SAMHÄLLSBYGGNAD

BYGGTEKNIK

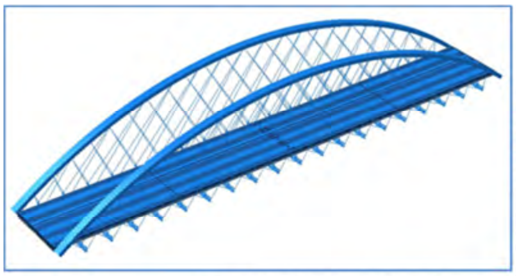


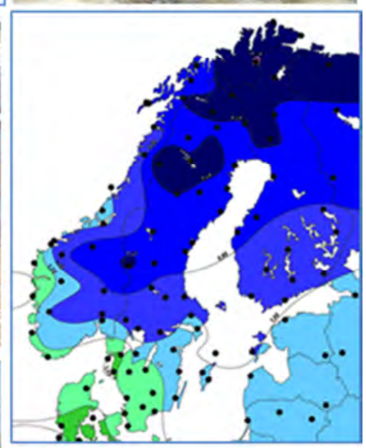

Durable Timber Bridges
Final Report and Guidelines

Compiled by Anna Pousette, RISE, Kjell Arne Malo, NTNU, Sven Thelandersson, Lund University, Stefania Fortino, VTT, Lauri Salokangas, Aalto University, James Wacker, USDA

SP Rapport 2017:25

Durable Timber Bridges

Final Report and Guidelines

Compiled by Anna Pousette, RISE, Kjell Arne Malo, NTNU,

Sven Thelandersson, Lund University, Stefania Fortino, VTT,

Lauri Salokangas, Aalto University, James Wacker, USDA

Abstract

Durable Timber Bridges

Final Report and Guidelines

This is the final report from the project DuraTB - Durable Timber Bridges. The goal of the project was to contribute to the development of sustainable timber bridges by making guidelines for moisture design and developing new and improved bridge concepts and details in terms of durability and maintenance aspects.

In this report the analyzes, surveys, results and guidelines are described. More detailed descriptions are referred to the many publications that the project has delivered.

The research leading to these results has received funding from the WoddWisdom-Net Research Programme which is a transnational R&D programme jointly funded by national funding organisations within the framework of the ERA-NET WoodWisdom-Net 2.

Keywords: timber bridges, durability, moisture, design, timber bridge consepts, timber bridge details

RISE Research Institutes of Sweden

SP Rapport 2017:25
ISSN 0284-5172
Skellefteå 2017

Table of contents

Preface

This is the final report from the project DuraTB - Durable Timber Bridges. It is the joint report of all parts and participants in the project.

The project was a Wood Wisdom-net project with participants from Norway, Sweden, Finland, and the United States. Project coordinator was Kjell Arne Malo, NTNU, Norway. Swedish national coordinator was Anna Pousette, RISE, and Finnish national coordnator was Stefania Fortino, VTT. The project was funded under the WW-Net + research program as part of the ERA-NET Plus Scheme in the Seventh Framework Programme (FP7) of the European Commission. National funding was made by Norges forskningsråd in Norway, Vinnova in Sweden, and Tekes in Finland and by the participants from industriy, road authoritites, cities and organizations.

Participating companies and organizations were:
Norwegian University of Science and Technology, NTNU, Norway (Project Coordinator);
Moelven Limtre AS, Norway;
Norwegian Public Road Authorities Statens vegvesen, Norway;
RISE Research Institutes of Sweden, Sweden;
Lund University, Sweden;
Moelven Töreboda AB, Sweden;
Martinsons Byggsystem KB, Sweden;
Limträteknik AB, Sweden;
Swedish Transport Administration Trafikverket, Sweden;
Teknologian Tutkimuskeskus VTT, Finland;
Aalto University, Finland;
Finnish Transport Agency, Finland;
Federation of the Finnish Woodworking Industries, Finland;
Versowood Oy, Finland;
Late- Rakenteet Oy, Finland;
MetsäWood, Finland;
City of Espoo (Municipality);
Finland, City of Helsinki (Municipality), Finland;
Forest Products Laboratory, USDA Forest Service, USA;
Leibniz University Hannover.

These guidelines have been compiled by Anna Pousette, RISE, Kjell Arne Malo, NTNU, Sven Thelandersson, Lund university, Stefania Fortino, VTT, Lauri Salokangas, Aalto University, and James Wacker, USDA, but many persons participating in the project have contributed as authors or reviewers of the content.

May 2017
Kjell Arne Malo, NTNU

Disclaimer

The design methods described in this report cannot be used as a basis for legal actions against the authors following material or immaterial damage due to applications of the presented methodologies.

1 Introduction about timber bridges and durability

1.1 Timber bridges

Great technological development in the wood and construction industry during the last decades has resulted in increased use of wood. Timber bridges have proven to be very competitive to short and medium span bridges with a span of 5 to 40 m and sometimes with longer spans. Timber bridges are well suited for this span range, and they offer quick installation on site. Because of the low weight they can also use existing foundations in the replacement of old bridges. In recent years more and more timber bridges have been built in several countries and because of the positive response, an even greater increase is expected in the future. There is an economic potential of having an alternative material for bridge construction except steel and concrete. From an architectural point of view, wood is also a material with great potential.

Environment concerns and awareness of the global warming has increased the interest of wood as a building material. Wood is the only construction material that is renewable and well maintained forests will increase to grow. Older trees are harvested and replaced by new trees transforming carbon dioxide, water and nutrients from the earth into a structural material by use of solar energy. This way the wood material stores a large amount of carbon dioxide as long as the wood is used in the structure.

Timber bridges can be built with different structural systems such as beams, slabs, trusses and arches, see more about bridge types in chapter 3. Timber bridges built today are typically made of glulam, which can have large cross-sections up to several square meters. Many wooden bridge decks are built as stress-laminated decks that in principle can be made continuous to any width or length. Usually the sizes of glulam elements and prefabricated bridges and bridge parts are limited by transportation from the factory to the building site. A timber bridge usually also contains other materials than wood, for example concrete in abutments and steel in fasteners.

Most materials used for construction of bridges have limited lifetime. Concrete gets carbonized, steel corrodes and timber may be attacked by fungi or insects. A large number of concrete and steel bridges built after the Second World War was assumed to have little need for maintenance. However, the current state of many of these bridges does not support this assumption; and there is now a vast gap between the needs for maintenance/repair of these bridges and the work actually performed. In many cases the bridges are beyond repair and new bridges are needed.

It is a common perception that the expected lifetime of a timber structure is only a fraction of that of a concrete or steel structure. In spite of this some timber structures like the Norwegian stave churches and the covered bridges in Switzerland are among the most durable structures. On the other hand there are timber structures that show serious decay after only a few years in service due to elevated levels of moisture and consequently growth of fungi and rot. This is also the case for many timber bridges in Europe. The prerequisites for a long life are good design and details, good materials and good strategies for maintenance and repair. Design of the details is essential to obtain good durability.

Figure 1.1 Pedestrian bridge of timber, Sweden

1.2 Design codes and durability of wood

The Eurocodes are the European standards that provide common structural design rules for design of structures and component products, and should be used within the member states of EU and EFTA. Bridges for public use are often monumental structures with expected design working life of about 100 years according to Eurocode EN 1990 (2002). The Swedish Transport Administration, however, requires 40 or 80 years for wooden bridges with higher demands for 80 years in respect of maintenance plan and covering of the main structure. The principle stated in EN 1990, Basis of design for durability, reads "The structure shall be designed such that deterioration over its design working life does not impair the performance of the structure below that intended, having due regard to its environment and the anticipated level of maintenance". Furthermore it is stated that the environmental conditions shall be identified so their significance can be assessed. Finally, it is also stated that the degree of any deterioration may be estimated on the basis of calculations, experimental investigation, and experience from earlier constructions or a combinations of these considerations.

However, consulting Eurocode EN 1995-1-1 (2004) about design of timber structures and the specific part on timber bridges EN 1995-2 (2004), no method, guidelines or data for evaluation of deterioration are given, only prescriptive rules for improvement are mentioned, like avoiding standing water and the use of preservatives. Consequently timber bridge designers have no measures for estimating lifetime of wooden structures. Hopefully these guidelines can contribute to improve this.

The Eurocodes on timber bridges allow in principle the designer a choice of (a) sufficient flashing or sheltering details, (b) use of naturally durable timbers according to EN 350-2 (1994), or (c) use of preservatives in pressure-treated materials. In North-America however, the AASHTO regulations and the Canadian bridge code require timber used in bridges to be treated with preservatives applied by pressure treatment as presented by Wacker, Groenier (2010). A comprehensive guide on most aspects regarding timber bridges in the North-America can be found in Ritter (1990).

1.2.1 Wood species

Different wood species have different natural resistance to attacks by wood-destroying organisms such as fungi and insects. Wood used in buildings and structures may be divided into softwoods (conifers) and hardwoods (deciduous). Many timber bridges in northern Europe are built of softwoods, mainly Scots pine and Norwegian spruce, as these are the most common trees in the forests. In North-America the most common wood species in bridges are Douglas fir and Southern pine, sometimes in combinations with other species. Hardwoods have a different structure of the wood and many hardwoods have good natural durability, for example oak.

Wood is a fibrous material, and the wood fibres of softwoods are oriented in the direction of the stem. The growth of the tree depends on the location and climate and each year some wood is added to the cross-section of the stem. These annual rings are a few millimetres thick. The outer parts of the wood in the tree, the sapwood, transport nutrients and water in the growing tree. Heartwood is the dead inner part which no longer transports water. It has increased decay-resistance compared to the sapwood as it forms in the transition zone when the cells die and deposit chemical extractives and these chemicals provide natural durability of the wood. Because of dead cells and extractives it is very difficult to pressure-treat heartwood with preservatives and only the sapwood can be treated.

Wood is an anisotropic material, which means that its properties are different in different directions. Parallel to grain, that is along with the fibres in the longitudinal direction of the stem, wood is significantly stronger than perpendicular to grain, that is across the fibres. This applies whether the applied load causes a compressive, tensile and bending stress in the timber. The strength of the wood is partly due to the wood density and on how well the grain is consistent with the direction of the forces that occur when the timber is loaded. Fibre direction deviates from the direction of forces at for example knots. The strength is also influenced by the wood humidity, temperature and the duration of loading. Dry wood is stronger than wet and cold wood is stronger than warm.

1.2.2 Preservative treatments

In northern Europe and in North-America, depending on national regulations, it is currently quite common to use toxic preservatives in order to reduce biological deterioration and thereby extend the lifetime of timber bridges. Preservative treatments with toxins can be very effective to enable the use wood in exposed environments.

However, in some countries e.g. Sweden, wood preservatives including chromium, arsenic or creosote are not accepted because of environmental concerns. The use of toxic preservatives in many of the wooden bridges reduces the perception of environmental friendliness in the society, and the trend is that the authorities are becoming more restrictive. Non-toxic preservative methods are on the market, but so far their costs, effectiveness and effects on the mechanical wood properties exclude them as competitive candidates for use in bridges. It is also well known that many bridge designs suffer from over-reliance on preservative treatment and have elevated moisture content as shown by Alampalli et al (2008). The use of preservatives like creosote may also leave a negative impression due to sweating; furthermore, water protective membranes often used in decks might get damaged due to lack of chemical resistance against such preservatives.

Figure 1.2 Construction of timber truss bridge, Norway

1.2.3 Service classes and use classes

The current design code for timber structures EN 1995-1-1 (2004) defines a set of three service classes which are relevant to the designer for assigning strength values and calculating deformations of structural timber. These service classes are determined by the wood moisture content corresponding to the humidity and temperature which are expected to prevail in service. The wood moisture content is also important for biological durability, but the system of service classes in EN 1995-1-1 (2004) and the system of use classes in EN 335 (2013), differ in their considerations of the effects of moisture. The use classes in EN 335 (2013) represent different situations to which wood can be exposed, but they are not performance classes and give no guidance for how long wood and wood-based products will last in service.

According to this system most timber bridges will end up in service class 2 or 3, and in use class 1, 2 or 3 depending on cover, and the risk and duration of wetting. Information about the natural durability of wood is given in EN 350-2 [10] for the various species. It should be noted that this information is based on specimen in ground contact, which should never be the case for wooden bridges. EN 350-2 [10] classifies Nordic softwoods (pine and spruce) in durability class 4 on a scale from 1 to 5 where 1 means very durable, while 5 indicates non-durable. This applies to heartwood while sapwood is in class 5. An attempt to link natural durability of wood with respect to fungi and the use classes is made in EN 460 (1994), but the outcome is merely a guide on use of preservatives based solely on use classes and durability classes. A more easily accessible guidance to this approach might be found in Sétra (2007).

Biological deterioration reduces the structural carrying cross section of wooden members (although not necessarily the cross section itself). It is a time-dependent effect that damages parts of the material and hence reduces the load-carrying area of structural members. Biological deterioration seems to have periods where the decay is reversed or set-back to some extent as described in EN 350-2 (1994). Classification of details and sets of performance models or curves can be a useful methodology to prevent fracture in structures due to biological deterioration. Such a classification is made in Australia for some typical outdoor applications like fences, pergolas, cross-arms and decking, leading to tables with typical service life or depth of decay after a certain time as shown by MacKenzie (2012). The tables depend on the durability class of the wood species, the treatment and the climate zone, and each table is valid for one typical structural design.

For structures in use class 2, 3 and 4 the design details of a timber component, the degree of prevention of water penetration, drainage and ventilation together with local climatic conditions and maintenance procedures, influence the long-term performance as presented in EN 460 (1994). Moreover, the ability to absorb water is important for the life of wood, and this property is linked to the degree of pressure treatability of wood. In case of fungi attacks, a size effect seems to occur so the service life of a timber component can be expected to increase in proportion to its thickness. This is especially interesting for timber bridges as they are likely to have very large cross-sections.

Figure 1.3 Timber arch bridge, Finland

1.3 Design of durable timber bridges

The durability of a timber bridge is governed by the design of the bridge. Timber bridge design resulting in too high humidity in the wood will lead to the appearance of fungi which in turn can cause serious damage. The most important objective of timber bridge design is therefore to avoid excessive humidity in the wood. Many of the durable bridges in Switzerland and USA are covered by a complete roof. But these bridges are mainly pedestrian bridges or made for vehicles very different from todays 20 meters long trucks. On a rainy day a modern truck-train at high speed will create a considerable blast wave which will carry a large spray of water and bring it into the bridge structure, covered by a roof. In such situation the roof may in fact reduce the ability of rapid drying and lead to high moisture in the structure. Hence, the covering of bridges by a roof is a doubtful approach for road bridges. On the other hand, bridges with the deck on top of the supporting structure will protect it from weathering, and have demonstrated a better state of preservation than those where the deck was between or below the carrying structure as shown by Kropf (1996).

The design of a bridge depends on many factors and is often given by topography, required waterway clearance, load, appearance, economy, etc. Decisions made at an early planning stage can have a decisive influence on the long-term behaviour of the structure. The less the structure protects itself, the more effort must be invested in protecting individual parts. Much of this can be resolved at the drawing table, assuming the design engineer is responsive to the needs and limits of the construction material - and keeps in mind that sun exposure and high temperatures might also damage wood. The differential change in volume due to unequal moisture distribution through a wood cross-section and in combination with the very low strength perpendicular to the grain, can develop longitudinal checks that can grow into large cracks. Large cracks in connection areas may reduce the strength of both connections and members. By combining good detail design with supplemental measures, i. e. cover, water repellent surface coating, and/or chemical treatment where needed, it is possible to provide weather exposed wooden structures for a service life comparable to other construction materials – and still keep the advantage of wood as an ecological material without disposal problems according to Kropf (1996). Ideally the advice of a wood expert should be included at the initial stage but today there is a considerable lack of education and competence in timber bridge building among architects, consultants and authorities. Therefore, this guide has been developed to help and support.

Several criteria must be taken into account when modern bridges are designed: the strength of the bridge must be guaranteed to provide a safe passageway for the planned traffic; the vibrations and deflections of the bridge deck must be limited according to standards so that passage over the bridge feels safe (comfort criteria); the sustainability must be ensured throughout the design life with a reasonable level of maintenance.

In Figure 1.1 a model for durability performance is incorporated in a graphical visualization of the design process for a timber bridge to complement the safety performance and the serviceability performance. Single arrow heads indicate one-directional flow of information or influence, e.g. the material properties of a chosen material influence the safety performance, but the safety performance does not change the material properties. Arrow heads in both ends means that information and influence can move both ways and implies in principle an iterative procedure.

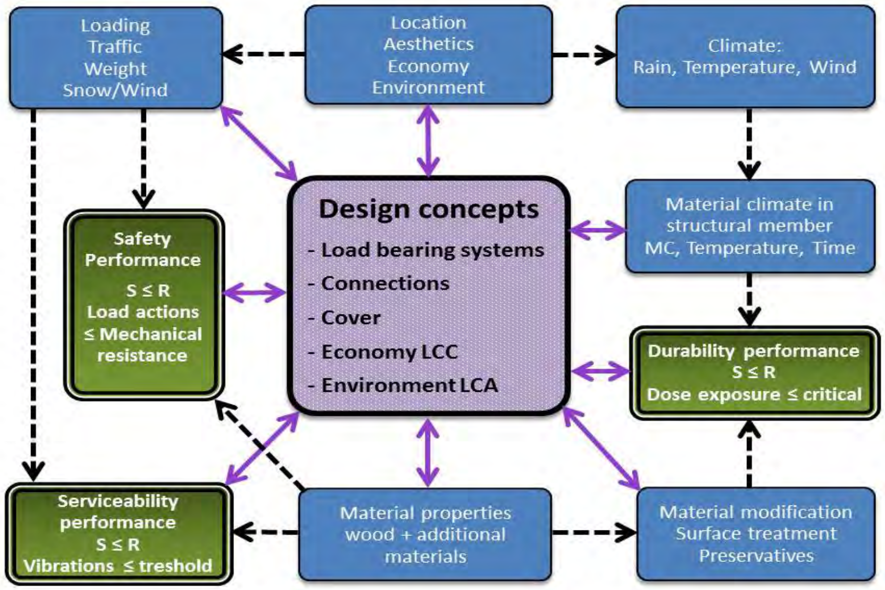

Figure 1.1. Design process for a timber bridge.

1.4 References, chapter 1

Alampalli, S.; Duwadi, S. R.; Herman, R. S.; Kleinhans, D. D.; Mahmoud, K.; Ray, J. C.; Wacker, J. P.; Yazdani, N. (2008). Bridge Workshop: Enhancing Bridge Performance, February 21-22, 2008, Reston, Virginia: workshop report. [S.l.]: The American Society of Civil Engineers, Structural Engineering Institute, 2008.

EN 1990 (2002). Eurocode - Basis of structural design. European Committee for Standardization, Bruxelles, Belgium, April 2002.

EN 1995-1-1 (2004). Eurocode 5: Design of timber structures – Part 1-1: General – Common rules and rules for buildings/incl Amendment A1, European Committee for Standardization, Bruxelles, Belgium, November 2004/2008.

EN 1995-2:2004 Eurocode 5: Design of timber structures – Part 2: Bridges, European Committee for Standardization, Bruxelles, Belgium, November 2004.

EN 335 (2013). Durability of wood and wood-based products – Use classes: Definitions, application to solid wood and wood-based products. European Committee for Standardization, Bruxelles, Belgium, March 2013.

EN 350-2 (1994). Durability of wood and wood-based products – Natural durability of solid wood – Part 2: Guide to natural durability and treatability of selected wood species of importance in Europe. European Committee for Standardization, Bruxelles, Belgium, May 1994.

EN 460 (1994) Durability of wood and wood-based products – Natural durability of solid wood – Guide to the durability requirements for wood to be used in hazard classes. Committee for Standardization, Bruxelles, Belgium, May 1994.

Kropf FW (1996). “Durability and detail design-the result of 15 years of systematic improvements”. Paper presented at the National conference on wood transportation structures, Madison, the USA, October 1996.

MacKenzie C. (2012): Timber service life design. Design guide for durability. Technical design guide issued by Forest and Wood Products Australia. ISBN 978-1-920883-16-4, 2012. Available from woodsolutions.com.au.

Ritter, M.: (1990). Timber Bridges, Design, construction, inspection and maintanance. US Department of Agriculture, Washington DC, USA, 1990.

Sétra (2007). Timber Bridges. How to ensure their durability. Technical Guide. © 2007 Sétra - Reference: 0743A - ISRN: EQ-SETRA--07-ED40--FR+ENG, This document is available and can be downloaded on Sétra website: http://www.setra.equipement.gouv.fr

Wacker, J.; Groenier, J. (2010). Comparative analysis of design codes for timber bridges in Canada, the United States, and Europe. Transportation research record. No. 2200 (2010): p. 163-168.

2. Performance based service life design of timber bridges[1]

2.1 Introduction, overview of methodology

2.1.1 General

This chapter deals with wood in outdoor above ground applications, i.e. use class 3 according to EN 335-2 (2013), focusing on applications relevant for timber bridges, see Figure 2.1. The degradation mechanism considered is the risk for fungal decay. Onset of decay is defined as a limit state of fungal attack according to rating 1 in EN 252 (2015). The consequences related to violation of the limit state should be considered as high for timber elements being part of the load bearing structural system in the bridge. The notional acceptance of probability of violation of the limit state should then be based on the target reliability for structures defined in EN 1990 (2002). For non-load bearing wood elements in the bridge, such as weather protection panels, a higher probability of failure can be accepted.

Figure 2.1 Vihantasalmi bridge, Finland.

The service life of a wood structure with respect to fungal decay mainly depends on :

- Climatic exposure, i.e. geographical site, local climate, degree of protection against rain, distance to ground, detailing with respect to moisture trapping and maintenance measures. A combined measure of moisture content and temperature in the wood is relevant for the risk of decay.
- Material resistance; different materials such as untreated spruce, pressure treated pine sapwood and larch heartwood display different resistance against decay.

---

[1] **Disclaimer**
The design method described in this chapter can not be used as a basis for legal actions against the authors following material or immaterial damage due to application of the presented methodology.

The exposure is primarily affected by the design and construction of the bridge and is as a whole independent of which material is used.

The resistance is primarily a function of the choice of material.

The method proposed in this guideline is to evaluate relevant wood members, details and joints in the bridge individually with regard to durability and service life. The first step is to determine whether the member or detail is fully protected from exposure to free water (from rain, splash or run-off water), see flow chart in Figure 2.2.

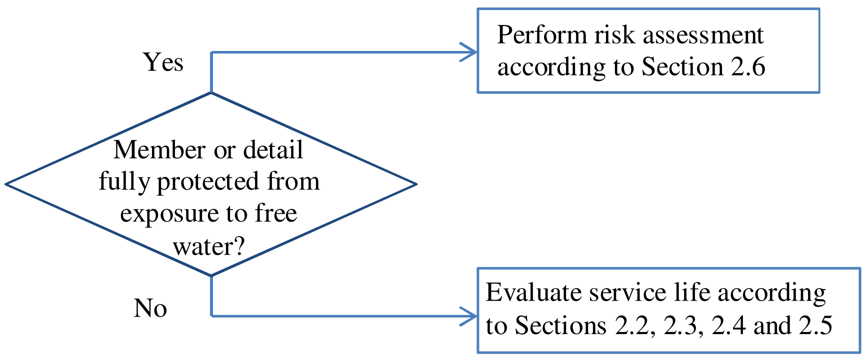

Figure 2.2. Flow chart for choice of assessment method for member/detail of bridge

Timber members which are fully sheltered from free water (rain, splash, runoff water) are normally not vulnerable to decay fungi, see EN 460 (1994), SETRA (2006). Most protective systems can be divided into one of three categories:

- Water barrier and ventilated air gap, e.g. ventilated cladding or metal sheeting
- Water barrier without air gap, e.g. impermeable layer under the paving on timber decks
- Protective roof, e.g. members sheltered by a deck or by an actual roof structure

Full sheltering from above can e.g. be assumed for the bottom side of a bridge deck with water tight membrane. Also wood in zones where *e/d* >2 according to Figure 2.8 can be assumed fully protected.

2.1.2 Wood fully protected from free water

In the case of full protection from free water, the risk of leakage in the water barrier has to be assessed. This is illustrated by the event tree shown in Figure 2.3. A methodology for risk assessment is described in Section 2.6.

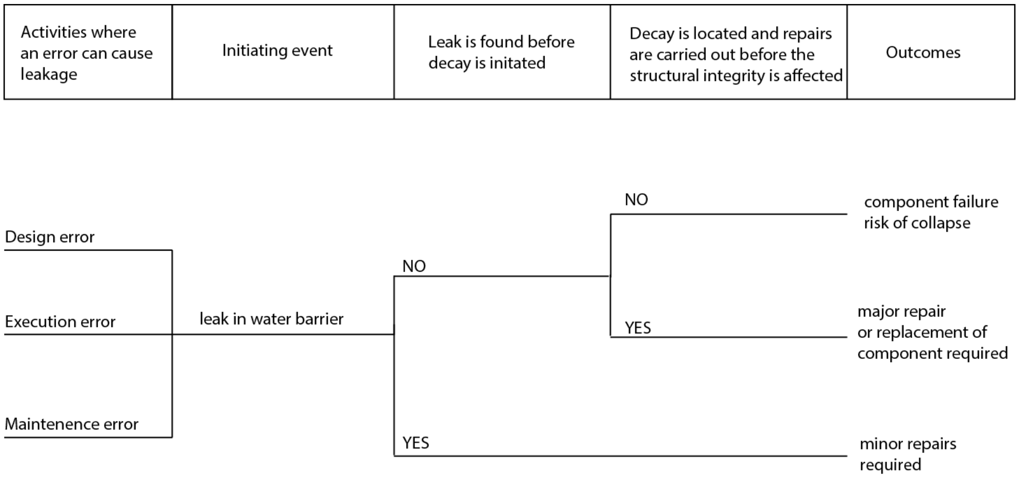

Figure 2.3. Event tree showing possible outcomes from a leak in the water barrier

2.1.3 Wood exposed to free water

For members or details which are exposed to free water, the design method proposed here implies that the climate exposure is assessed and compared with the resistance of the selected material. A selected design solution and choice of material is accepted if

Exposure ≤ Resistance

Mathematically this can be expressed as

$$D_{Ed} = D_{Ek}\gamma_d \leq D_{Rd} \qquad (2.1)$$

where D_{Ek} is a characteristic dose value for the exposure, D_{Rd} is a design value of the resistance expressed as a dose and γ_d depends on severity class. The severity class refers to the expected consequences if the limit state is violated. If the condition in Eq. (2.1) is fulfilled, then the design meets the service life requirements; otherwise the design and/or material properties can be changed to meet the requirements. The concept of dose, which has the unit time (in days), is a combined measure of moisture content, temperature and duration, see e.g. Isaksson et al. (2013).

Figure 2.4. Reference element for climate exposure – horizontally exposed spruce board without moisture traps. (Photo: Tord Isaksson, Lund University).

The definitions of D_{Ek} and D_{Rd} are related to the following reference situations. The reference exposure in terms of an annual dose D_{E0} is defined for a horizontal wooden element exposed to outdoor conditions in terms of precipitation, relative humidity and temperature, see Figure 2.4. This reference exposure depends on the climate at the geographical site considered. The reference element is without moisture traps. The effect of e.g. detail design and local conditions is accounted for by using different factors resulting in a characteristic exposure D_{Ek} for a specific design detail.

The material resistance to onset of decay is defined by a design value D_{Rd} which depends on species, modification and preservative treatment. Important aspects here are material specific properties regarding water uptake and inherent protection against fungal decay. Norway spruce (*Picea abies*) is chosen as reference material.

The exposure of the reference detail (without water traps) is relatively favourable in terms of avoiding decay. Most design situations mean higher risk for moisture trapping and consequently longer periods of higher moisture content in the material with increased risk for onset of decay. These situations are accounted for by using exposure factors as described in section 2.3.

The evaluation of a given member or detail exposed to free water can be made in the following steps:

1. Determine the required service life (Section 2.2).
2. Determine severity class and the corresponding value of the factor γ_d (Section 2.2).
3. Determine the annual dose D_{E0} for the exposure depending on geographical site (Section 2.3).
4. Determine an exposure factor, which considers local climate conditions. Important factors here are intensity of driving rain, topography of the terrain and degree of protection from surrounding buildings and vegetation (Section 2.3).
5. Determine exposure factors (Section 2.3) for
    a) rain sheltering
    b) distance to ground
    c) detailing of the considered component/detail
6. Steps 2-5 gives a design value D_{Ed} for the annual exposure dose in the considered detail or member
7. Select material and determine the relevant value of D_{Rd} (Section 2.4).
8. Determine the expected service life as $\frac{D_{Rd}}{D_{Ed}}$ years (Section 2.5).
9. Check if the selected design and choice of material meets the required service life
10. If not, modify input in steps 4 to 7

Descriptions of how exposure and resistance can be determined are given in Sections 2.3 and 2.4 respectively.

2.2 Service life requirements for bridge structures.

2.2.1 General

The design of structures and details in timber bridges with respect to durability and expected service life concerns mainly two aspects:

- Timber bridge structures designed according to Eurocodes (EN 1995-2: 2004; EN 1995-1-1:2004; EN 1990:2002) and national applications.
- Aesthetical and economical requirements which are normally project specific and defined together with the client.

Performance in terms of aesthetics and economics is not regulated in codes. The requirements of the client are based on expectations regarding e.g. maintenance, life cycle costs and appearance. For bridges the requirements are most often based on maintenance and economic assessment.

The level of performance requirements on durability should be considered in relation to the consequences of non-performance, e.g. personal injuries, deaths, economical losses and the costs and measures necessary to reach a certain durability.

This guideline separates between the above mentioned two aspects of durability in terms of consequence. The durability of structural components follows the requirements stated in Eurocode [EN 1990(2002), EN 1995-1-1 (2004)]. Non-structural components are treated by choice of consequence class, see section 2.2.3.

2.2.2 Durability requirements for structural components

According to Eurocode (EN 1990:2002) a structure shall be designed to have adequate:

- structural resistance,
- serviceability and
- durability

The requirement on durability should accordingly be considered as equal to requirements on resistance and serviceability. A general principle concerning durability is given in EN 1990 (2002) as

"The structure shall be designed such that deterioration over its design working life does not impair the performance of the structure below that intended, having due regard to its environment and the anticipated level of maintenance."

For methods to verify durability, reference is made to the material dependent Eurocodes EN 1992-EN 1999. Concerning timber bridges EN 1995-2 gives only general principles summarised as

"The effect of direct weathering by precipitation or solar radiation of structural timber members can be reduced by constructional preservation measures, or by using timber with sufficient natural durability, or timber preservatively treated against biological attacks."

In this guideline a method to verify the compliance to the durability requirements based on estimated service life is described.

General requirements for load-bearing structures regarding design working life are given as indicative values in EN 1990 (2002), see Table 2.1. These values are applied here for timber bridges.

Table 2.1. Indicative design working life according to EN 1990 (2002).

Design working life category	Indicative design working life (years)	Examples
1	10	Temporary structures[1]
2	10 to 25	Replaceable structural parts, e.g. gantry girders, bearings
3	15 to 30	Agricultural and similar structures
4	50	Building structures and other common structures
5	100	Monumental building structures, bridges and other civil engineering structures
[1] Structures or parts of structures that can be dismantled with a view to being re-used should not be considered as temporary		

Structural design of timber bridges is based on requirements for structural resistance and serviceability. Durability design shall secure that these requirements are fulfilled during the intended service life.

2.2.3 Durability severity class

The reliability of durability design used here is differentiated depending on the consequences of having a service life which is shorter than the expected service life. This is done by introducing a factor γ_d depending on severity class, see Table 2.2. The chosen class should depend on the expected consequences related to damage from decay within the expected service life.

It is clear that primary load bearing structural elements in a timber bridge belong to the highest consequence class 3 with γ_d = 1,0. This can be seen as a reference case. For non-structural wooden elements, the severity class can be taken depending on the intended use and the possibility of replacement and maintenance. Wooden panels for weather protection of load-bearing structural elements can be taken as class 1 if the intention is to replace them at regular intervals. Some secondary structural elements, where failure has no consequences for humans and which can be replaced easily may be assigned to severity class 2.

Generally, for non-structural elements not covered by the structural Eurocodes, durability requirements should be decided by the designer in cooperation with the client.

Table 2.2. Definition of severity classes for durability.

Severity class	γ_d
1. Low (e.g. where it is accepted and easy to replace a limited number of components if decay should be initiated within expected service life)	0.6
2. Medium (e.g. when the expected economical and practical consequences are significant)	0.8
3. High (risk for human injuries or loss of lives)	1.0

2.3 Exposure conditions for rain exposed elements and details

2.3.1 General

The exposure shall be evaluated for different locations and detail designs of the bridge structure. We can distinguish between two cases. Structural elements and details are either

1. subjected to exposure from free water (rain, splash or run-off water)
2. protected from rain exposure by e.g. protective cladding or effective sheltering from above

For case 2 the risk of decay can be neglected as long as the protective measures work as intended. The designer must however carefully consider the risk of failure/leakage of the protection. How this can be done is described in Section 2.6. How effective sheltering from above is defined is described in section 2.1.1.

For case 1 with rain exposure, the annual dose D_{Ek} shall be seen as a "characteristic value", including safety margins accounting for uncertainties. The methods described below may also be used for elements and details protected from rain to evaluate the risk associated with leakage or malfunction of the protection system and as a basis for decisions about inspection strategies.

The exposure for rain exposed elements is assumed to depend on

- Geographical location determining global climate conditions
- Local climate conditions
- The degree of sheltering from rain
- Distance from ground
- Detail design of the wood component considered

In this guideline the annual exposure dose is determined as

$$D_{Ek} = k_{E1} \cdot k_{E2} \cdot k_{E3} \cdot k_{E4} \cdot D_{E0} \cdot c_a \tag{2.2}$$

where

D_{E0} annual reference exposure dose depending on geographical location/global climate
k_{E1} factor describing the effect of local climate conditions and driving rain
k_{E2} factor describing the effect of sheltering
k_{E3} factor describing the effect of distance from ground
k_{E4} factor describing the effect of detail design (risk of trapping water)
c_a = 1,4 (calibration factor estimated on the basis reality checks, safety considerations and expert estimates, see section 2.7)

How the factors in Eq. (2.2) are determined is described below in separate sections. The exposure dose intends to describe the severity in terms of combined moisture and temperature conditions favourable for development of decay fungi. It has been derived with the aid of the performance model described in Isaksson et al (2015).

2.3.2 Annual reference exposure dose D_{E0}

The annual reference exposure dose D_{E0} is a function of geographical location and describes the climatic effects for the reference object, i.e. a horizontal wooden element exposed to outdoor conditions in terms of precipitation, relative humidity and temperature, see Figure 2.4.

The base value D_{E0} of the exposure has been estimated with the help of the simplified logistic dose model (SLM) described in Isaksson et al (2013). The SLM-model (in the form of a dose-response relationship) is used to evaluate the combined effect of moisture content, temperature and the time variation of these parameters on the potential for decay fungi to germinate and grow.

The macroclimate for a standard year at different sites is based on the software Meteonorm (http://meteonorm.com, 2015). The climate data in the form of relative humidity and rain is used to calculate moisture content in the reference wood element at depth of 10 mm using a simple numerical model developed in DURA-TB, see Niklewski et al (2016a) and Niklewski et al (2016b). The temperature in the wood element was assumed to be the same as the air temperature.

The annual reference doses for a large number of locations in Europe were calculated. The results are displayed in the form of contour plots on a map produced by interpolations between the analysed sites, see Figure 2.5. In this way geographical zones are identified. The annual dose for a standard year within each of the zones are given in Table 2.3. Magnification of the same map for Scandinavia is shown in Figure 2.6.

Table 2.3. Annual exposure dose D_{E0} for the zones displayed in Figures 2.5 and 2.6. Valid for the reference object shown in Figure 2.4.

Zone	Annual exposure dose D_{E0} (days)		
	Mean	Range	Color code
a	66	63-69	
b	60	57-63	
c	55	52-57	
d	49	46-52	
e	43	40-46	
f	37	34-40	
g	32	29-34	
h	26	23-29	
i	20	17-23	
k	15	12-17	
m	9	6-12	

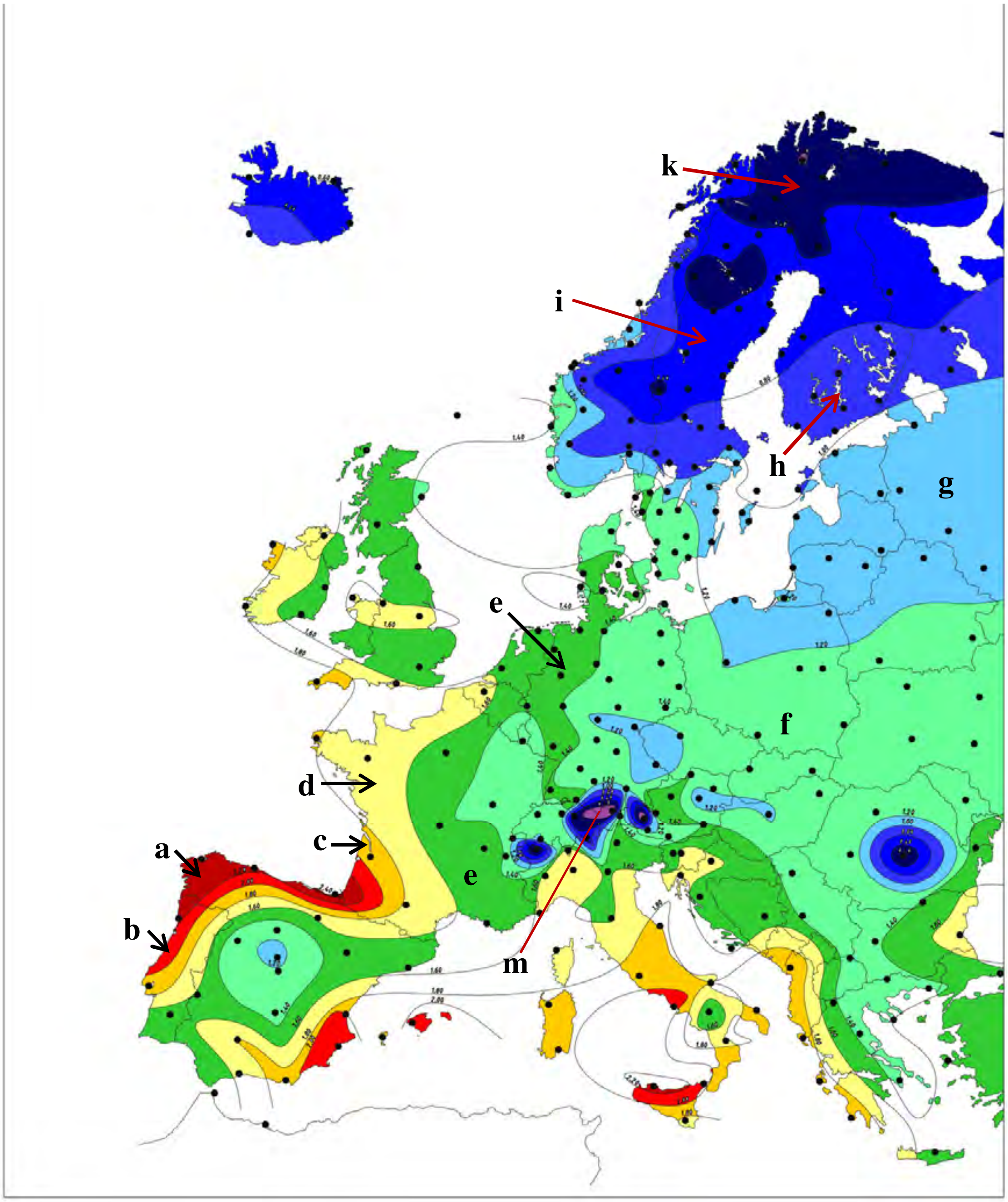

Figure 2.5. Zones for Europe for estimation of annual exposure dose

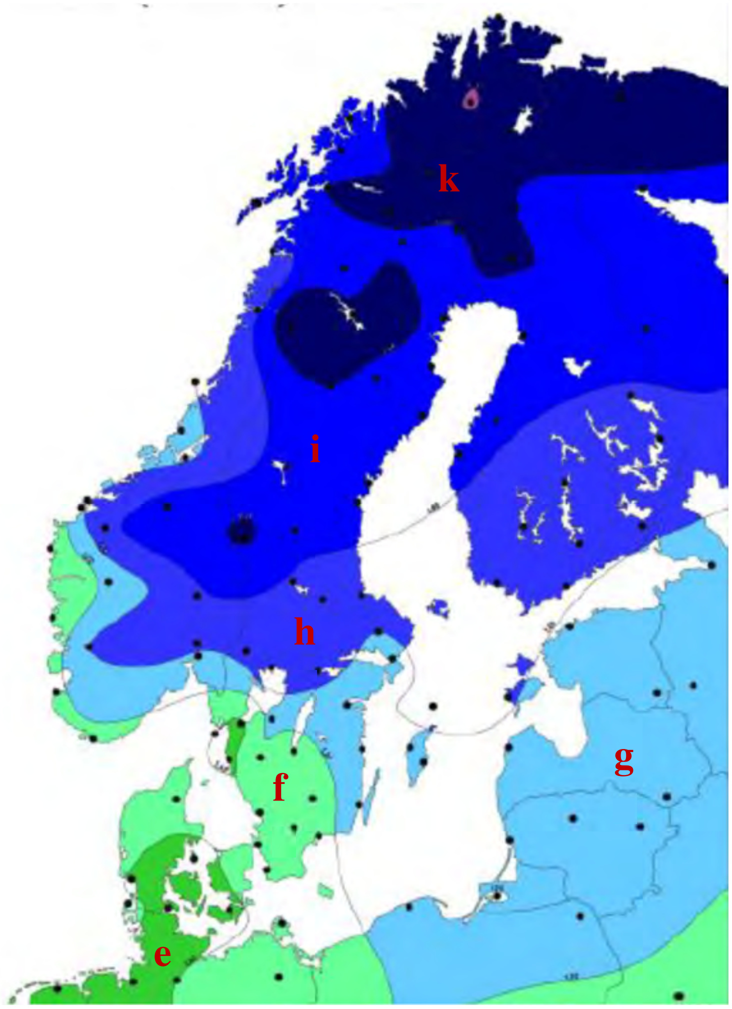

Figure 2.6. Magnification of map in Figure 2.3 for Scandinavia

2.3.3 Local exposure conditions

The local conditions in terms of risk for driving rain and protection from topography and adjacent buildings, vegetation and other obstacles will affect the exposure of vertical surfaces. This is described in terms of three classes: light, medium and severe, as shown in Table 2.4. The factor k_{E1} is assumed to be valid for wood facing the dominating wind direction, since this case gives the most severe exposure. Adjustments for less exposed directions are not made, because the design normally does not vary between different directions. Note that for horizontal rain-exposed surfaces local conditions should always be taken as severe.

The local conditions can be accounted for by using the factor k_{E1} according to Table 2.4. It is a function of

- the extent of free driving rain at the bridge site
- the degree of protection from the surroundings outside the bridge itself

Information about free driving rain may be obtained from meteorological data. Free driving rain is present when high wind and rain occurs simultaneously. As an example, in Figure 2.7

a map is shown for Europe indicating the frequency of free driving rain in terms of an index. It is proposed here that free driving rain should be considered (i.e. answer yes in the second column of Table 2.4) in zones with index > 1,6, but not in zones with index < 1,6.

Table 2.4. The effect of local exposure conditions for vertical wood surfaces.[1]

Degree of exposure	Protective effects are present	Driving rain expected at the site	k_{E1}
Light	Yes	No	0.8
Medium	Yes	Yes	0.9
Medium	No	No	0,9
Severe	No	Yes	1.0

[1]For horizontal rain-exposed surfaces k_{E1} = 1,0 should be chosen.

Since the experimental test results forming the basis for annual dose calculations are based on severe conditions (free driving rain and without shelter), this case is chosen as reference with k_{E1}=1.0.

Reduction in exposure effects may be identified at the bridge site by considering the potential of protection from the free driving rain based on topography and surrounding buildings or other facilities. In cases where this effect is difficult to estimate the advice is to be conservative and disregard the effect. The values in Table 2.4 are not based on experimental results but more on expert opinions. The effect of local conditions is normally not possible to change or improve by the designer.

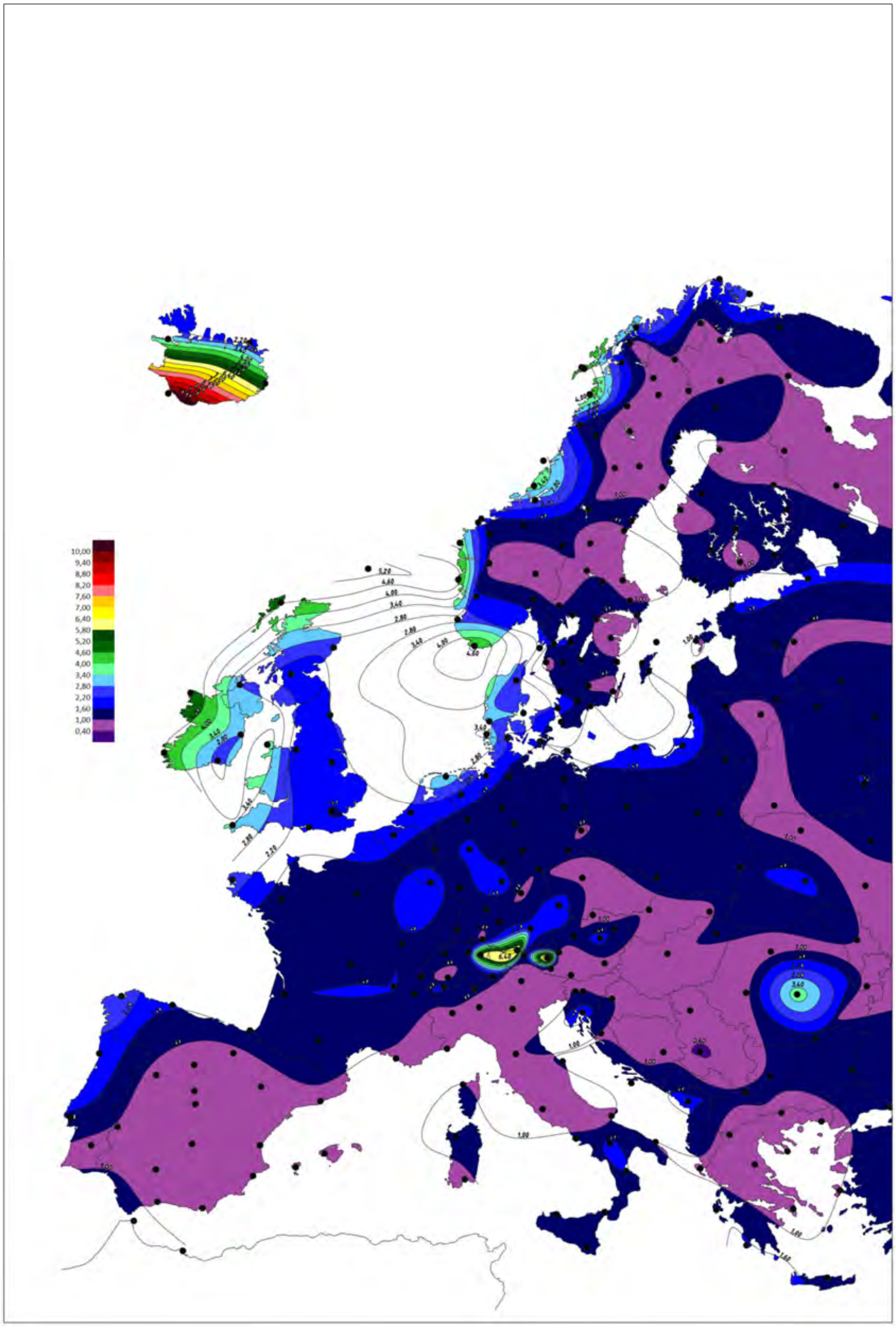

Figure 2.7. Map indicating intensity of free driving rain over Europe in the form of an index. For zones with index higher than 1,6 driving rain can be regarded as frequent, while in zones with index less than 1,6 effect of driving rain can be neglected in Table 2.4.

2.3.4 Degree of sheltering and distance from ground

The effect of rain sheltering above the detail considered is evaluated based on field tests described in Bornemann et al (2012). See also SETRA (2006). This effect is described by the factor k_{E2}, see Eq. (2.2). It is assumed to be a function of the ratio *e/d*, where *e* is the width of the overhang and *d* is the relative position of the detail considered, see Figure 2.8.

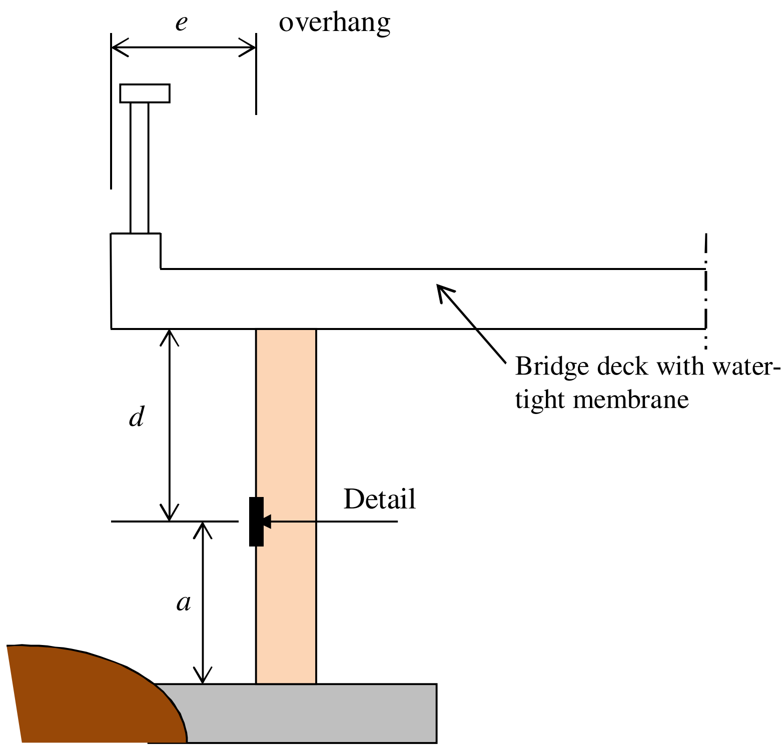

Figure 2.8. Definitions of measures for overhang *e* and distance *a* from ground.

Sheltering from overhang can be taken into account by reduction with the factor k_{E2} according to

$$k_{E2} = 1 - 0{,}2\frac{e}{d} \quad \text{if} \quad 0 < \frac{e}{d} \le 1 \tag{2.3}$$

$$k_{E2} = 0{,}8 \quad \text{if} \quad \frac{e}{d} > 1$$

This equation is illustrated graphically in Figure 2.9.

Distance from ground is considered as an increase of exposure for details closer than 400 mm from the ground level. Distances less than 100 mm are not considered since such a design is clearly not appropriate and durability effects are very uncertain. The effect is described by the factor k_{E3} which is calculated from

$$k_{E3} = \frac{700 - a}{300} \quad \text{if} \quad 100 < a \le 400 mm \tag{2.4}$$

$$k_{E3} = 1{,}0 \quad \text{if} \quad a > 400 \text{ m}$$

with *a* in mm. This equation is illustrated in Figure 2.10.

The definition of the distance to ground can sometimes be problematic for timber elements supported on concrete foundations, see e.g. pictures in Annexe A. The vertical distance to the ground soil should always be considered. But the question is if the distance from the wood should be measured to the concrete support or not? In such cases the user have to make an assessment whether splashing from rain on the concrete surface could affect the moisture exposure of the timber or not. Note that the effect of support detailing is covered by the factor k_{E4} , which is described in Section 2.3.5.

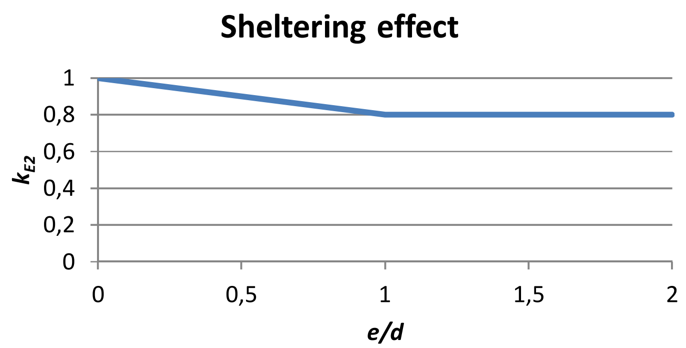

Figure 2.9. Effect of sheltering is described by the factor k_{E2}, with *e* and *d* defined in Figure 2.6. For *e/d* > 2, full rain protection can be assumed.

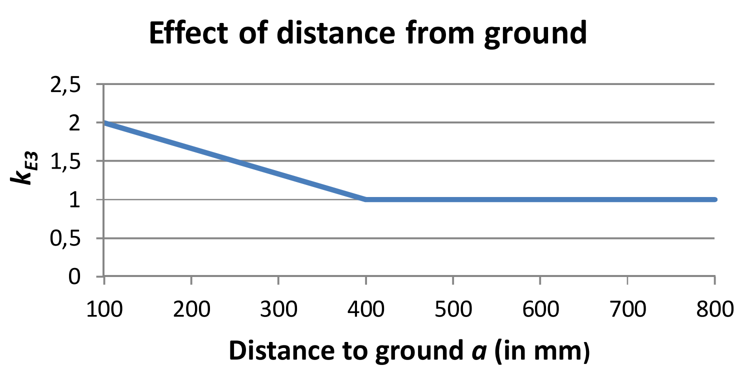

Figure 2.10. Effect of distance *a* from ground is described by the factor k_{E3}.

2.3.5 Effect of detail design

The effect of detail design is evaluated based on field tests carried out in the DURA-TB project, where a number of bridge details were exposed outdoors while the moisture content was measured continuously, see Niklewski et al (2016c). The simplified logistic dose model (SLM), see Isaksson et al (2013), was used to post-process the moisture content measurements to calculate the annual dose. Each detail was then assigned to one out of five classes ranging from excellent to poor. The relative annual dose, compared to a reference, is described by the factor k_{E4} (see table 2.5).

Table 2.5. Rating of details with respect to exposure.

Class	Description	Example	k_{E4}
Excellent	Design characterized by excellent ventilation (air gap > 10 mm) and no standing water. For example: a vertical surface without connecting members or with sufficient gap between members[1]	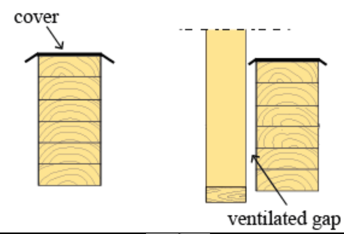	0,8
Good	Design characterized by excellent ventilation but standing water after rain events. For example: horizontal surface without connecting member.		1,0
Medium	Design characterized by poor ventilation but limited exposure to water. For example, vertical contact areas without sufficient air gap.	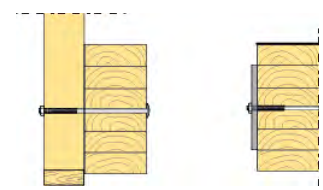	1,25
Fair	Design characterized by poor ventilation and high exposure to water **or** end-grain with good ventilation and limited exposure to water.[1] For example: horizontal contact areas and end-grain with sufficient air gap.	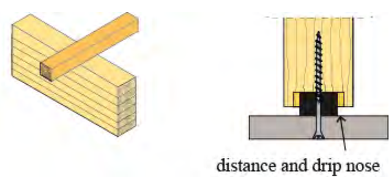	1,5
Poor	Design characterized by exposed end-grain with no ventilation and very high exposure to water. For example: end-grain contact area without air gap.	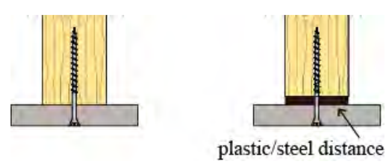	2

[1)] It is assumed that the gap is kept completely free from dirt and vegetation

For details different from the examples shown, the user must assess the degree of moisture exposure and relate to one of the five classes listed in Table 2.5. The main criteria should be the degree of rain exposure and the possibility of fast drying to avoid moisture traps. In case of uncertainty a more severe class should be chosen.

In evaluating details, the risk of soil and dirt being trapped in critical spots should be considered. Another risk could be that vegetation will lead to increased risk of moisture being trapped.

Annex A shows a few examples of how the grading can be performed.

Note again that timber which is sheltered from rain, for example by protective cladding or sheltering from elements above, is not dealt with here. For this case see Section 2.6.

2.4 Wood material resistance

2.4.1 General principle

The resistance of different wood species and treated wood products in above ground applications is primarily dependent on the degree of inherent material resistance against fungal decay, but also on the wetting ability of the respective material. The resistance dose D_{Rd} is therefore defined as:

$$D_{Rd} = D_{crit} \cdot k_{wa} \cdot k_{inh} \tag{2.5}$$

D_{crit}	critical dose corresponding to decay rating 1 (slight attack) according to EN 252 (2015)
k_{wa}	factor accounting for the wetting ability of the tested material [-], relative to the reference Norway spruce
k_{inh}	factor accounting for the inherent protective properties of the tested material against decay [-], relative to the reference Norway spruce

D_{crit} was evaluated for Scots pine sapwood and Douglas fir heartwood according to Isaksson et al. (2013). The critical dose can be considered to correspond to decay rating 1 according to EN 252 (2015). Differences between species and/or treatments can be accounted for by defining differences in moisture uptake and decay inhibiting properties. The variability found in tests is significant but the critical dose can be estimated to be around 325 days under favourable conditions for fungal decay (Isaksson et al. 2013). It should be noted, however, that the occurrence of brown rot in some cases can lead to significantly lower values.

The factors k_{wa} and k_{inh} can be estimated from testing. This is described in Annexe II where results from Meyer-Veltrup et al. (2016) for a number of natural wood species and some treated wood products are summarized.

2.4.2 Material resistance for selected materials commonly used in bridge construction

Material resistance (D_{Rd}) values of selected species and treated materials are given in Table 2.6. Given the same exposure, the column to the right expresses how many dose days more or less a certain material needs to reach decay rating 1 compared to Norway spruce.

The values in Table 2.6 are rounded values based on the test results presented in Annex II, see also Meyer-Veltrup et al. (2016). For preservative treated materials the factors are based on more subjective estimates indirectly supported by general experience from field tests, see e.g. Isaksson et al. (2015). All values should be interpreted as mean values. Necessary safety margins accounting for uncertainties are considered via the calibration factor c_a, see Sections 2.3.1 and 2.7.

For materials and treatments not included in table 2.6 estimates of resistance can be based on the information given in Annexe II.

Table 2.6. Material resistance dose D_{Rd} (design value)

Wood species	**D_{Rd} (days)**	**Relative D_{Rd} (reference: Norway spruce)**
Norway spruce (*Picea abies*)	325	1.0
Scots pine sapwood (*Pinus sylvestris*)	300	0.9
Scots pine heartwood (*Pinus sylvestris*)	850	2.6
European larch heartwood (*Larix decidua*)	1900	5.8
Douglas fir heartwood (*Pseudosuga menziesii*)	1700	5.2
Preservative-treated wood NTR AB[1]	1700	*5.2*
Preservative-treated wood NTR A[2]	2600	8.0

[1] Accepted for use class 3.2 according to EN 335 (2013)
[2] Accepted for use class 4 according to EN 335 (2013)

2.5 Estimation of service life

The expected service life of the member or detail considered can be calculated as

$$\text{Expected service life} = \frac{D_{Rd}}{D_{Ed}}(years)$$

where

D_{Rd} = design resistance (in dose days) for the chosen material, which is determined according to Section 2.4.
$D_{Ed} = D_{Ek} \cdot \gamma_d$ with
D_{Ek} = characteristic annual exposure (in dose days per year), which is determined according to Section 2.3
γ_d = severity factor, see Section 2.2.

The expected service life can now be compared to the required service life, see Section 2.2. The overall reliability of the methodology is verified against reality checks described in Section 2.7 and Annexe III.

2.6 Risk assessment for water protected elements and details

This section gives some general guidelines on how to deal with the risk of decay in cases where structural elements or details are protected from rain exposure. The background is a number of cases where damage has been reported in protected bridge components due to leaks, often resulting from failure of the protective system, see Pousette & Fjellström (2016). Since protective systems are often used as substitutes to preservative treatment, failure of the protective system can lead to rather quick decay progression. Therefore, the engineer should consider the risks related to leaks with potential effects on durability. Protective systems considered can consist of non-loadbearing elements (e.g. wood panels or steel sheets) designed specifically to protect main components as well as sheltering from above by other structural elements (e.g. bridge deck with water tight membrane).

A leak in the water barrier, due to either error in design, execution or maintenance, will cause local wetting of a timber component. If the leak is not located and fixed, the wood will start to decay after a certain time, depending on the possibility for leaking water to dry out between rain events. In situations where the decay damage is not located and repaired, deterioration will progress over time to a point where the structural integrity of the component is affected. Figure 2.3 provides an overview over the events.

There are several mitigation strategies to reduce the consequences related to leaks. Here the following three are considered: (1) to reduce the risk of leak, (2) to find and fix the leak before decay starts and (3) to repair the decay damage before component fails. The simple flow chart in Figure 2.11 can be used to identify suitable measures.

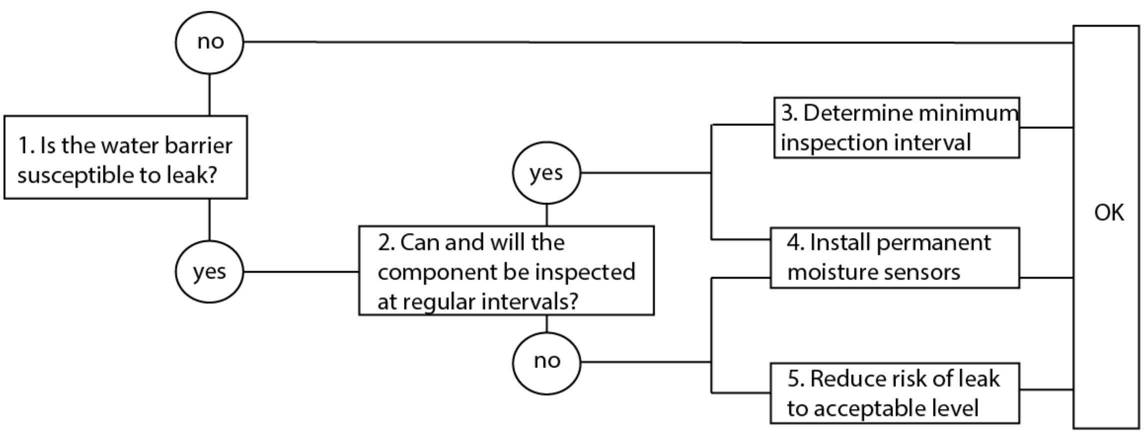

Figure 2.11 – Strategies to reduce the risk of decay related consequences when using structural protection.

The questions and mitigation measures displayed in Figure 2.11 are discussed below.

1) *Is the water barrier susceptible to leak?*

It is up to the designer to determine if a leak in the water barrier is plausible. The answer to this question is in most cases yes, but the probability of leaks occurring varies with design, detailing and quality control during construction. A water proof membrane in a timber deck may fail although with low probability if the installation is made in a correct way. Leakage through metal sheeting or timber cladding designed specifically to protect the component from water is also generally plausible. If the designer decides to disregard the risk of leakage, it should be substantiated by documented experience from practice.

2) *Can and will the component be inspected with regular intervals?*

Since the probability of leakage usually cannot be neglected, regular inspections are generally important. The designer should consider the the question whether a leakage can be detected or not and if a component can be inspected with reasonable effort or not? If risk of leakage can not be disregarded the designer should specify the need for regular inspections as a condition for the design to be feasible.

3) *Determine minimum inspection interval*

The maximum time between inspections should not exceed the service life which could be expected if the protection system fails or leak occurs. To estimate this, the methodology described in Sections 2.3-2.5 can be used. The following sequence can be applied in the assessment.

- Assume as an accidental event that the water barrier is leaking and provides no sheltering effect.
- Estimate the service life as described in Sections 2.3-2.5**.** The estimated service life then represents the time from start of the leakage to achieve decay rating 1 according to EN 252 (2015).
- Check the condition of the bridge at regular intervals. The maximum time between inspections should not exceed the service life given that leakage have occured.

This strategy will provide a reasonable safety against failure even if an existing leakage problem is not detected in the inspection. When decay reaches level 1 it can usually be seen visually during an inspection. Even in the worst case scenario when decay is initiated just after the inspection occasion, the problem can normally be dealt with at the next inspection occasion, since the time from initiation of decay until severe decay (say decay level 3) have been developed is of the same order of magnitude as the time needed to achieve decay level 1.

4) *Install permanent moisture sensors*

Finding a leak during an inspection can be difficult, especially if the inspection does not coincide with a rain event. Health monitoring using continuous moisture measurements have been used with some success and provides an efficient way to ensure good durability in high risk locations such as abutments or critical details. However, covering larger areas with monitoring (e.g. the whole area of a beam or a deck) is difficult.

5) *Reduce the risk of leak to acceptable level*

When inspection or monitoring of a component is not a viable option, measures should be taken to reduce the risk of a leak in the water barrier. Strict quality control of the construction work and of the finished bridge as well as third-party review of design solutions can be used to reduce the risk of errors.

2.7 Calibration factor c_a and verification by reality checks

All elements in the service life design described so far are mainly expressed in relative terms. The question is whether the method will give an adequate safety margin against non-performance. The only possible approach at the present level of knowledge is to check if the system will give reasonable results in accordance with generally accepted and known experience. For this reason, verification of the guideline against a limited number of reality checks has been made as described in Annexe III. Each reality check consists of a case from practice, for which the guideline is applied and where the real performance is known. Based on these reality checks and subjective estimates of uncertainties of various elements in the design method, the calibration factor was taken as

$$c_a = 1,4$$

The main motives behind this choice are:

- This value seems to give an adequate safety margin compared with the observed performance in the reality checks in annexe III.
- A high safety margin is motivated for timber bridges considering the consequences if load-bearing elements should fail.
- The reference value of material resistance for spruce given in Table 2.6 may in some cases be overestimated since the occurrence of brown rot can lead to lower values.

General conclusions from the reality checks, described in annexe III is that untreated spruce used without weather protection, can be expected to have a very limited service life, usually of the order of a few years. This is predicted with good accuracy by the design tool.

For chemically treated wood, long service life seems to be possible even in case of poor detailing. The reality checks performed indicate that the design tool is conservative for properly treated wood, even if uncertainties remain due to lack of information about the treatment method used for the bridges investigated in the reality checks.

2.8 References, chapter 2

Bornemann T, Brischke C, Lück J-M (2012). *Comparative studies on the moisture performance and durability of wooden facades*. Proceedings IRG annual meeting 2012. IRG/WP 12-20492. The International Research Group on Wood Protection.

Brischke C (2007*) Investigation of decay influencing factors for service life prediction of exposed wooden components*. Doctoral thesis, University of Hamburg. http://ediss.sub.uni-hamburg.de/volltexte/2007/3515/.

CEN/TS 15083-1 (2005) Durability of wood and wood-based products - Determination of the natural durability of solid wood against wood-destroying fungi, test methods - Part 1: Basidiomycetes. CEN (European committee for standardization), Brussels, Belgium.

CEN/TS 15083-2 (2005) Durability of wood and wood-based products - Determination of the natural durability of solid wood against wood-destroying fungi, test methods - Part 2: Soft rotting micro-fungi. EN (European committee for standardization), Brussels, Belgium.

EN 113 (1996) Wood preservatives - Method of test for determining the protective effectiveness against wood destroying basidiomycetes - Determination of the toxic values. CEN (European committee for standardization), Brussels, Belgium.

EN 1990 (2002). *Basis of structural design*. European Committee for Standardisation, Brussels.

EN 1995-1-1 (2004). *Design of timber structures –Part 1-1: General – Common rules and rules for buildings*. European Committee for Standardisation, Brussels.

EN 1995-2 (2004). *Design of timber structures - Part 2: Bridges*. European Committee for Standardisation, Brussels.

EN 252 (2015). *Wood preservatives. Field test methods for determining the relative protective effectiveness in ground contact.* European Committee for Standardisation. Brussels.

EN 335 (2013). *Durability of wood and wood-based products – Use classes: Definitions, application to solid wood and wood-based products*. European Committee for Standardisation. Brussels

EN 460 (1994). Durability of wood and wood-based products – Natural durability of solid wood – guide to the durability requirements for wood to be used in hazard classes. European Committee for Standardisation. Brussels

ENV 807 (2001) Wood preservatives - Determination of the effectiveness against soft rotting micro-fungi and other soil inhabiting micro-organisms. CEN (European committee for standardization), Brussels, Belgium.

Isaksson T, Brischke C, Thelandersson S (2013) Development of decay performance models for outdoor timber structures. Materials and Structures 46, 1209-1225.

Isaksson T, Thelandersson S, Jermer J, Brischke C (2015). *Service life of wood in outdoor above ground applications: Engineering design guideline – Background document*. Report TVBK-3067. Div. of Structural Engineering Lund University, Sweden. Can be downloaded at www.kstr.lth.se

Just A., Gustafsson A., Pousette A., Just E., Tuhkanen E.,Fjellström P.A. (2017). Wooden bridges in Nordic countries: Resistance reearch analysis with proposals. SP report 4P05308, Skellefteå/Tallinn.

Meteonorm (2015). *Global Meteorological Database for Engineers. Planners and Education*. http://www.meteonorm.com/ METEOTEST.

Meyer-Veltrup L, Brischke C, Alfredsen G, Humar M, Flæte P-O, Isaksson T, Larsson Brelid P, Westin M, Jermer J (2016) The combined effect of wetting ability and durability on outdoor performance of wood – development and verification of a new prediction approach. Wood Science and Technology. Submitted for publication.

Niklewski J, Fredriksson M, Isaksson T (2016a) Moisture content prediction of rain-exposed wood: Test and evaluation of a simple numerical model for durability applications. Building and Environment 97, 126-136.

Niklewski J, Frühwald-Hansson E, Brischke C, Kavurmaci D (2016b). *Development of decay hazard maps based on decay prediction models.* Proceedings of 47th IRG annual meeting 2016. IRG/WP 16-20588. The International Research Group on Wood Protection, Lisbon, Portugal.

Niklewski J, Frühwald Hansson E, Pousette A, Fjällström P-A (2016c) Durability of rain-exposed timber bridge joints and components. Proceedings of WCTE World Conference on Timber Engineering, Vienna, Austria.

Pousette A., Fjellström P-A. (2016). Experiences from timber bridge inspections in Sweden – examples of influences of moisture. SP Report 2016:45, Skellefteå, Sweden.

prEN 16818 (2015) Durability of wood and wood-based products - Moisture dynamics of wood and wood-based products. CEN (European committee for standardization), Brussels, Belgium

SETRA (2006). *Technical Guide. Timber Bridges- How to ensure their durability.* Service d´Ètudes techniques des routes et autoroutes. France.

Suttie E, Englund F, Viitanen H, Thelandersson S, Jermer J, Grüll G (2011). *Proforma and guidance document for performance inspection of exterior wood cladding and decking*. BRE Report 274243-2011.

Van Acker J, De Windt I, Li W, Van den Bulcke J (2014) Critical parameters on moisture dynamics in relation to time of wetness as factor in service life prediction. Stockholm: International Research Group on Wood Protection, IRG/WP/14-20555.

Annex I – Grading of timber bridge details -examples

The pictures below show bridge details and corresponding values for the factor k_{E4}

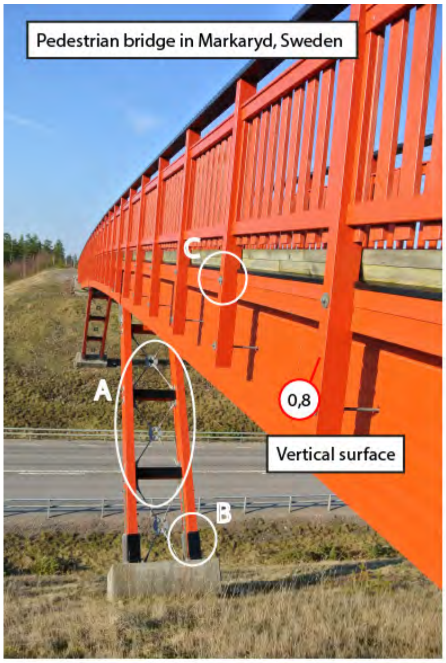

Annexe II: Wood material resistance – background

II.1. General methodology

The approach in the guideline aimed at defining material resistance is based on the combined effect of wetting ability and durability for service life prediction of wood exposed above ground. Therefore, a tool was sought to provide wetting ability and durability data for a comprehensive engineering design and performance concept.

Various standardised and non-standardised methods for determining the durability and wetting ability of wood have been reported (e. g. Van Acker et al. 2014), but no guidance for utilising them is so far provided by European standards. Furthermore, a feasible set of test methods is not yet commonly accepted, but a pre-standard is under consideration, prEN 16818 (2015). Within this guideline wetting ability was determined on the base of different short and medium term water uptake and release tests (Meyer-Veltrup et al. 2016).

II.2 General procedure

The resistance of different wood species and treatments of wood is primarily dependent on the degree of protection against fungal decay (durability), but also on the wetting ability of the respective material. The resistance dose D_{Rd} is therefore defined as:

$$D_{Rd} = D_{crit} \cdot k_{wa} \cdot k_{inh} \qquad \text{(II.1)}$$

D_{crit}	critical dose corresponding to decay rating 1 (slight attack) according to EN 252 (2015)
k_{wa}	factor accounting for the wetting ability of the tested material [-], relative to the reference Norway spruce
k_{inh}	factor accounting for the inherent protective properties of the tested material against decay [-], relative to the reference Norway spruce

D_{crit} was evaluated for Scots pine sapwood and Douglas fir heartwood according to Isaksson et al. (2013). It was found that the critical dose corresponding to decay rating 1 according to EN 252 (2015) can be seen as more or less independent from the wood species. Instead, differences between species and/or treatments can be accounted for by defining differences in moisture uptake and decay inhibiting properties. For the two wood species the critical dose was found to be around 325 days with favourable conditions for fungal decay (Isaksson et al. 2013). This critical dose can be determined for example by outdoor exposure of double-layer tests (Brischke 2007).

II.3 Wetting ability k_{wa}

Differences in moisture characteristics of different species and treatments influence the moisture content and consequently also the durability of the material. Norway spruce is used in this guideline as a reference material to identify the critical dose D_{crit}, see also Isaksson et al (2013). The critical dose, given the same climatic exposure, will not be reached at the same time for other materials. Refractory species such as Douglas fir heartwood have a lower water uptake than more permeable species such as Scots pine sapwood which means that the critical dose will be reached first by Scots pine sapwood. The effect of differences in water uptake is accounted for by adjusting the critical dose D_{crit} with a factor k_{wa}. In order to reflect different relevant mechanisms responsible for moisture dynamics of wood under real in-service situations the four following test procedures were applied to determine k_{wa}:

- Liquid water uptake of oven-dried wood by submersion during 24 h ($W24_{submersion}$)
- Water vapour uptake of oven-dried wood in water saturated atmosphere (100 % RH) during 24 h ($W24_{100\ \%\ RH}$)
- Water release (desorption) of fibre saturated wood at 0 % RH during 24 h ($W24_{0\ \%\ RH}$)
- Capillary water uptake of wood with end-grain in contact with liquid water during 200 s (*CWU*)

The resulting factors describing the wetting ability (k_{wa}) are given in Table II.1 for selected materials according to Meyer-Veltrup et al. (2016).

II.4 Material-inherent resistance k_{inh}

Differences in inherent resistance of different species and treatments influence the durability of the material. To evaluate relative protective effects of different materials and treatments k_{inh} factors were calculated as follows.

$$k_{inh} = \frac{1}{2}\left[\frac{\sum_{i=1}^{n_i} k_{inh,soil,i}}{n_i} + \frac{\sum_{j=1}^{n_j} k_{inh,non-soil,j}}{n_j}\right] \tag{II.2}$$

k_{inh}	factor accounting for the inherent protective properties of the material against decay [-]
$k_{inh,\ soil,\ i}$	factor accounting for the inherent protective properties of the material against decay in test i with soil contact [-]
$k_{inh,\ non\text{-}soil,\ j}$	factor accounting for the inherent protective properties of the material against decay in test j without soil contact [-]
n_i , n_j	number of tests

In order to reflect different types of exposure and types of decay results from tests with and without soil contact, i.e. with and without soft rot attack, the following factors were used:

- $k_{inh,\ non\text{-}soil}$:
  - Resistance tests with different Basidiomycete monocultures (brown and white rot) according to EN 113 (1996) and/or CEN/TS 15083-1 (2005)
- $k_{inh,\ soil}$:
  - Resistance tests against soft rot and other soil inhabiting microorganisms according to ENV 807 (2001) and/or CEN/TS 15083-2 (2005)
  - Resistance field tests with ground contact (“graveyard tests”) according to EN 252 (2015)

To avoid unrealistically high relative values (factors) a threshold was set on the base of results from above ground field tests with untreated wood (Meyer-Veltrup et al. 2016) for both factors leaving the values in the following range: $0 < k_{wa} \leq 5$ and $0 < k_{inh} \leq 5$. This threshold may be reviewed in the future.

The resulting factors describing the inherent protective properties (k_{inh}) are given in Table II.2 for selected materials according to Meyer-Veltrup et al. (2016).

Table II.1. The factor k_{wa} accounts for the wetting ability of different wood species and wood-based materials (Meyer-Veltrup et al. 2016).

Wood species	Botanical name	W24 submersion	W24 100 % RH	W24 0 % RH	CWU	Mean
				k_{wa} [-]		
Hardwoods						
Norway maple	*Acer platanoides*	0.94	1.18	0.99	0.37	0.87
Aspen	*Populus tremula*	0.91	1.13	1.09	0.65	0.95
Birch	*Betula pendula*	0.84	1.16	1.09	0.36	0.86
English oak	*Quercus robur*	1.19	1.44	0.82	0.67	1.03
Beech	*Fagus sylvatica*	0.92	1.15	0.92	0.31	0.82
Teak	*Tectona grandis*	2.38	2.90	0.88	1.28	1.86
Black locust	*Robinia pseudoacacia*	2.33	2.11	1.60	1.29	1.83
Softwoods						
Norway spruce	*Picea abies*	1.00	1.00	1.00	1.00	1.00
Southern Yellow Pine (SYP)	*Pinus* spp.	0.89	1.01	1.45	0.58	0.98
Scots pine heart	*Pinus sylvestris*	0.83	1.10	0.92	1.19	1.01
Scots pine sap	*Pinus sylvestris*	0.59	1.03	1.01	0.28	0.73
Western Red Cedar (WRC)	*Thuja plicata*	1.11	1.61	0.72	0.27	0.93
Juniper	*Juniperus communis*	1.30	1.43	0.77	1.20	1.17
Siberian larch	*Larix sibirica*	1.04	1.30	0.91	0.46	0.93
European larch	*Larix decidua*	1.67	1.83	0.94	0.72	1.29
Douglas fir	*Pseudotsuga menziesii*	1.61	1.57	0.87	0.54	1.15
Modified materials						
Oil-heat treated Spruce	*Picea abies*	1.99	2.91	1.67	1.60	1.73
Oil-heat treated Ash	*Fraxinus excelsior*	1.73	2.35	1.95	0.88	2.04
Thermally modified Scots pine	*Pinus sylvestris*	1.18	2.38	2.52	1.39	1.87
Acetylated SYP (acetyl content: 19 %)[1]	*Pinus* spp.	1.32	2.86	3.20	0.76	2.03
Acetylated Radiata pine (acetyl content: 20 %)[1]	*Pinus radiata*	1.33	2.84	3.45	1.15	2.19
Furfurylated SYP (WPG: 50 %)[1]	*Pinus* spp.	1.73	2.23	2.49	1.45	1.97
Furfurylated Scots pine (WPG: 40 %)[1]	*Pinus sylvestris*	2.79	3.30	4.40	1.54	3.01

[1]Weight percent gain of furfurylated wood and acetyl content of acetylated wood according to manufacturer's data.

Table II.2. The factor k_{inh} accounts for the protective inherent resistance of different wood species and wood-based materials (Meyer-Veltrup et al. 2016).

Wood species	Botanical name	Non-soil[2]	Soil[3]	mean
			k_{inh} [-]	
Hardwoods				
Norway maple	*Acer platanoides*	0.88	1.56	1.22
Aspen	*Populus tremula*	0.80	1.62	1.21
Birch	*Betula pendula*	0.72	1.30	1.01
English oak	*Quercus robur*	5.00	5.00	5.00
Beech	*Fagus sylvatica*	1.01	1.32	1.17
Teak	*Tectona grandis*	5.00	5.00	5.00
Black locust	*Robinia pseudoacacia*	5.00	2.72	3.86
Softwoods				
Norway spruce	*Picea abies*	1.00	1.00	1.00
Southern Yellow Pine (SYP)	*Pinus spp.*	3.69	0.87	2.28
Scots pine heart	*Pinus sylvestris*	2.85	2.36	2.61
Scots pine sap	*Pinus sylvestris*	0.80	1.76	1.28
Western Red Cedar (WRC)	*Thuja plicata*	5.00	1.97	3.48
Juniper	*Juniperus communis*	5.00	5.00	5.00
Siberian larch	*Larix sibirica*	2.52	5.00	3.76
European larch	*Larix decidua*	4.13	5.00	4.56
Douglas fir	*Pseudotsuga menziesii*	4.20	5.00	4.60
Modified materials				
Oil-heat treated Spruce	*Picea abies*	5.00	4.58	4.79
Oil-heat treated Ash	*Fraxinus excelsior*	5.00	5.00	5.00
Thermally modified Scots pine	*Pinus sylvestris*	5.00	4.40	4.70
Acetylated SYP (acetyl content: 19 %)[1]	*Pinus* spp.	5.00	5.00	5.00
Acetylated Radiata pine (acetyl content: 20 %)[1]	*Pinus radiata*	5.00	3.75	4.38
Furfurylated SYP (WPG: 50 %)[1]	*Pinus* spp.	4.51	5.00	4.75
Furfurylated Scots pine (WPG: 40 %)[1]	*Pinus sylvestris*	5.00	5.00	5.00

[1]Weight percent gain of furfurylated wood and acetyl content of acetylated wood according to manufacturer's data.

[2]mean value of resistance tests with different Basidiomycete monocultures (brown and white rot) according to EN 113 (1996) and/or CEN/TS 15083-1 (2005)

[3]mean value of resistance tests against soft rot and other soil inhabiting microorganisms according to ENV 807 (2001) and/or CEN/TS 15083-2 (2005) and resistance field tests with ground contact ("graveyard tests") according to EN 252 (2015)

II.5 Material resistance

Based on the determined values for k_{wa} and k_{inh} the material resistance D_{Rd} can be calculated. The resulting values for the different materials and species as well as the relative resistance dose, when using Norway spruce as reference, are given in Table II.3. Given the same exposure, the relative D_{Rd} expresses how many days more or less a certain material needs to reach decay rating 1 (slight attack) compared to Norway spruce.

Table II.3. The material resistance D_{Rd} for different species, calculated from k_{wa} (Table 2.5), k_{inh} (Table 2.6) and a critical dose D_{crit}=325 days.

Wood species	Botanical name	D_{Rd} [d]	Relative D_{Rd} [2] [-]
Hardwoods			
Norway maple	*Acer platanoides*	344	1.06
Aspen	*Populus tremula*	373	1.15
Birch	*Betula pendula*	284	0.87
English oak	*Quercus robur*	1670	5.14
Beech	*Fagus sylvatica*	313	0.96
Teak	*Tectona grandis*	3027	9.32
Black locust	*Robinia pseudoacacia*	2298	7.07
Softwoods			
Norway spruce	*Picea abies*	325	1.00
Southern Yellow Pine (SYP)	*Pinus* spp.	727	2.24
Scots pine heart	*Pinus sylvestris*	856	2.63
Scots pine sap	*Pinus sylvestris*	304	0.93
Western Red Cedar (WRC)	*Thuja plicata*	1049	3.23
Juniper	*Juniperus communis*	1909	5.87
Siberian larch	*Larix sibirica*	1136	3.50
European larch	*Larix decidua*	1914	5.89
Douglas fir	*Pseudotsuga menziesii*	1716	5.28
Modified materials			
Oil-heat treated Spruce	*Picea abies*	2691	8.28
Oil-haet treated Ash	*Fraxinus excelsior*	3314	10.20
Thermally modified Scots pine	*Pinus sylvestris*	2850	8.77
Acetylated SYP (acetyl content: 19 %)[1]	*Pinus* spp.	3305	10.17
Acetylated Radiata pine (acetyl content: 20 %)[1]	*Pinus radiata*	3119	9.60
Furfurylated SYP (WPG: 50 %)[1]	*Pinus* spp.	3049	9.38
Furfurylated Scots pine (WPG: 40 %)[1]	*Pinus sylvestris*	4886	15.03

[1]Weight percent gain of furfurylated wood and acetyl content of acetylated wood according to manufacturer's data.

[2]Relative to Norway spruce

Annexe III. Verification by reality checks

III.1 General

The general format of the guideline was adopted from an earlier project named WoodBuild described in Isaksson et al (2015). Reality checks collected in the project Woodexter and documented in Suttie et al (2011) were used to verify the methodology. 34 cases of claddings or deckings from Sweden were investigated. The design tool delivered correct predictions of service life for 30 cases (88 %). The remaining 4 cases gave conservative predictions, i.e. the service life was underestimated by the method.

A number of cases for timber bridges collected in the DURA-TB project are described below and compared to the output of the design tool, given that the calibration factor c_a = 1,4.

III.2 Swedish bridge cases

Pousette & Fjellström (2016) describe 9 cases from bridge inspections in Sweden as a part of the DURA-TB project. In one of these cases the age of the bridge at inspection was only 3 years, which makes it unsuitable as a reality check. Service lives for the remaining 8 cases estimated with the present method are listed in Table III.1.

Table III.1. Estimates of service life for 8 Swedish cases described in Pousette et al (2016).

Case	Description	γ_d	D_{E0}	k_{E1}	k_{E2}	k_{E3}	k_{E4}	D_{Ed}*	*Material*	D_{Rd}	*Estimated service life (y)*
S1	Railing post Bjurholm	0,8	20	1,0	1	2	2	84,6	Spruce	325	3,6
S2	Railing post Ekerö	0,8	32	1,0	1	1	1,5	53,8	Spruce	325	6,0
S3	Railing panel Vaxholm	0,8	32	0,9	1	1	1,5	48,4	Pine NTR A	2600	53,7
S4	Railing panel Borås	0,8	37	1,0	1	1	1,5	62,2	Spruce	325	5,2
S5	SLTD[1] Skellefteå	1	20	0,9	1	1	1,25	31,5	Pine NTR A	2600	82,5
S6	SLTD[1] Lumnäs	1	20	1,0	1	1	1,5	42,0	Spruce	325	7,7
S7	SLTD[1] Södertälje	1	32	1,0	1	1	1,25	56,0	Spruce	325	5,8
S8	SLTD[1] Hädanberg	1	20	0,9	1	1	1,0	25,2	Spruce	325	12,9

*Calculated from Eq. (2.2) with c_a =1,4

[1] SLTD= Stress laminated timber deck.

Information about the actual status of these bridges at the time of inspection is available, and is compared with the predicted service lives in Table III.2. For all 8 cases, the observations at the time of inspection did not contradict the prediction by the design tool. However the strength of evidence was different between the cases, e.g. when the age of inspection differs significantly from the predicted service life. A subjective estimate of the strength of evidence is given in the last column of Table III.2. This estimate also to some extent takes into account the extent of decay observed in the inspection. The strength of evidence can be regarded as high in 4 of the 8 cases.

Table III.2. Comparison between predicted service life (Table III.1) and observations from inspections.

Case	Material	Predicted service life (y)	Age at inspection (y)	Decay observed	Correct prediction ?	Strength of evidence
S1	Spruce	3,6	6	Yes	Yes	High
S2	Spruce	6,0	7	Yes	Yes	High
S3	NTR A	53,7	19	No	Yes	Medium
S4	Spruce	5,2	11	Yes	Yes	High
S5	NTR A	82,5	20	No	Yes	Medium
S6	Spruce	7,7	12	Yes	Yes	High
S7	Spruce	5,8	16	Yes	Yes	Medium
S8	Spruce	12,9	5	No	Yes	Weak

III.3 Bridge cases from Estonia

Just et al (2017) describe a number of cases from inspections of timber bridges in Estonia performed in 2014. 11 cases suitable for reality checks were selected from this investigation. Service lives for these cases estimated with the present method are listed in Table III.3.

Table III.3. Estimates of service life for bridge cases from Estonia described in Just et al (2017).

Case	Description	γ_d	D_{E0}	k_{E1}	k_{E2}	k_{E3}	k_{E4}	D_{Ed}*	*Material*	D_{Rd}	*Estimated service life (y)*
E1	Footbridge Vaida	1	32	1,0	1	1	1,5	67,2	Spruce	325	4,8
E2	Footbridge Reopalu	1	32	1,0	1	1	1,5	67,2	Pine NTR AB[1]	1700	25
E3	Tehvandi Beam support	1	32	1,0	1	2	2	179,2	Pine NTR AB[1]	1700	9,5
E4	Tehvandi Railing	0,8	32	1,0	1	1	1,5	53,8	Spruce	325	6,0
E5	Beam support Keisripalu	1	32	1,0	1	2	2	179,2	Pine NTR AB[1]	1700	9,5
E6	Arches Törva	1	32	1,0	1	1	1,25	56	Pine	860	15
E7	Arch/beams Merirahu	1	32	1,0	1	1	1	44,8	Spruce	325	7,3
E8	Deck Lucati	1	32	1,0	1	1	1,5	67,2	Spruce	325	4,8
E9	Arch Lucati	1	32	1,0	1	1	1,5	67,2	Spruce	325	4,8
E10	Beam support Tagavere	1	32	1,0	1	2	2	179,2	Pine NTR AB[1]	1700	9,5
E11	Railing posts Kärdla	0,8	32	1,0	1	2	2	143,4	Spruce	325	2,3

*Calculated from Eq. (2.2) with c_a =1,4

[1]No information about the type of chemical impregnation is available in the documentation. For this reason quality corresponding to NTR AB has been assumed here.

Information about the actual status of these bridge components at the time of inspection is compared with predicted service lives in Table III.4. For 8 of the 11 cases, the observations at the time of inspection did not contradict the prediction by the design tool. For 3 cases (E3,E5 and E10) the design tool conservatively underestimates the service life. All these 3 cases concern preservative treated pine, where the type of treatment has been conservatively assumed to be equivalent to NTR AB.

The strength of evidence was regarded as high in 7 of the 11 cases. In these cases the material investigated is spruce. For 4 of the cases, all with treated wood, there is considerable uncertainty mainly due to lack of information about the quality of the treatment used.

Table III.4. Comparison between predicted service life (Table III.3) and observations from inspections.

Case	Material	Predicted service life (y)	Age at in-spection (y)	Decay observed	Correct prediction?	Strength of evidence
E1	Spruce	4,8	6	Yes	Yes	High
E2	Treated	25	6	No	Yes	Weak
E3	Treated	9,5	10	No	No	Weak
E4	Spruce	6,0	10	Yes	Yes	High
E5	Treated	9,5	11	No	No	Weak
E6	Pine	15	26	Yes	Yes	High
E7	Spruce	7,3	13	Yes	Yes	High
E8	Spruce	4,8	9	Yes	Yes	High
E9	Spruce	4,8	9	Yes	Yes	High
E10	Treated	9,5	16	No	No	Weak
E11	Spruce	2,3	7	Yes	Yes	High

3 Design concepts for durable timber bridges

3.1 Types of bridges and structural systems

Bridges are usually categorized by their main support system. In terms of span length these systems are:

- Plates
- Beams
- Trusses
- Arches
- Cables (cable stayed or suspension)

Beams and plates are well suited for short span lengths and can easily be combined into ribbed decks. For longer span other structural systems such as trusses and arches are used together with timber, concrete or steel decks. Cable stayed and suspension bridges are sometimes used, for long pedestrian bridges, but should also be considered for road bridges.

3.1.1 Plate bridges

The plate or slab constitutes not only the support structure of the bridge, but also its deck. A wooden slab type bridge can be built by screw-laminating solid wood planks, but it is not much used. Previously, also nail- or spike-laminating planks have been tried in some countries. Usually, the slab bridge or deck-plate is produced by stress-laminating lamellas in the longitudinal direction of the bridge by pre-stressing rods. The lamellas can be stressed together, either at a factory or on site, depending on the bridge size. The deck can be designed with butt joints, making it possible to manufacture long continuous bridge deck. Normally, no special wind bracing is needed. These wooden decks are usually provided with a water-tight layer and pavement surface, which protects the wood against moisture from above. Together with a cladding along the edges, this gives the bearing structure a good weather protection which ensures low maintenance costs and long life. Stress-laminated timber slabs can provide light decks for truss and arch bridges.

Figure 3.1 Stress-laminated plate bridge, span 17 m, Lövösundet, Holmsund, Sweden

3.1.2 **Beam bridges**

Short span bridges are often made as simple beam-type glulam structures, as simply supported single span bridges or as multiple span bridges. The main beams span in the lengthwise direction, and depending on the deck, transverse crossbeams may be necessary. On top of the beams there is usually a transverse timber deck with a wearing layer of wooden planks added. The traditional beam bridge typically has floor beams and an open plank deck, which can be suitable for pedestrian bridges and small road bridges. An alternative to crossbeams is to use a concrete plate on top of the main beams, with shear-connectors in-between forming a composite system. However, in some cases it is preferred to avoid composite action between the wooden structure and the concrete slab due to differences in expected creep and temperature behaviour. Open timber decks give little shelter to the main beams, which should be sheltered by claddings. With a deck plate of concrete or wood on top, only the outside of the beams may need a cladding.

Figure 3.2 Beam bridge with timber deck (Täfteån, Sweden)

3.1.3 **Truss bridges**

Trusses in modern bridges are mostly made of glulam members. The truss can be placed beneath or above the carriageway. The choice depends on available free height under the carriageway, as well as on aesthetical, economical and durability considerations. The trusses are prefabricated in as large parts as possible, commonly limited by transport regulations and road obstacles. Splices in the chords are usually placed at locations suitable for assembly of the separate parts on site. Connections and splices are made of dowels in combination with slotted-in steel plates. Pedestrian truss bridges with connections and splices made with bolts are suitable for spans up to 30 m. Here, the trusses are placed on both sides of the deck and can be used to fasten handrails.

Figure 3.3 Flisa bridge, Norway, truss with longest span of 70 m. Photo: K. A. Malo

Figure 3.4 Connection with slotted-in steel plates and dowels

3.1.4 **Arch bridges**

Arches are often used in timber bridge design for longer spans. They have massive wood cross-sections or for longer spans the arches may be formed by trusses. The use of a truss arch is beneficial in order to handle the large moment actions originating from the point loads transferred from the deck by vertical hangers. A structural feature of the arch is large horizontal thrusts at the footings that can be accommodated by use of heavy foundations. For shorter bridges a tension tie can be a better and cheaper solution. Arches are sometimes stabilized in the transverse direction by bracing or frames. Three-hinge arches are often used due to transport and manufacturing reasons.

Figure 3.5 Fretheim bridge, span 38 m, with three-hinged glulam arches, stress-laminated timber deck, steel hangers, steel cross-beams and no horizontal wind truss between arches. Photo: Sweco Norway AS

3.1.5 **Design basics and loads**

There are many types of timber bridges. The type of bridge that is most suitable in each case depends on spans, free height, type of traffic, etc. Bridge design includes verifications for ultimate and serviceability limit states for combinations of actions. In Europe the requirements for design are specified in the Eurocodes, EN 1990-1999. Moreover, there are national requirements and regulations. In Europe, actions on timber bridges should be determined according to the relevant parts of Eurocode EN 1991 (CEN 1991 2002): densities, self-weight, snow loads, wind actions, thermal actions, actions during execution, accidental actions and traffic loads on bridges.

Traffic loads on bridges correspond to the impact of traffic on the bridge in vertical and horizontal direction due to vehicle weights, braking and acceleration forces, centrifugal and transverse forces, loads on footways and cycle tracks, crowd loading, etc. Timber bridges are used both as road bridges and as pedestrian bridges, which means different loads and design requirements. The load models of road traffic contain large concentrated loads (wheel loads) acting on a specified surface area and a uniformly distributed load for each lane. For pedestrian traffic there are two types of loads: a uniformly distributed load corresponding to people and crowds, and concentrated loads (wheel loads) of a service vehicle. Vibrations caused by pedestrians are important when designing timber structures, due to their light weight. Both vertical and horizontal vibrations can cause an anxiety for pedestrians on the structure.

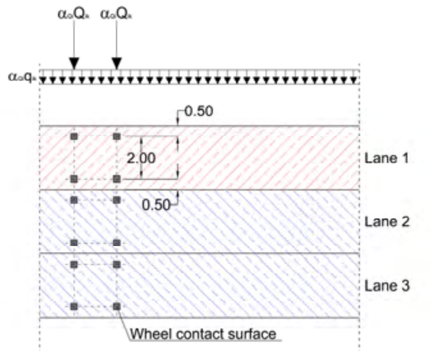

Figure 3.6 Example of traffic loads on road bridge

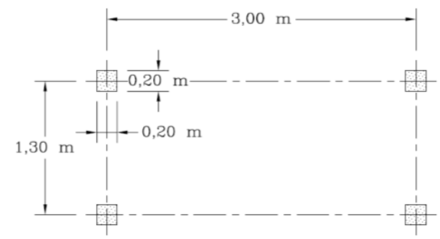

Figure 3.7 Example of wheel loads on pedestrian bridge

Pedestrian wooden bridges often have timber railings. Railings on road bridges must withstand the required impact forces of vehicles and are evaluated by full-scale crash tests according to standards. Most often, steel railings are used on wooden road bridges and the connection of the rail posts to the timber deck needs to be verified.

The design of connections in timber bridges is important for both load-bearing capacity and durability. Fasteners such as bolts, screws and dowels are mostly used. They are either axially or shear loaded. For connections with large forces, e.g. in truss bridges, steel gusset plates placed in sawn slots in the wooden members to be connected, can be used in connection with steel dowels. Steel is also used in other components of timber bridges such as cross beams and vertical hangers. Bearings and expansion joints may also be important bridge details, but usually simpler lay-outs can be used for timber bridges than for bridges in other materials. Design basics and loads can be found in Eurocode standards, whereas requirements in terms of materials and workmanship are given in national rules, which can differ quite significantly from country to country.

3.1.6 **Design loads on timber bridges**

Herein, the design is based on the Eurocodes which in turn are based on the limit state concept used in conjunction with a partial factor method. EN 1990 Basis of design (CEN 1990 2002) (commonly denoted Eurocode 0) states how the fundamental limit states shall be verified by design. For each of the two fundamental limit states, ultimate limit states (ULS) and serviceability limit state (SLS), several scenarios are defined. Eurocode 0 has guidelines as to how the actions in each scenario shall be combined by the use of partial factors giving a design value, indicated by subscript “d”, of the combined effects of the actions. The actions are given by the EN 1991-x series of standards like (CEN 1991-2 2003) Traffic load on bridges and (CEN 1991-1-4 2002) for wind action. Note that for timber bridges additional evaluations might be necessary for self-weight due to effects of moisture and use of preservatives. Furthermore, moisture might give considerable dimensional changes which need to be considered, as do temperature effects.

3.1.7 **Design values**

Eurocode 5 Part 1-1 Design of timber structures (CEN 1995 2004) and Part 2 Bridges (CEN 1995-2 2004) describe the principles and requirements for safety, serviceability and durability of timber bridges. The mechanical behaviour of wooden materials shows considerable time and moisture dependencies. Long duration of the loading (DOL) decreases the measureable strength of the material significantly; this effect is accounted for in modern design codes. Wood is also a hygroscopic material, i.e. water is exchanged with the surroundings. Increase of moisture content (MC) leads, in general, to a decrease in strength and stiffness properties. In air, the moisture content (MC) and exchange of water are dependent on the relative humidity (RH). Most material properties of wood are related to standardized climatic condition (RH 65% and a temperature of 20° C) leading to approximately 12 % MC. Furthermore, standardized DOL (Duration Of Load) is used in order to have a common reference for determination of the mechanical properties.

The effects from DOL and MC cannot be neglected in design of timber structures and are taken into account in a simplified manner through the use of a modification factor k_{mod}, which in turn is dependent on the climatic conditions (MC) and the duration of the loads (DOL), applicable to the timber structure during its design life. The climatic conditions are characterized by one of the three service classes, each of which is related to the expected MC during a given design life (CEN 1995 2004). Service class 2 may be applied to timber bridges where the timber parts are properly covered and not exposed directly to rain and water, while in all other cases service class 3 should be used for timber bridges.

Any given load is associated with one of the five specified load durations, ranging from instantaneous (wind) to permanent (self-weight). Traffic loading on bridges is normally assumed to be short term loading. The design value for a strength or resistance property is calculated by

$$R_d = k_{\mathrm{mod}} \frac{R_k}{\gamma_m} \tag{0.1}$$

Recommended values for the modification factor k_{mod} and the material factor γ_m are stated in (CEN 1995 2004) and (CEN 1995-2 2004). The partial factor for material properties γ_m depends on the type of wood-based product as well as on the design problem at hand. All safety and strength properties are based on the use of the characteristic (5%) value R_k (denoted by use of subscripts *k* or *05*), while serviceability issues like deformation and vibration make use of the mean values of the material properties (subscript *mean*).

3.2 Short to medium span bridges

3.2.1 Pedestrian timber bridges

There are many variations of the short plate bridges for pedestrians. One of the most common types for small pedestrian bridges is the horizontally pre-stressed slab. It consists of horizontally placed, equally high, adjacent placed glulam beams, which are pre-stressed together by steel tendons anchored at the edges of the deck (Figure 3.8). Horizontally pre-stressed beam bridge with timber deck can is constructed similarly (Figure 3.9).

The advantage of a pre-stressed short span bridge is that the whole bridge can be finished at the factory. The bridge can then be transported to the site and installed by lifting it on supports.

Figure 3.8 Pre-stressed slab bridge

Figure 3.9 Pre-stressed beam

Short span beam bridges may usually be constructed as single span bridges. Somewhat longer spans can be achieved by using cantilevers at the ends. A span of 30 m can be reached for pedestrian bridges using simple glulam beams (Figure 3.10).

Durability of small timber bridges can be increased by protecting the beams with painting or cladding. Whole bridges may be protected by sun radiation and rain by using a roof or a shelter as shown in Figure 3.11.

Figure 3.10 Cantilever beam bridge

Figure 3.11 Timber bridge equipped with canopy

3.2.2 **Timber-Concrete Composite Bridges**

Earliest TCC bridges were built in USA in 1930s and 1940s. After the World War II, the use of composite girders spread to Australia and New Zealand. In Europe, TCC bridges were adopted in 1990s. Since then, TCC bridges have gradually been built in countries as Finland, Brazil, Portugal, Switzerland, France, Germany and Austria (Rodrigues, Dias et al. 2013). It can be roughly estimated that a few hundreds of TCC bridges are now in use around the world.

Figure 3.12 Timber-concrete bridge

Figure 3.13 Timber beam and concrete slab

The spans of existing TCC bridges are usually short, below 20 m. However, in the deck of Vihantasalmi Bridge in Finland, a span of 42 m has been reached. A review of Finnish TCC bridges has been presented by (Jutila and Salokangas 2010). More on the use of TCC bridges can be found in (Jaaranen 2016).

Two types of TCC bridge decks have been used in practice:

- Concrete slab connected to a deck plate of timber beams
- Concrete slab connected to timber beams.

The latter system is more common today.

Besides the effective composite action under vertical loading, TCC bridges have some considerable advantages compared to other types of timber deck bridges:

- The concrete deck can be used also for traffic road timber bridges.
- Water insulation layers can be realized in a similar way as in concrete slab bridges to prevent water leakages.
- The timber beams are below the deck and protected by rain and sun radiation.

The good condition of timber beams after 20 years of service can be seen in Figure 3.13.

Usually, timber members are manufactured and equipped with shear connectors in the factory, and then transported to the bridge site and lifted on supports. The concrete deck is finally cast in-situ on the bridge site.

Figure 3.14 Timber beams installed before casting of the concrete slab

Figure 3.15 Transporting a timber beam member for composite deck

During the construction and the casting of the deck, two different supporting methods can be used:

- Shored method: when the timber members are supported in the span during the construction and concrete casting.
- Un-shored method: when the timber members are un-supported during the construction of the concrete deck.

The behaviour of a TCC bridge under loading depends largely on the composite action provided by the shear connection between the two materials. The principle of a timber-concrete beam is shown in Figure 3.16.

By connecting the concrete slab to timber beam with shear connectors makes the beam behave more effective in structural sense. So the stiffness of the cantilever increase and deflection decrease.

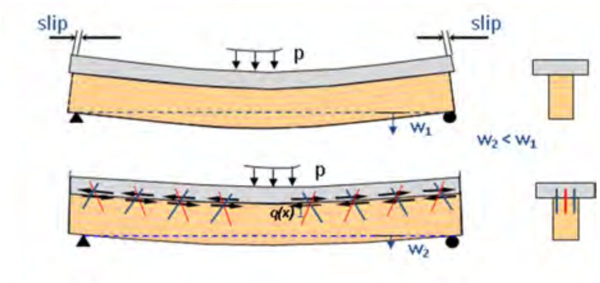

Figure 3.16 The effect of shear connectors to the slip and the deflection of the beam

The selection of the construction method has a remarkable influence on the final structural behaviour of the bridge. Bridge designers must decide which method should be used in each particular case. By using shored method, the intermediate supports of the deck are removed after that the concrete has hardened. After the removal, the deck is performing as a composite structure for all vertical loads. So, the self-weight of the superstructure starts loading the composite structure as soon as the intermediate supports are removed.

By using the un-shored method, the permanent loads, including the weight of concrete mass during the casting, load the timber members. In this case, the deck is working as composite structure only for the loads applied after the concrete has cured and hardened.

However, different stiffness and arrangements of the shear connectors have a large impact on the deformations and the stress distributions of the bridge components. By increasing the stiffness of the connectors, deformations and stresses decrease, but the forces in the connectors increase. In addition to the effects of the external loads, e.g. permanent and traffic loads, the different material behaviour of the components and the environmental variations can cause large effects. Thermal strains, shrinkage, or swelling of wooden members, due to varying moisture content, severely affect also the behaviour of the composite girder. All these phenomena cause deformations. Due to the composite action, stresses are induced in different material parts of TCC bridges.

Both material components of TCC girders (wood and concrete) display more or less time-dependent behaviours. Wood is affected not only by usual creep, but also by mechano-sorptive creep. Concrete is affected not only by creep but also by slips of connections or at the interface of the different materials. Moreover, the interaction between the components and the flexibility of the connectors introduce additional complexity on the creep behaviour of TCC structures. Creep will increase the deformations and will change the stress distribution in the structure during its whole lifetime. As previously explained, the construction method has also a strong influence on the structural behaviour of TCC bridges.

3.2.3 **Design of TCC Bridge**

The design of shear connectors suitable for TCC bridges is not covered in present Eurocodes (2017). The physical properties of connectors, like stiffness, must be obtained from other sources, e.g. from experimental test results.

3.2.3.1 Principle for Short-Term of Modelling for FE analysis

A common approach of analysing timber concrete composite floors in buildings is to use the γ-method given in the Annex B of the Eurocode EN 1995-1-1 (CEN 1995 2004). This can be applied by hand calculations. For bridges, the lateral load distribution should be defined, but the load factor approach is not given in Eurocodes. By using the lever rule and assuming rigid-diaphragms for the bridge deck one can estimate the transversal load distribution between the beams, but it may lead to erroneous solution.

Finite element (FE) model for timber concrete composite deck is suggested in Figure 3.17. By using this model, the effects of the lateral stiffness of the concrete slab, as well as flexible connectors between the slab and the timber beams, can be taken into account. The different parts of the deck are suggested to be discretized for FE analysis as follows:

- The concrete slab is modelled as grillage consisting of longitudinal and transversal concrete beams placed on the level of centre plane of the deck slab;
- The longitudinal timber beams are modelled as wooden beam elements;
- The shear connection between the concrete slab and the timber beams is modelled as a combination of connector elements and stiff separation elements.

The effective width (b_{ef}) of the longitudinal concrete beams used in the grillage model can be determined according EN 1992 (CEN 1992 2003). The centre plane of the grillage is distant a from the centreline of timber beams. A discretized FE model is shown in Figure 3.17.

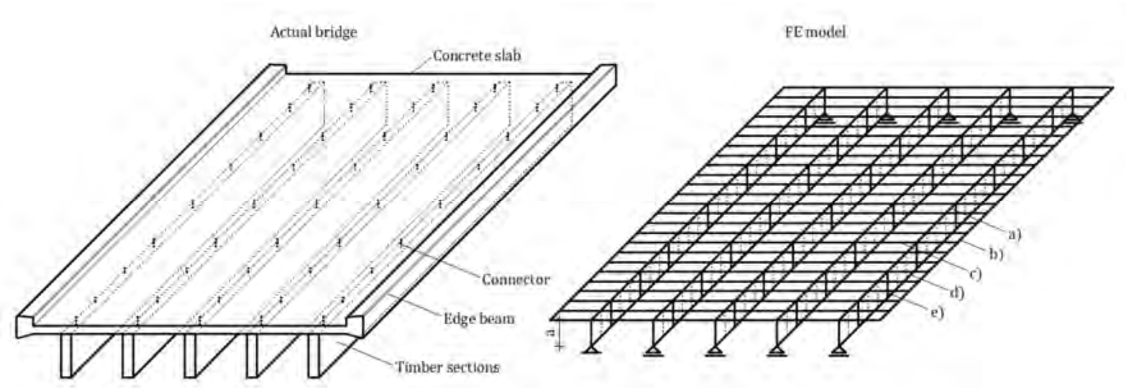

Figure 3.17 Deck model: (a) longitudinal beams in the grillage, (b) edge beams in the grillage, (c) transverse beams in the grillage, (d) timber beams and (e) connection

The connection between the timber beam and concrete slab is modelled by series flexible connectors (springs) and separations links (rigid members), see Figure 3.18.

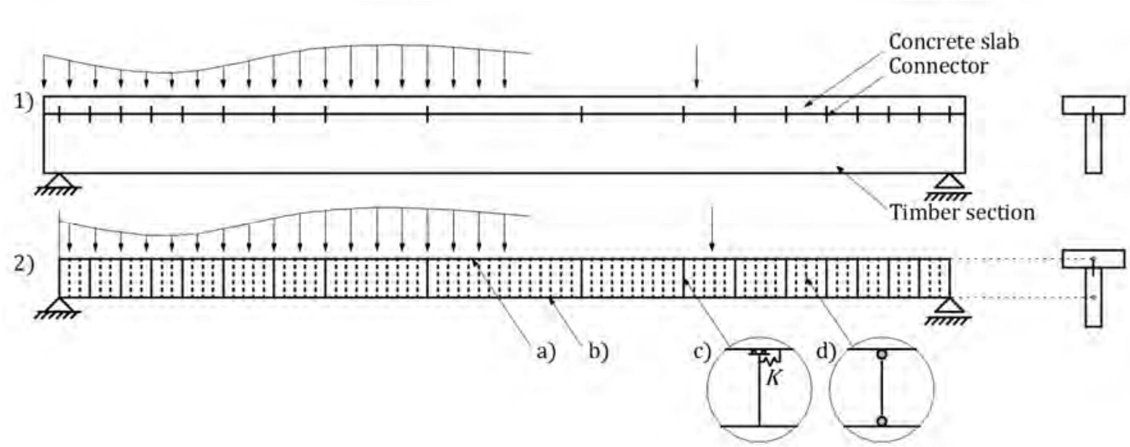

Figure 3.18 FE modelling scheme of TCC beam parts: a) concrete beam, b) timber beam, c) flexible connection member and d) rigid separation link

The connection model between the concrete slab and the timber beam c) has free rotational degree of freedom around longitudinal axis. In the transverse direction, the spring stiffness is introduced by using experimentally obtained values for slip modulus K of the actual connectors. The separation links are axially rigid pin-ended truss elements distributed along the bridge span. Rigid links are needed to guarantee a constant distance (a) between the centre plane of the concrete slab and the centre lines of timber beams.

The benefit of the presented model is that the forces and the deformations are obtained for different structural parts directly from the results of the analysis.

3.2.3.2 Method for Long-Term Analysis of TCC Bridge Deck

Time depending structures are usually analysed numerically together with incremental time step methods. However, such a tedious approach cannot be applied in practical bridge design. More simplified methods are needed to take account of the long-term behaviour. One simple method for TCC bridges has been proposed by (Fragiacomo 2006). In this approach, the total effect of the applied long-term loads is calculated as the sum of three sources:

- The effects of permanent and variable loads,
- The effects of concrete shrinkage,
- The effects of inelastic strains due to temperature and moisture content variations of wood.

The effects of the creep of concrete are taken into account by simply applying the effective modulus method. Even though the use of different material models is suggested, methods found in Eurocodes EN 1992-1-1 (CEN 1992 2003) and EN 1995-1-1 (CEN 1995 2004) could also be applied (Ceccotti 1995, Ceccotti 2003). In EN 1995-1-1 (CEN 1995 2004) only the final deformation factor is given, but for more detailed analyses intermediate duration deformation factors can be found in the literature. The effects of temperature variation should be calculated according to EN 1991-1-5 (CEN 1991 2003).

How to take account of the effects of moisture content (MC) variation is not considered in the current Eurocodes. Instead, some local guidelines are still available. The most relevant existing method is based on the assumption that the shored construction method is used (Fragiacomo 2006).

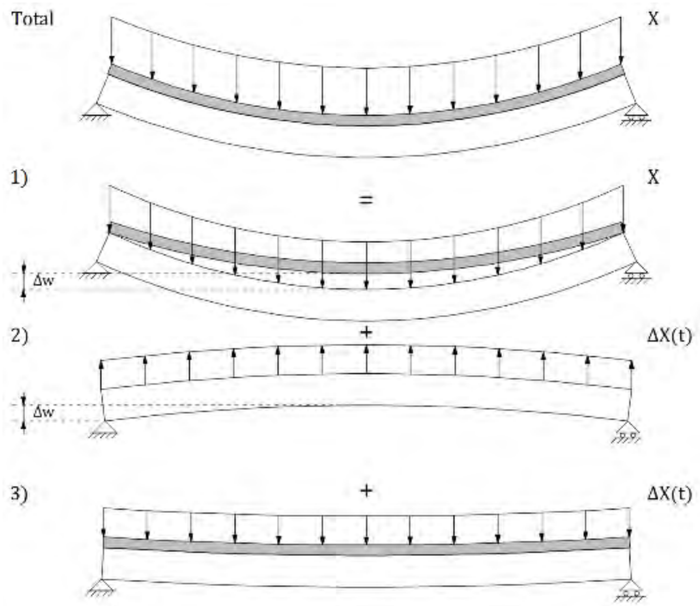

Figure 3.19 Superposition principle for the loads applied prior to concrete curing

Regarding the un-shored case (TCC bridge deck loaded before the concrete has fully cured), the following approach is suggested. The total effect after curing is obtained by superposing:

1) the effects of the load X to the timber components, including creep (using an effective modulus of elasticity for timber);
2) the effects of the restrained load $\Delta X(t)$ to the timber beams, excluding creep;
3) the effects of the restrained load $\Delta X(t)$ on the composite beam, including the influence of creep (using effective moduli of elasticity for timber, concrete and connectors) developing from the curing time t_c.

The superposition principle is shown in Figure 3.19. The restrained load, $\Delta X(t)$, is equal to the load required to restore the compatibility of the timber member and concrete slab after creep deformation, which occurs after that the slab has cured. The effective load ΔX at time t is given as

$$\Delta X(t) = X \frac{\varphi_t(t,t_i) - \varphi_t(t_c,t_i)}{1+\varphi_t(t,t_i)} \tag{0.2}$$

In the Equation (0.2), X is defined as the load acting on the beam, ϕ_t is the creep coefficient of timber members, t_i is time moment when the load is applied and t_c is the time instant when concrete is cured. A more detailed description of this approach can be found in (Jaaranen 2016).

3.3 Medium to long span bridges

For short spans, the bridge deck and the load-carrying structure may be integrated into one structure. For medium to long span timber bridges, this is normally not possible, either technically or economically. Hence, in the present context, medium to long timber bridges have a separate load-carrying structure supporting the bridge deck (in this section the brief term bridge therefore means a medium to long timber bridge).

The bridge has the following main parts: deck, railing, load supporting structure and abutments.

3.3.1 Bridge components

If suspended and cable-stayed bridges are excluded, the load-carrying structure for a medium to long timber bridge is in practice either trussworks, arches or a combination thereof. The load carrying structure may be located:

a) beneath and within the vertical projection of the deck;
b) on the sides of the deck (partly over and partly under the deck);
c) on the sides and above the deck.

From a durability point of view, case a) is a good choice when the elevation of the connected roads at the building site allows the load-carrying structure to be put beneath the bridge and the space under the bridge is sufficient. In this case, the timber support structure should be covered by a watertight deck. Shielding on the sides should also be considered in order to avoid wetting of the timber structures by lashing rain. The Old Town Bridge in Trondheim, Norway, is a good example. The load-carrying structure consists of four parallel Howe trusses beneath the timber deck. The timber deck has a watertight cover on top, and on both sides venetian blinds made of timber boards protect the lower parts of the outermost trusses, see Figure 3.20. The bridge was built in 1861.

Figure 3.20 Gamle Bybro, Trondheim, Norway.

For bridges with the load-carrying structures on the side of the deck, cases b) and c), some kind of cover of the structures is usually necessary for satisfactory durability. Some older bridges in USA and Switzerland are completely covered by roof and sidewalls, but this is nowadays an option mostly for pedestrian bridges. On a road bridge with heavy traffic, a twenty meter long lorry, on a rainy day, might carry a considerable amount of moisture into the bridge by turbulent water sprays. Having road bridges with complete roof and walls will slow down the drying inside the bridge and might lead to high levels of moisture. Therefore, the strategy most used today is to cover each structural part individually by some form of cladding, possibly in combination with preservative treatment.

Due to the need for constructive cover, it is evident that the structural parts, which need covering, should be as simple as possible since detailed covering leads to increased costs. Simple structural forms with few connections that need cover are therefore beneficial and are not vulnerable to malfunctions.

A timber bridge usually contains other materials, such as steel and concrete and materials for protection against water access to the wood materials. Reinforced concrete is used in the abutments and sometimes as decking. Steel is used in the fasteners of the timber joints, in hangers used in arches and sometimes as tension members in truss-work. In combination with stress-laminated timber decks, steel (transversal) crossbeams are mostly preferred due to higher stiffness, less height and smaller volume, leading to a more slender appearance of the bridge. Concrete decks can be designed either as a separate plate, or in composite action with timber members. In the latter case, concrete will be in compression, while the timber members will carry the tension. Two different layouts can be used: either distributed shear connectors leading to almost continuous shear force transfer between the parts, or concentrated connections between the concrete plate and the timber structure at the timber joints connecting the concrete slab directly to the slotted-in steel connector plates without contact between wood and concrete.

3.3.2 **Structural timber elements**

Most medium to long timber bridges built today make use of glulam. Glulam is a stack of parallel solid wood lamellas with a thin layer of glue in-between, brought together into a single structural element by applied external pressure during the curing of the glue. Several glulam stacks can be glued together side by side and this is usually denoted as block gluing. In this way, a wide range of cross-sectional sizes can be made, ranging from the size of solid timber to several square meters. The individual lamella is finger jointed and can therefore be made continuous in any practical length. Usually the size of a glulam element is limited by transportation from the factory to the bridge site.

3.3.3 **Structural modelling**

It is in general sufficient to use first order linear elastic models to distribute the effects of the actions in a wooden bridge structure. Care must be taken regarding the effect of duration of loads (DOL) since creep effects may influence the force distribution within a structure, especially in cases where different materials are combined. Somewhat simplified, it can be stated that for calculations in ULS the *characteristic* values of the material properties are used, while SLS makes use of the *mean* values.

For simple structural members having compressive stresses, geometrical instability must be checked either by simplified methods, like estimation of equivalent buckling (or effective) length, or by 3D computer models where second order effects (change in geometry) are included.

Wood is a highly anisotropic material that cannot be adequately represented by isotropic material models in 2D and 3D analyses. While the ratio E/G is about 2.6 for structural metals, this ratio is roughly 16 for wood. Consequently, general isotropic models requiring two parameters as input (E and G, or E and Poisson ratio) are deemed to fail for wood. The most used material model for 3D finite elements is the transverse isotropic linear elastic model, neglecting the difference between the tangential and radial directions, but including the difference between transverse and longitudinal directions. In this case, the material axes of the wooden elements have to be represented correctly.

For the overall behaviour of beam-like structural members (1D elements) good results are usually obtained by use of simple beam elements, provided that the shear deformations are included, i.e. use of Timoshenko beam elements.

For trusses having curved chords, one straight member between two neighbouring joints is not satisfactory. The out-of-straightness must be included in the structural model both for calculation of internal force distribution in linear models, as well as for the evaluations of stability of the structure.

Although trusses may be designed by using models with only pinned (moment free) joints, this is normally a poor model. Usually the chords are made continues in as long pieces as possible, limited by transportation or preservation requirements. Computations of internal stresses in trusses by the use of the simplified assumption of pinned joints in such cases fail to capture the real stresses. It is therefore recommended to model the structural parts as continuous beams if that is the case, and include the joints where they actually are located.

The rotational stiffness properties for shear-loaded mechanical joints in timber structures are very uncertain. Most of such joints will have less than half of the bending stiffness of the connected parts themselves. However, in some cases these connections might transfer moment actions although that was not intended in the design of the joints. Consequently, the outermost fasteners in those connections may become more loaded than the presumption made in the design calculations. Care should be taken in those cases where eccentricities or rotations might occur, in order to take possible moment action in the connection into account.

3.3.4 **Timber arch bridges**

The majority of timber arch bridges built in recent years has the arch above the deck and use vertical hangers to transfer the deck loading to the arches. Bridges featuring a monolithic cross-section in the arches are typically based on the three-hinged statically determined lay-out. In cases with longer spans the arches are made by use of truss-work which enhances the bending capacity of the arch without much increase in material use. These design concepts are well expressed at Tynset bridge (70 m span), see Figure 3.21. The connections used in the trussed arch usually consist of slotted-in steel plates combined with numerous of steel dowels. For the truss-work type of arches it may be more convenient to apply the two-hinged arch concepts.

The size of a prefabricated bridge part depends on the curvature and the length due to limitations in chemical treatment facilities as well as transport. Typically, parts exceeding a length of 30-35 m cause problems. For the truss-work type of arches this size-handling problem may be overcome by using the truss connections also as mounting connections. This can readily be done as the connections in a truss are exposed mainly to axial forces. However, the splicing of arches having massive cross sections is much harder since these also have to resist moment action.

Figure 3.21 Tynset bridge, Norway (photo: K. Bell)

In arch bridges with vertical hangers the moment actions in the arch are likely to become large due to traffic loads, introducing high concentrated forces in the arch. Furthermore, by introducing the loads into the arch by a few vertical hangers, the combination of shear stress and tension normal to grain may become very challenging; see more about this e.g. in (Bell 2010).

3.3.5 **Transverse forces and stability**

Usually the arches are made so slender that there is a need for sideway support to avoid instability. Arches unsupported along the span require clamping in the transverse direction at the supports. In accordance with St. Venant's principle, the effect of the clamping will diminish as the arches are made longer and more slender. For long span bridges, the height of the arches may be sufficient for a rigid frame to transfer sideway forces. The rigid corner of the moment carrying frame is then formed by the wind bracing at the top of the arches, connecting the two arches by, for instance, a K-shaped truss, transferring the lateral forces towards the supports. This design was chosen for Tynset bridge, see Figure 3.21. In this case the hangers are vertical and hinged at both ends transferring only vertical forces; hence, no horizontal forces from the arches are transferred to the deck by the hangers.

For smaller spans a simpler design has been utilized where the transverse actions have been transferred to the timber deck. This is achieved through the use of transverse U-shaped steel frames. Here, the hangers are replaced by beams rigidly connected to the crossbeams, thus providing the necessary transverse stability properties of the arches. The pre-stressed timber decks have high lateral stiffness and act as horizontal beams, transferring the transverse actions to the supports, see Figure 3.21.

3.3.6 **Durability issues**

The durability requirements have mainly been met by use of chemical treatments like CU and creosote impregnation, in combination with cover of details and connections. Often several levels of protection are used, such as a constructive layer on top of beams, arches and trusses in combination with a creosote impregnation of mostly the glulam elements. These protective measures are mainly working on the outer faces of the elements. In addition Cu-impregnation of each lamella takes care of the inner parts of the structural elements. The constructive layer on top also takes care of possible cracking on the topside of the element. This is the approach for durability used on Tynset bridge, see Figure 3.21.

It is expected that in the coming years more severe restrictions will be put forward on the use of environmental unfriendly chemicals and for long durability of timber bridges this can easily lead to increased costs. Considering Figure 3.21, it is quite obvious that "clean" designs, like the two smaller side spans of the Tynset bridge, are much easier to cover in some way than the complicated 3-D truss of the main span. An example of covering of a simple bow-string bridge is demonstrated by Fretheim bridge, Norway, see Figure 3.22. Here, copper cladding is used on the top faces, while the side faces are covered by ventilated venetian blinds.

Figure 3.22 Fretheim bridge, Norway (Photo by SWECO (SWECO NORGE AS))

Figure 3.23 Glulam cross-section with pit location pointing upwards and radial cracks

The basic principle to achieve durable timber structures is simple: it is all about keeping the water out of the wooden material in order to assure that the moisture content stays below 18 to 20 % (Scandinavian climate). Susceptible points for entrance of water are everywhere where water can be collected in liquid form like on horizontal upward surfaces, in cracks on horizontal and vertical surfaces, around details like fish-plates, screw discs, bearing shoes, and in drilled holes and cut-outs which are not pointing downwards. By controlling the orientation of lamellas in the glulam production, it is possible to assure that the location of the pit is on the upwards side. Most cracks in wood are radial cracks and consequently pointing downwards and therefore water will not be collected in these cracks, see the visualization on Figure 3.23. It should also be kept in mind that water is very rapidly transported into the wooden material if end-grains are brought in contact with liquid water. More on recent findings related to durability can be found in (Kleppe 2010) and (Pousette and Sandberg 2010).

Some countries like Switzerland and USA have several fully covered bridges showing good performance for centuries. However, this approach has mainly been used for pedestrian bridges; it is more questionable for road bridges. Heavy goods vehicles will on a rainy day transport considerable spray of water into the bridges and the cover may prevent effective ventilation and drying up. The result may be high levels of moisture content in the wood. Furthermore, the wind exposed area of fully covered bridges might be considerable, leading to strong requirements for transverse stiffness.

3.3.7 **Massive timber arch bridges**

3.3.7.1 Inclined hangers

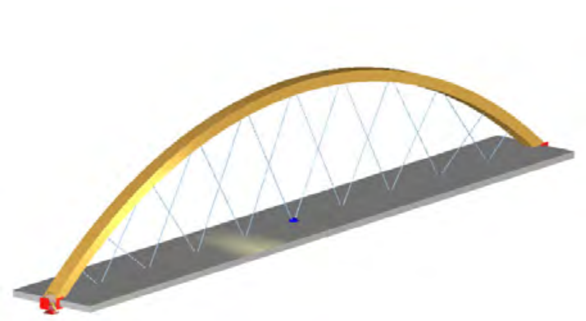

Figure 3.24 Network arch, after (Bell 2010)

For bridges exposed to traffic loading, the design case is often heavy loading located in a skew position. Using an arch with vertical hangers, this skew and relatively local loading will be transferred to the arch through the hangers as point loads. The result is a large moment action in the arch. For the truss-work arch this moment action is dealt with by a considerable increase of the internal moment arm. Another approach is to reduce the moment action. O. F. Nielsen (Nielsen 1929), nearly hundred years ago, appears to have pioneered hangers inclined in a V-configuration for bowstring arches, thus reducing the moment action into a more pure compressive arch bearing. This concept was further developed by P. Tveit (Tveit 1959) in the late 1950s, letting the inclined hangers cross each other more than once and denoting it "network arch bridge". A summary of his design considerations is available in (Tveit 1987). The effect of inclined hangers and network hanger design on bowstring arch bridges, like the one depicted on Figure 3.24, is clearly demonstrated in (Bell 2010), showing that the moment action in the arch might be reduced to roughly one quarter and might give reduced vertical displacement of the deck to nearly one sixth.

The most important feature of a network arch bridge is the use of inclined and crossing hangers, which typically cross each other twice or more. The use of inclined hangers dramatically lowers the moment in the arch and makes the bridges much stiffer. The current work is focused on network arch bridges for which both deck and arches are made of timber.

3.3.7.2 Stability of network arch

The in-plane stability of a network arch depends on the stiffness of the arch member as well as the deck and the distance between the hangers. In general it is forced to buckle in between the hanger fastening points, leading to good in-plane stability.

For the out-of-plane stability, the inclined hangers do not make much difference compared to vertical hangers. For a two-hinged network arch, sideways clamped at the supports, the two lowermost buckling modes are visualized in Figure 3.25. In fact, assuming that the load can be imposed on the arch in some way, the instability modes do not change much from an arch without hangers or a three-hinged arch with the same geometry. For the three hinged arch the critical buckling loads will be only slightly smaller. Usually, the out-of-plane stability is assured by coupling two arches together with a bracing in-between. However, in the present work a different approach will be explored.

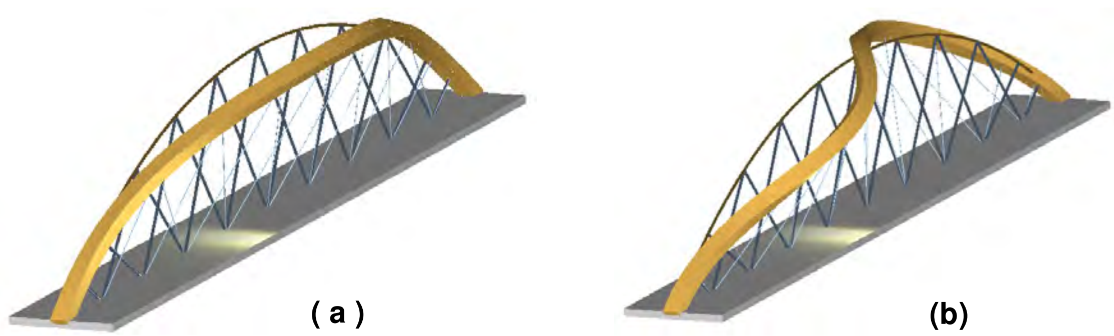

Figure 3.25 The two lowermost buckling modes for a network arch, after (Bell 2010)

Consider Figure 3.24, and assume that each of the hangers consists of two parallel rods. If the fasting points are displaced in the transverse direction in the deck for the two rods, the layout will be very similar to the familiar layout of the spokes in a bicycle wheel, see a visualization in Figure 3.26.

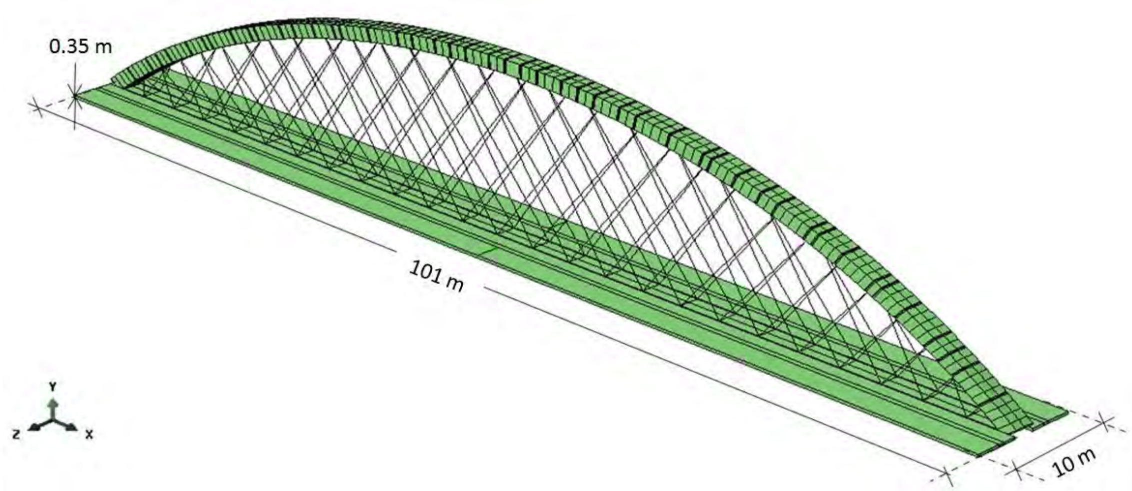

Figure 3.26 Network arch with double hangers in spoked wheel configuration.

A simple model to demonstrate the possible effect on stability from this spoked wheel configuration is shown in Figure 3.27. Figure 3.27 a) shows a situation with hangers only in the plane of the arch. If we assume that the arch tends to displace and rotate about the line between the support points, this rotation will be like a rigid body rotation and no lateral forces are activated to resist the rotation. However, in the spoked wheel configuration, see Figure 3.27 b), a lateral displacement or rotation about the support line will lead to an elongation of one of the hangers and thereby forces will develop to resist the lateral displacement.

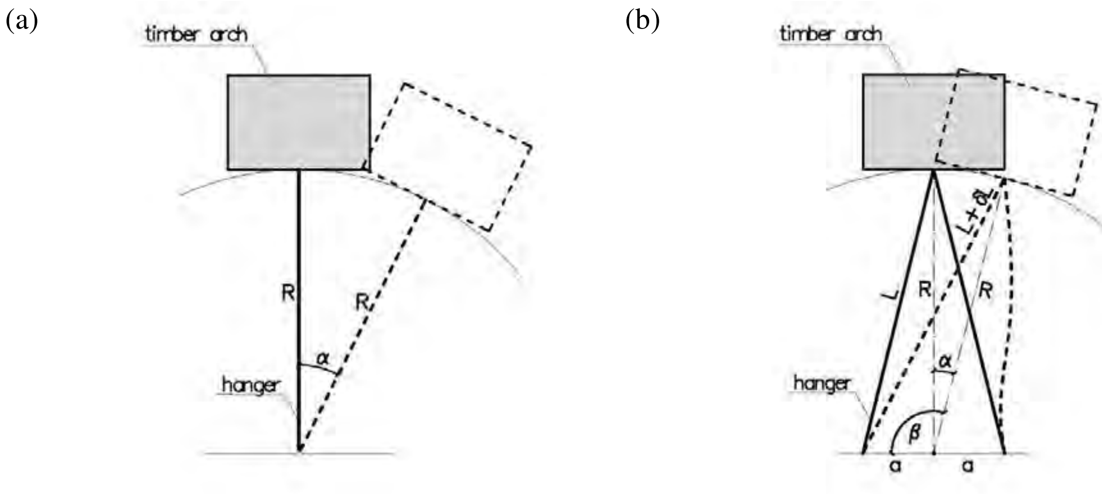

Figure 3.27 Lateral stiffness from spoked wheel configuration.

Assuming hangers of length L and a rigid body rotation α (radians) of the arch about the line between the end supports, the strain in a single tensile hanger in a transversely displaced position is obtained by simple kinematics and reads

$$\varepsilon = \sqrt{1 + \frac{2 \cdot a \cdot \alpha \cdot R}{L^2}} - 1 \qquad (0.3)$$

Here, a is the horizontal distance between the displaced fastening points of the hangers on the deck relative to the centreline of the arch, and R is the vertical distance from the fastening point in the arch to the line of rotation (line through the end supports).
Even for small rotations and values of a, there is considerable amount of strain in the tensile hangers in the spoked configuration, consider Equation (0.3). The actual values of a and R are of course dependent on the chosen design, but it is quite clear that arches having smaller arch rise, and hence shorter hangers, are beneficial from this point of view. Clearly the largest effect is obtained close to the supports and becomes considerable less at mid-span due to the variation of hanger length. Therefore, the sideway support effect will vary along the span in the same manner.

Eurocode 5-1-1 (CEN 1995 2004) recommends a minimum out of vertical alignment by

$$\alpha \geq 0.005\sqrt{5/R} \qquad (0.4)$$

to be used in building calculations. An example of the stabilizing effect can be made by use of the following assumptions: the allowed horizontal deflection is limited to twice the value of α (Equation (0.4)), hangers have 45° inclination and the vertical distance between arch and deck $R = 10$ m. The resulting estimate of the stabilizing force of a single hanger is dependent of the initial out-of-plane location a, and is plotted in Figure 3.28.

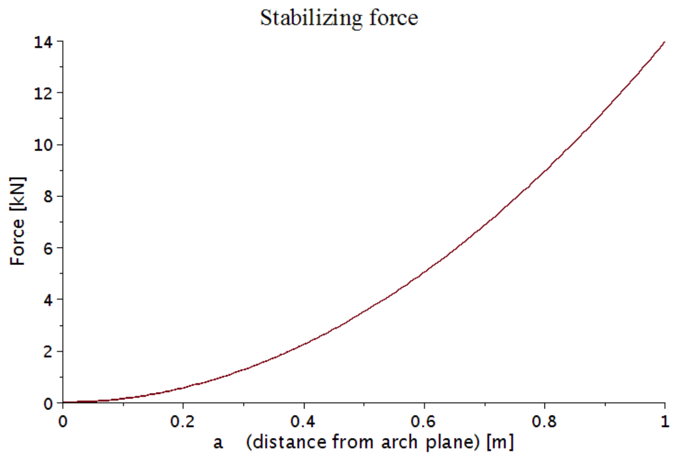

Figure 3.28 Stabilizing force from spoked and inclined hangers

The stabilizing force shows a nonlinear increase with increasing horizontal offset a. It represents an interesting feature for horizontal stabilization of arches that can limit the need for wind trusses. Therefore, the transverse distance between the fastening points of the hangers ($2a$) should be made large in order to improve sideway stability.

The area determined by the vertical projection of the arches onto the deck cannot be used for traffic purposes since the entrance will be blocked by the arches. Therefore, this area can be used for inclined and spoked (transversely displaced) hangers and possibly guard railings. Moreover, the arches should be clamped at the supports in transverse direction.

The height (depth) and width of the cross-sections together with the rise-to-span ratio and the out-of-the-plane support condition of the arch strongly influence the stability properties. The in-plane stability of a network arch is high and it may be reasonable to let the width of the cross-section be larger than the height in order to increase the out-of-plane stability. Furthermore, although the compressive forces in the arch will increase together with a slight increase in moment actions, it will be beneficial for the sideway stability to use an arch with quite low rise to span ratio.

3.3.8 **Hangers**

3.3.8.1 Inclination of hangers in the plane of the arch

The objective of the use of inclined hangers or network arch design is to reduce the moment in the arch, letting it carry the loads by mainly compressive stresses. This leads to a great reduction in the amount of material needed for the arch. The side-effect, which might occur from the use of inclined hangers, is that some of the hangers may become relaxed or even get compressive stresses if the end-fastening allows it. This can lead to buckled hangers and possibly a visual or practical problem. It can also have an influence on the stability of the arch as the in-plane buckling length is dependent on the distance between the hangers, and relaxed hangers are ineffective in this regard.

3.3.8.2 Hanger patterns

The hanger outline of the network arch bridges is crucial for the force distribution in the structure. The hanger patterns are characterized by number of hangers, their orientations, and the locations of fastening points in the structure. The hanger patterns influence strongly the bending moment distribution in the arch and the deck. General typologies of patterns in arch bridges are shown in Figure 4.1.

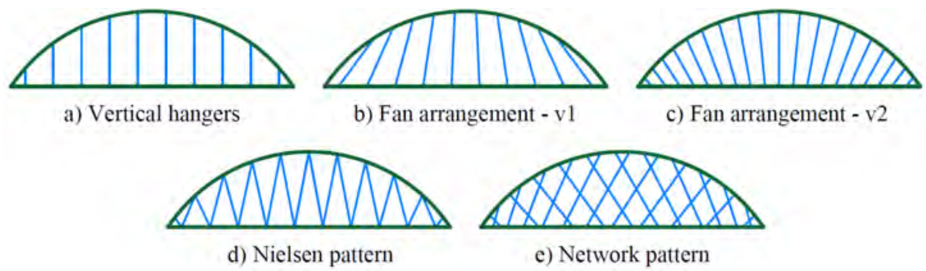

Figure 3.29 Hanger patterns in arch bridges

In order to design network pattern geometry, consider the following variables:

- number of hanger sets in the arch,
- number of hangers in one set,
- distance between hangers in one set,
- hanger inclination, i.e. the angle between the hanger and either the deck, the arch, or the arch radius or tangent (Schanack 2008).

A set of hangers is a group of hangers which are inclined towards the same direction, see Figure 3.29 a. A second set is usually symmetrical to the first one with respect to the centreline of the bridge. In practice, the number of hanger sets in a bridge is most often equal to two, see Figure 3.29 e. According to (Tveit 1966), three or more hanger sets might be worth considering for temporary bridges with light and flexible decks; see Figure 3.30 b-c. However, for timber network arch bridges it is recommended to stay with two sets of hangers.

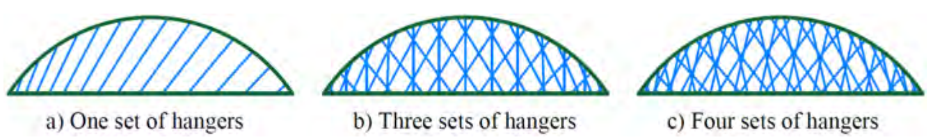

Figure 3.30 Patterns with different number of hanger sets

The number of hangers in a set depends primarily on the bridge length and the type of traffic. The longer the bridge and the heavier the traffic, the more hangers are recommended. Theoretically infinite number of hangers leads to the best arch performance. The number of hangers depends also on the bridge static system and the deck type. For bridges with light decks supported by crossbeams, the hangers may conveniently be attached to the crossbeams. Hence, their number will be limited by the number of crossbeams. However, in cases where an edge deck beam is present, the hangers can be fixed to it and their number become independent of crossbeams.

The distances between the hangers in a set as well as the inclination of the hangers vary depending on the pattern type. Several network patterns are used, and the most common ones are described in the following.

3.3.8.3 Pattern with constant inclination of hangers

The main premise of this pattern is that the inclination of the hangers, defined relative to the deck, is the same for all hangers and therefore *α=constant*, see Figure 3.31a. Another name of this pattern is *rhombic pattern*. In an alternative pattern with constant inclination of hangers, they are evenly distributed along the arch. However, the principle of generating both patterns is the same.

3.3.8.4 Pattern with constant change of inclination of hangers

In this pattern the hangers in a set have a constant incremental change in their inclination. Therefore, two parameters describe the pattern: the starting angle α and the constant angle change $\Delta\alpha$. Depending on the desired geometrical effect, the angle change can be both positive and negative. An example of a pattern with constant, negative change of hanger inclination for hangers that are evenly distributed along the arch is depicted in Figure 3.31 b.

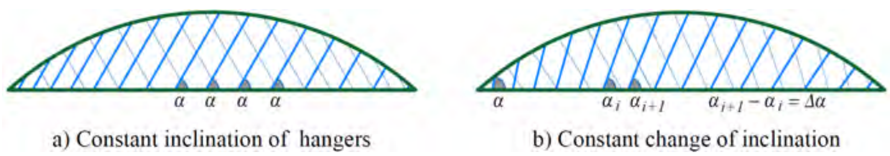

Figure 3.31 Different network patterns

3.3.8.5 Radial pattern

The angle between arch radius and the hangers is constant in the radial pattern type. This pattern was developed by Brunn and Schanack (Brunn and Schanack 2003), following a parametric studies performed on a 100 m long bridge designed for train traffic. The outline of the radial pattern, where hangers are equally distributed along the arch is presented in Figure 3.32.

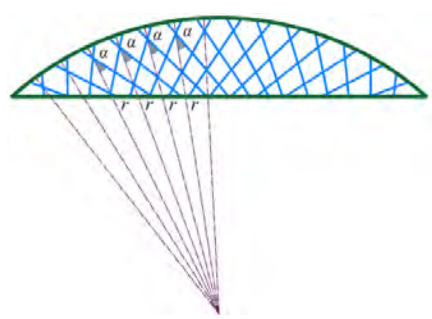

Figure 3.32 Radial network pattern

3.3.9 **Bridge design issues**

The choice of an efficient network pattern is one of the design challenges for network bridges. However, more aspects need to be carefully considered during the design of timber network arch bridges.

3.3.9.1 Deck type and boundary conditions

One of the governing topics is the choice of the deck type. A concrete deck and a timber arch is an option which was chosen for the 88m long Steien bridge located in Norway (Veie and Abrahamsen 2013). An alternative is a deck made of stress-laminated timber planks, supported on the transversal beams.

The choice of deck type is also a choice of boundary conditions. Using a concrete deck, it is possible to have a heavy edge beam, which connects the ends of the arch, creating a stiff 'frame' filled with a hanger net. Such a solution is common for many of the types of so-called *tied arch bridge* or *bowstring arch*, where usually the structure is statically indeterminate internally, but determinate externally, see references (Ryall, Parke et al. 2000, Pipinato 2016). Such a design can be treated as a simply supported beam. In addition, hangers can be fixed anywhere in the deck as well as in the arch; in other words there are few limitations. Using a timber deck, the transversal crossbeams are natural points for hanger attachment.

In network arch bridges with timber deck on transversal crossbeams, there is not necessarily any longitudinal ties or edge beams connecting the two arch ends. However, both arch and deck should have symmetrical boundary conditions, i.e. pinned arch and deck, or pinned arch and roller support at both deck ends. Obviously, it is possible to have a tie or a beam, but for long spans, it would require a quite heavy steel element, disproportionate to the remaining structure. It may be better to transfer the horizontal forces to the ground by using the abutments to carry the horizontal thrust. For short and medium long bridges, a steel tie or edge beam can be introduced to limit or avoid horizontal reactions at the supports.

3.3.9.2 Arch rise, buckling and wind truss

The arch rise is related to both force distribution and arch stability. Bridge designs having hangers only in a single plane and without other transverse stiffening structures will not provide sufficient sideway stability of the bridge, necessitating wind bracing. Alternatively, the arches can be tilted towards each other as a 'basket handle'. In both design alternatives, connections on the side faces of the wooden arches are common, but undesirable. For good durability of the wooden elements, such a solution is not optimal due to the risk of moisture trapping and challenging covering of the connections.

An alternative approach is to apply a double inclination of hangers, so-called *spoked configuration of hangers* (Malo, Ostrycharczyk et al. 2013), see Figure 3.33. By introducing out-of-plane spacing with spoked hangers, limited by the vertical projection of the arch cross section, the buckling lengths can be reduced by more than half. Combining double inclination of hangers with rectangular cross section of the arch where the width-to-height ratio is more than 1.5, the out-of-plane instability problem can be reduced to the point that no, or limited, wind bracing is needed.

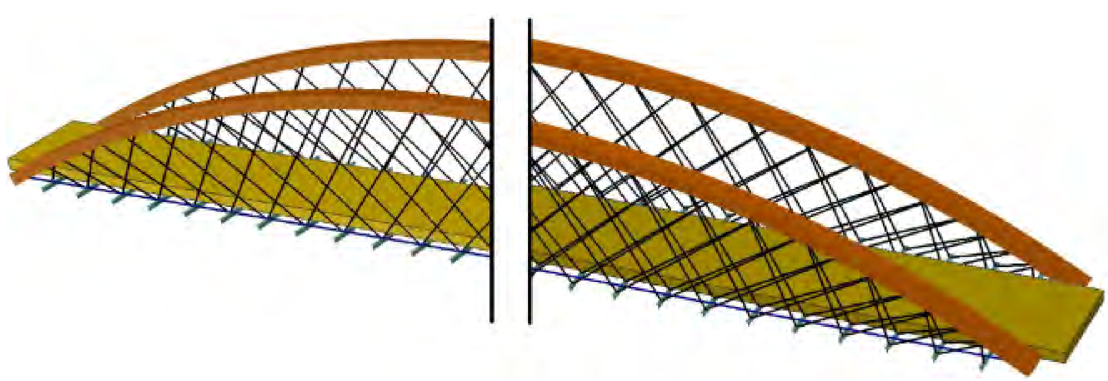

Figure 3.33 Network arch bridge: classic (on the left) and with spoked configuration of hangers (on the right)

3.3.10 **Recommendations**

3.3.10.1 Arch rise

The choice of the arch rise for a network arch bridge depends on whether or not a wind bracing is present. For bridges with wind truss bracing, the recommended arch rise is in the range of 10-25% of the bridge length. For bridges without a wind truss bracing, the arch rise should be limited to 10-18% of the bridge length. According to research conducted at NTNU under the DuraTB project, optimal arch rises for bridges with spoked hangers are in the range 13-18% of the bridge length (Ostrycharczyk and Malo 2017).

3.3.10.2 Cross beams

In Table 3-1 the minimal recommended number of crossbeams is stated for network arch bridges of different lengths. The recommended number has been obtained by numerical analyses performed at NTNU using various arch rises combined with a wide range of spread angles in radial network patterns (Ostrycharczyk and Malo 2017). The maximal bending moment in the arch, resulting from unfavourable skew loading, has been used as deciding parameter.

Table 3-1 Recommended minimal number of transversal crossbeams for different bridge lengths

Recommended minimal number of crossbeams	Bridge length L[m]						
	30	40	50	60	80	100	120
n [-]	6	7	8	9	13	15	15

Circular cross-sections of the cross-beams avoid moisture trapping under a timber deck and give good ventilation between the crossbeams and the deck. However, depending on the deck width and on the hanger fastening locations (or the presence of edge beams), this might not be the most economical solution. Traditional 'I' beams with reduced cross section towards the ends or underpinned beams can in many cases be more efficient and hence a better choice. A circular cross-section is beneficial for inclined hangers since, regardless of the resultant force direction, circular cross-sections have the same strength and stiffness properties. In any case, large contact surfaces with water trapping abilities between the crossbeams and the timber deck should be avoided.

3.3.10.3 Arch shape

Figure 3.34 presents the relation between the maximum bending moments M in the arch and the hanger angle α. The bending moments have been determined for circular and parabolic arch shapes and network radial pattern with evenly distributed fastening points on the deck. Note that the bending moments represent the maximum moment in the arch, obtained for the most unfavourable load case of skew loading applied on the bridge deck. In addition, the percentages of relaxed hangers H obtained for the most unfavourable skew loading on the deck are also presented on Figure 3.34. The results were obtained using a bridge model of 100 m length and 17 m arch rise (height). It is quite clear that a circular arch shape is more advantageous than a parabolic shape. These results are valid for radial pattern with evenly distributed fastening points on the deck.

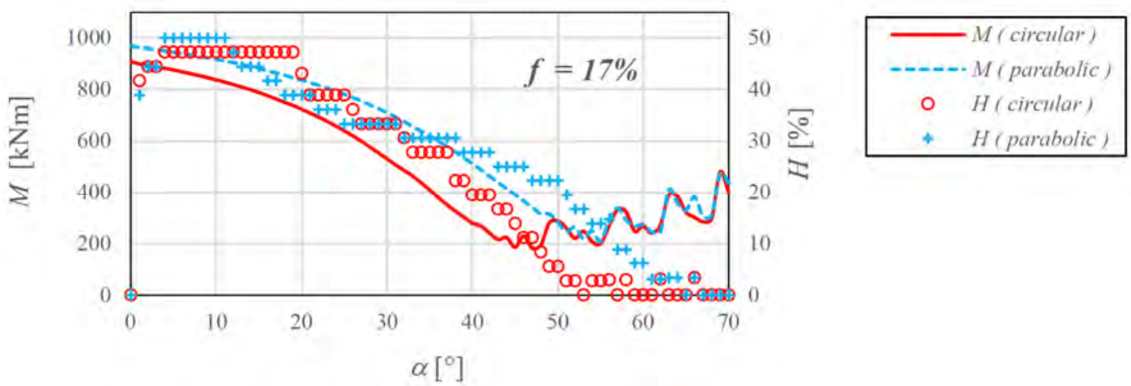

Figure 3.34 Maximum bending moment and percentage of relaxed hangers H as a function of angle α in network radial pattern

3.3.10.4 Hangers and radial patterns

Evenly spaced crossbeams usually support bridges with stress-laminated timber decks. The crossbeams constitute a natural base for hanger fastening, and hence the hangers will be evenly distributed along the deck. Consequently, the hangers will probably be randomly distributed along the arch. It may not always give the best structural performance of the bridge since it may happen that two hangers have coinciding fastening points on the arch, resulting in a considerable increase in moments at this location. To avoid this layout, visual judgement is suggested. It is not recommended that hangers share fastening points within the central (1/3) part of the arch.

Since a timber or steel deck is a light type of deck, its weight does not fully pre-stress hangers for all the load positions, so it can happen that some of them become relaxed (i.e. do not transfer tension force) during use. As long as the number of zero-force hangers is low, it is not a problem from a structural point of view. However, from a practical point of view the hangers should be fastened and interconnected in such a way that rattle and buckling are avoided. The number of relaxed hangers appearing in the structure is dependent on the chosen pattern and its features (deck-hanger angle or angle change).

In the design of network patterns for bridges with crossbeams, the hangers located towards the ends of the arch may need special attention. While the hangers in the central part of the arch are, most likely, evenly distributed according to a chosen pattern type, the edge hangers may be candidates for manual adjustments to avoid nearly horizontally oriented hangers. In radial patterns this can be performed in a systematic way by implementing the so-called *modified radial pattern*. In this pattern the focal point, which is the centre of the radial rays, is shifted in the vertical direction so that the edge hangers become steeper, while hangers in central part of the arch remain almost in the same position. In Figure 3.35 two examples of patterns for a network bridge are presented. In both cases the bridge length is L = 50 m, the arch rise f = 9 m and the angle between radial ray and hanger is α = 42.5°. The bridge on the left-hand side of the figure refers to a classic radial pattern, while on the right-hand side the modified radial pattern is presented. The focal point is vertically shifted a distance of 50 m.

Table 3-2 shows recommended values of angle α and angle change $\Delta\alpha$ for different types of patterns, i.e. patterns with constant inclination of hangers, with constant change of inclination and radial patterns where hangers are evenly distributed along the deck. The data are based on studies performed at NTNU on a 100m long timber bridge with a timber deck supported by 18 transversal crossbeams. Maximum bending moment and maximum number of relaxed hangers under the most unfavourable position of skew loading were the main criteria during the analyses.

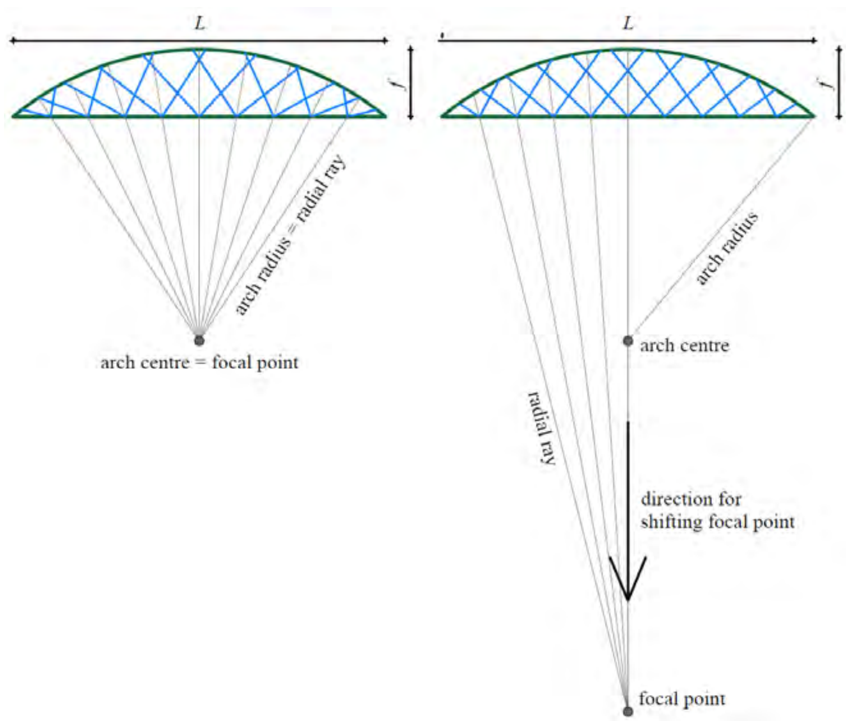

Figure 3.35. Radial network patterns: classic (on the left) and modified (on the right)

Table 3-2 Recommended value of angle for different pattern types

Arch rise		Pattern type		
percentage of bridge span	Type	constant inclination of hangers	constant change of inclination	radial pattern (without modifications)
		α	α ; $\Delta\alpha$	α
$10\% \rightarrow 13\%$	Shallow	$40° \rightarrow 45°$	$50° \rightarrow 70°$; $-1,5° \rightarrow -4,0°$	$48° \rightarrow 65°$
$14\% \rightarrow 20\%$	Medium	$45° \rightarrow 45°$	$55° \rightarrow 75°$; $-1,0° \rightarrow -3,5°$	$40° \rightarrow 55°$
$21\% \rightarrow 25\%$	High rise	$48° \rightarrow 58°$	$65° \rightarrow 80°$; $-1,0° \rightarrow -4,0°$	$38° \rightarrow 54°$

3.3.11 **Bridge details**

In the development of a bridge concept consisting of with timber network arches and spoked hangers, emphasis has been put on design solutions which will have good durability without heavy use of preservatives. For most bridge structures, this implies that the structures will have to be covered in some way. Therefore, all upward and nearly horizontal wooden surfaces are designed without any connections or any other protruding details. Furthermore, fastening of load-bearing components on vertical wooden surfaces has also been minimized or is absent. Such a design strategy will reduce or eliminate potential moisture traps, reduce the moisture content in the wood and make the timber bridge more durable. It will also reduce cost of proper covering as well as future maintenance costs. Low moisture content in wood makes the use of toxic preservatives unnecessary and the environmental footprint improves. Easy covering of the load-bearing structures is a major issue, and the design solution focus on watertight cover of the horizontal or upwards wooden surfaces and ventilated cover of vertical faces.

A computer model of a 111 m bridge is shown in Figure 3.36. This design proposal was worked out during a master thesis project at NTNU (Eilertsen and Haddal 2016). All hangers are fastened on the downward face of the wooden arches, without any penetration of upwards or vertical surfaces.

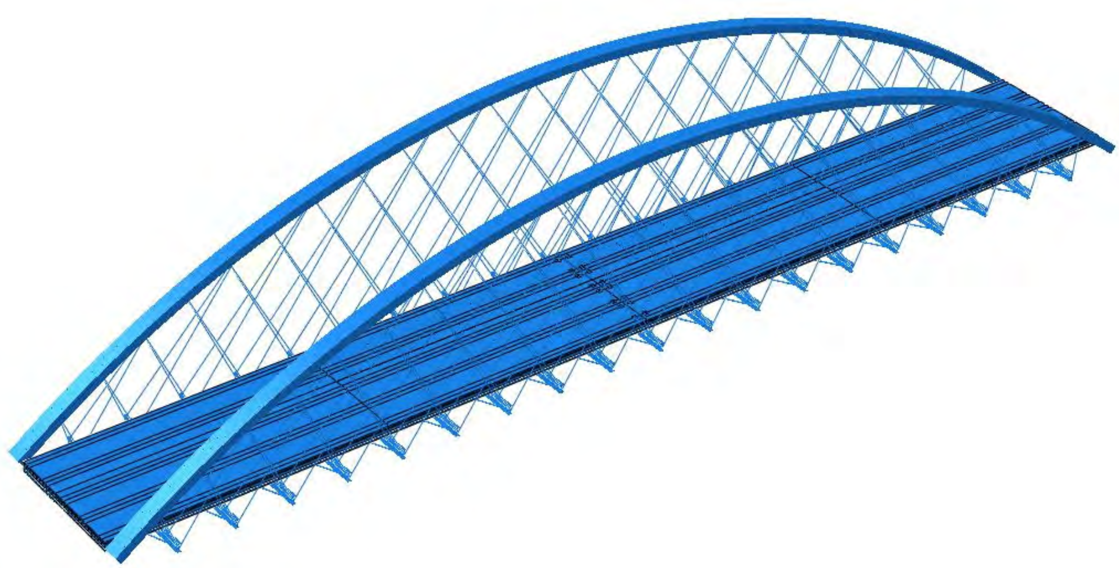

Figure 3.36 Timber bridge concept with network arch and spoked hangers

A sketch of a possible design of a footing detail is given in Figure 3.37. The arch has rotational freedom in the plane of the arch, but it is clamped with respect to lateral displacements. The clamping of the wooden arch to the steel details is made by use of long threaded rods as these connections can be made very rigid without any initial slip. Basically, the same technology is used for potential splices of the arches; see the drawing in the middle of Figure 3.37. Here, two sets of threaded rods have been used, coupled together with mechanical steel couplers.

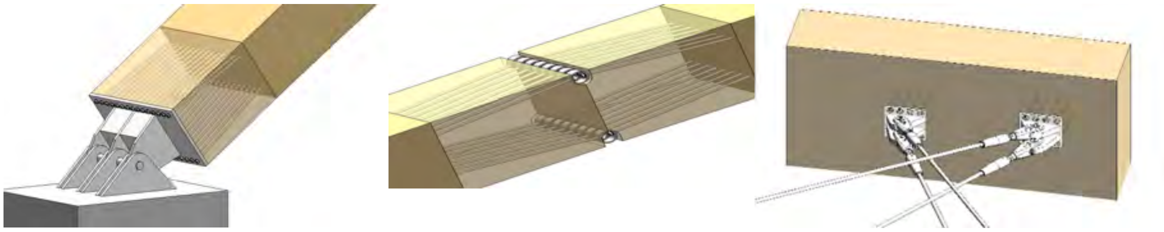

Footing Splice Hanger fastening

Figure 3.37 Arch detailing

The hangers are also fastened by use of threaded rods embedded in the wooden arches. Little mounting effort is required for these types of connections, and they have good properties and may be installed in nearly any angle to the grain. However, installation along the grain should be avoided since potential cracks due to drying and wetting in wood will be along the grain.

The network arch bridge is an efficient bridge concept which may enhance the competitiveness of timber bridges. A network arch bridge becomes very stiff in the plane of the arches. It is also possible to use this concept to build long bridges without the need for truss-works for wind forces or instability, by using hangers in a spoked configuration, i.e. hangers which are inclined both in the plane of the arches and in the transvers direction.

3.4 Design of timber components

3.4.1 Design strength for structural timber members

Some design formulas essential for timber bridges are presented in the following, but it should be emphasized that these represent only a subset, and references are made to (CEN 1995 2004) and (CEN 1995-2 2004) for more comprehensive information. In the following it is assumed that the axis along the structural member is denoted *x*, while *y* and *z* are the principal axes of the cross-section. Furthermore, it is assumed that bending about the strong axis is about the *y*-axis.

3.4.1.1 Bending and axial actions

The design strength in Eurocode 5 (CEN 1995 2004) and (CEN 1995-2 2004) is formulated on the basis of linear elastic methods combined with the use of various factors k_{xx} where the subscript is dependent on the physical effect it applies to. The factors k_{xx} account for effects neglected by the simplified and linear elastic calculations. For timber members having stresses mainly in the direction of the longitudinal material axes, the following requirements apply;

For bending and axial tension:

$$\frac{\sigma_{t,0,d}}{f_{t,0,d}}+\frac{\sigma_{m,y,d}}{f_{m,y,d}}+k_m\frac{\sigma_{m,z,d}}{f_{m,z,d}}\leq 1 \quad \text{and} \quad \frac{\sigma_{t,0,d}}{f_{t,0,d}}+k_m\frac{\sigma_{m,y,d}}{f_{m,y,d}}+\frac{\sigma_{m,z,d}}{f_{m,z,d}}\leq 1 \qquad (0.5)$$

For rectangular cross-sectional shapes the bending stress redistribution shape factor k_m can be set equal to 0.7, while it should be set to 1.0 for other cross-sections (CEN 1995 2004).

For combined bending and axial compression of members prone to buckling:

$$\frac{\sigma_{c,0,d}}{k_{c,y} f_{c,0,d}} + \frac{\sigma_{m,y,d}}{f_{m,y,d}} + k_m \frac{\sigma_{m,z,d}}{f_{m,z,d}} \leq 1 \quad \text{and} \quad \frac{\sigma_{c,0,d}}{k_{c,z} f_{c,0,d}} + k_m \frac{\sigma_{m,y,d}}{f_{m,y,d}} + \frac{\sigma_{m,z,d}}{f_{m,z,d}} \leq 1 \qquad (0.6)$$

Here the buckling effect is brought into the design formulas by use of the factors $k_{c,y}$ and $k_{c,z}$ where subscript c indicates compression, and y or z relates to buckling about the y-axis or z-axis, respectively. The buckling factor $k_{c,i}$ is defined as

$$k_{c,i} = 1 \Big/ \left(k_i + \sqrt{k_i^2 - \lambda_{rel,i}^2} \right) \quad \text{and} \quad k_i = 0.5\left[1 + \beta_c \left(\lambda_{rel,i} - 0.3\right) + \lambda_{rel,i}^2\right] \qquad (0.7)$$

where y or z shall replace subscript i. The member slenderness λ_i enters the expressions through a material scaled relative slenderness defined as:

$$\lambda_{rel,i} = \frac{\lambda_i}{\pi} \sqrt{\frac{f_{c,0,k}}{E_{0,05}}} \qquad (0.8)$$

The factor β_c reflects the fact that highly industrialized products, like glulam and LVL, have in general smaller geometrical imperfections, so $\beta_c = 0.2$ for solid timber and $\beta_c = 0.1$ for glulam and LVL.

Members subjected to bending about the strong axis shall also be checked for lateral-torsional instability by:

$$\frac{\sigma_{m,d}}{k_{crit} f_{md}} \leq 1 \quad \text{and} \quad \left(\frac{\sigma_{m,d}}{k_{crit} f_{md}}\right)^2 + \frac{\sigma_{c,0,d}}{k_{c,z} f_{c,0,d}} \leq 1 \qquad (0.9)$$

The latter expression of Eq. (0.9) takes into account the possible interaction of lateral-torsional instability and weak axis buckling. The reduction factor due to lateral-torsional instability k_{crit} is determined by the simplified expression

$$k_{crit} = \begin{cases} 1 & \text{for } \lambda_{rel,m} \leq 0.75 \\ 1.56 - 0.75\lambda_{rel,m} & \text{for } 0.75 < \lambda_{rel,m} \leq 1.4 \\ 1/\lambda_{rel,m}^2 & \text{for } \lambda_{rel,m} > 1.4 \end{cases} \quad \text{where} \quad \lambda_{rel,m} = \sqrt{\frac{f_{m,k}}{\sigma_{m,crit}}} \qquad (0.10)$$

The critical bending stress level is determined by classical theory for lateral-torsional instability for elastic members. For timber, warping of cross-sections can usually be neglected leading to:

$$\sigma_{m,crit} = \frac{M_{y,crit}}{W_y} = \frac{\pi\sqrt{E_{0,05} I_z G_{0,05} I_{tor}}}{l_{ef} W_y} \qquad (0.11)$$

Here, W_y is the section modulus about the strong y-axis, I_z is the second moment of area about the weak axis and I_{tor} is the torsional moment of area. The effective length of the structural members is denoted l_{ef} and the ratio of l_{ef}/l is usually in the range 0.5 to 1.0 where l is the actual length of the member.

3.4.1.2 Shear action

The shear strength along the grain is quite low for most wood species and for high beams this might limit the utilization of the timber member. The design requirement is

$$\frac{\tau_d}{k_v f_{vd}} \leq 1 \tag{0.12}$$

The shear stress along and normal to grain ($\tau_{zxd} = \tau_{xzd}$) is calculated by

$$\tau_d = \frac{V_{zd} S_y}{I_y b_{ef}} = \frac{3V_{zd}}{2h_{ef} b_{ef}} \tag{0.13}$$

The latter expression in Eq. (0.13) is only valid for rectangular cross-sections. The introduction of an effective width b_{ef} is meant to account for the risk of cracking due to wetting and drying; it is defined as $b_{ef} = k_{crack} b$, where k_{crack} represents the relative amount of non-cracked material. The effective height h_{ef} will only be smaller than the height of the cross-section h in cases where some material is locally removed, as in connections and notches. If a notch leads to a combination of tension normal to grain and shear stresses, a critical stress concentration may occur. This situation is accounted for by a correction factor k_v for the strength, see Eq.(0.12), which in such a case will be less than 1.0. In other cases k_v equals unity.

3.4.1.3 Local effects

Stresses may be transferred between wooden members by compressive contact stresses between mating surfaces, or by use of additional elements like metallic fasteners. Contact stresses on inclined surfaces should be related to the material axes of the wood or checked by simplified rules offered by the codes, see e.g. (CEN 1995 2004). For contact stresses normal to grain on small surfaces relative to the member size, an increase in capacity is normally achieved and can be utilized in design calculations.

The use of fasteners normally requires removal of some material due to drilling of holes or cutting of grooves or similar. The removal of material reduces the effective load-bearing cross-section and this must be taken into account, and it is especially important in cases with tensile stress evaluation σ_{t0d} and $\sigma_{m,d}$ for use in Eq.(0.5).

3.4.1.4 Fastening of hangers

For fastening of hangers by use of groups of fasteners embedded in timber elements, the tensile force component normal to the grain direction can lead to cracking along the grain due to the small strength of wood with respect to tension normal grain. The design check can be performed by fracture mechanics based models like:

$$F_{90.Rk} = 14b\sqrt{\frac{h_e}{1-{h_e}/{h}}} \tag{0.14}$$

where b is the width of the cross-section, and h and h_e are the total and effective height, respectively. More information is given in (CEN 1995 2004).

3.4.1.5 Curved and tapered members

Special rules apply for curved glulam members, taking into account the reduction in strength due to bending of lamellas during production, and the occurrence of tensile stresses normal to grain due to straightening bending moments. In many cases, interaction of stress components may be the design case. For wooden members with tapered cross-sections, the stresses at the surface with inclination relative to the grain direction will have a multi-axial stress state, which also need special consideration. Most design codes have guidelines for the handling of these effects, see e.g. (CEN 1995 2004).

For straightening moment loading arch bridges, the induced tensile stresses normal grain σ_{t90d} due to moment, in combination with shear stresses τ_d, might severely limit the load capacity. The current design verification in (CEN 1995 2004) is based on linear interaction of $\sigma_{t,90d}$ and τ_d with modifications for various stress distribution and size effects:

$$\frac{\tau_d}{f_{vd}} + \frac{\sigma_{t,90d}}{k_{dis}k_{vol}f_{t,90d}} \leq 1 \tag{0.15}$$

The size effects on fracture due to tensile stresses normal grain k_{vol} may become very severe and in moment-exposed arches, it will likely become the design case.

3.5 Fasteners in wooden bridges

3.5.1 Design of laterally loaded connections

3.5.1.1 Fasteners

Metallic fasteners made of steel with grades ranging from 4.6 to 8.8 are mostly used. For modern timber bridges, the rod type connections (dowels, bolts and screws) are most popular. The fasteners are either axially or shear loaded. It should be noted that for timber bridges all metallic parts should have adequate protection against corrosion. Stainless steel dowels are widely used for non-covered bridges, but zinc coating (hot-dipped) is also quite common.

3.5.1.2 Dowel type connection

A dowel is a smooth rod cut in appropriate lengths and is very similar to a bolt, but lacks the threads, nut and head. The dowel cannot transfer forces in the direction of its own rod axis; otherwise the nominal capacity of dowels and bolts is similar. The most effective dowel-type connection is achieved by the use of slotted-in steel-plates where the capacity of the dowel is balanced with the capacity of the wooden layers between the plates. A conceptual model of a dowel type connection is visualized to the left in Figure 3.38, while to the right a similar joint from a bridge is depicted.

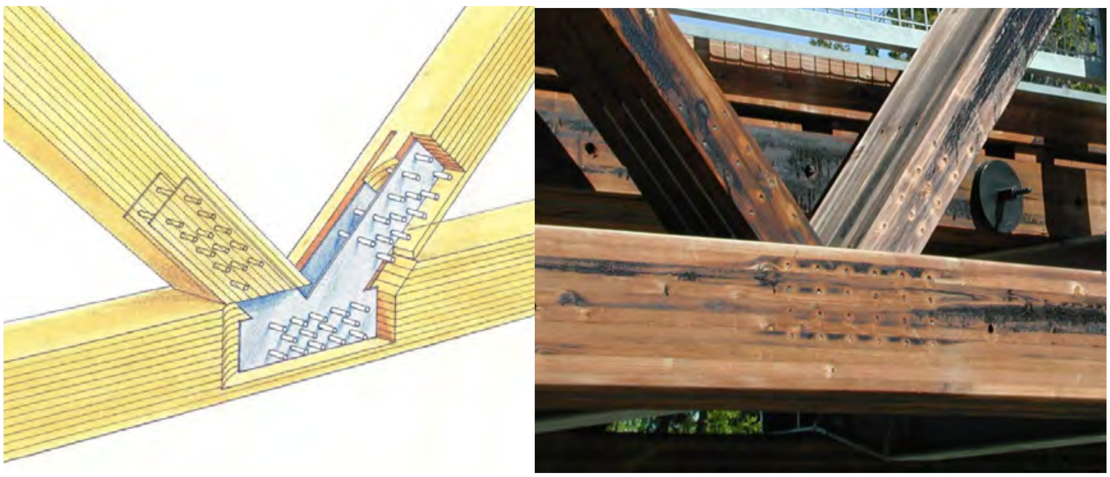

Figure 3.38 Dowel type joint with slotted-in steel plates.

Typically, a shear-loaded connection will transmit forces from a structural member to one or more fasteners, which in turn will transfer the forces to the receiving structural member. This leads to three natural steps in the design of timber connection using fasteners: evaluation of the capacity of the transmitting member, the receiving member, and finally the capacity of the transferring elements, e.g. the fasteners.

There is a number of possible failure modes, as illustrated in Figure 3.39. Failure mode 1) is due to limited embedment strength or capacity of the fasteners; design considerations usually aim at this failure mode since this is the most ductile type of failures. Failure mode 2) is splitting along a row of fasteners in the grain direction; adequate spacing in the fibre direction and end/edge distances minimizes this failure. In addition, a reduced computational capacity is used depending on the spacing and the number of fasteners on rows parallel to the grain. Failure mode 3) should be avoided by use of proper end distance. Failure mode 4) is a block shear failure and may occur in connections with steel plates and numerous and dense groups of fasteners. Failure mode 5) is a tension failure in the net section and may often govern the design capacity. Failure mode 6) is splitting due to tension normal to grain, a load exposure that always should be minimized. However, in many cases, a force component normal to grain occurs and a splitting check should be performed.

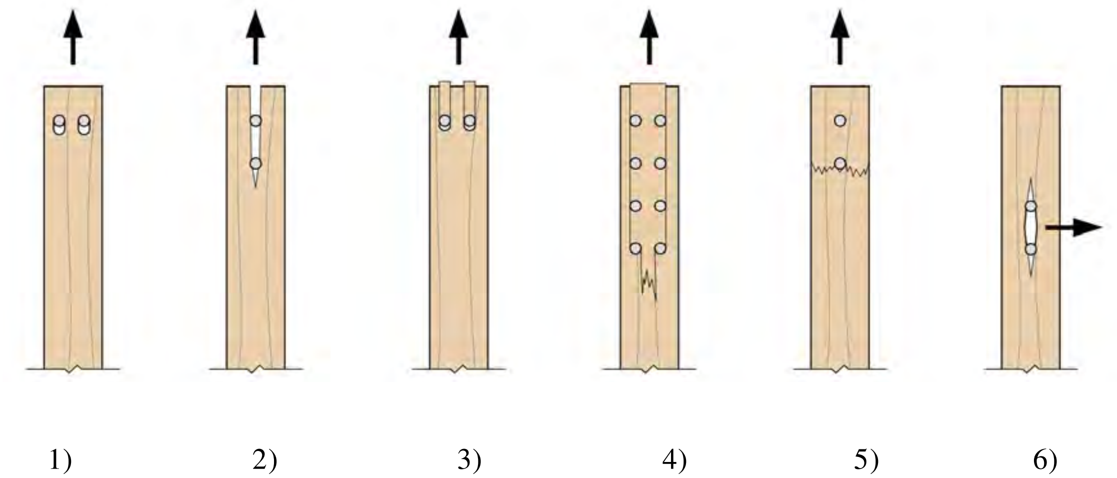

Figure 3.39 Basic failure modes for wood in steel-to-wood dowel type connection.

3.5.1.3 Design expressions for dowel type fasteners with multiple slotted-in plates

Theory for load-carrying capacity of connections using shear-loaded rod-type connections is usually based on work done by K.W. Johansen (Johansen 1949). The theory is based on the assumptions of rigid plasticity where the crushing or embedding strength of the wood as well as the yielding of the rods have perfect rigid plastic behaviour. A set of possible plastic failure mechanisms is visualized in Figure 3.40 for wood to steel connections. For multiple slotted-in steel-plates in a structural wooden member, only failure mechanisms c, d and e on Figure 3.40 are relevant for the external (outermost) shear-planes in a connection, while l or m will govern the internal shear planes.

Eqs.(0.16) give the capacity expressions for the external shear-planes (per shear plane and fastener). Here t_1 is the minimum of the thickness of the external (outer) wooden layer and the penetration depth of the rod, d is the diameter of the rod, $f_{h,k}$ is the characteristic embedding strength of the wood. Note that the embedding strength $f_{h,k}$ is dependent on the angle between grain and the force direction in the rod (see in (CEN 1995 2004)). $M_{y,Rk}$ is the characteristic bending strength of the rod.

$$F_{v,Rk} = \min \begin{Bmatrix} f_{h,k} \cdot t_1 \cdot d & \text{(c)} \\ f_{h,k} \cdot t_1 \cdot d \left[\sqrt{2 + \dfrac{4M_{y,Rk}}{f_{h,k} \cdot d \cdot t_1^2}} - 1 \right] & \text{(d)} \\ 2.3 \cdot \sqrt{\cdot M_{y,Rk} \cdot f_{h,k} \cdot d} & \text{(e)} \end{Bmatrix} \qquad (0.16)$$

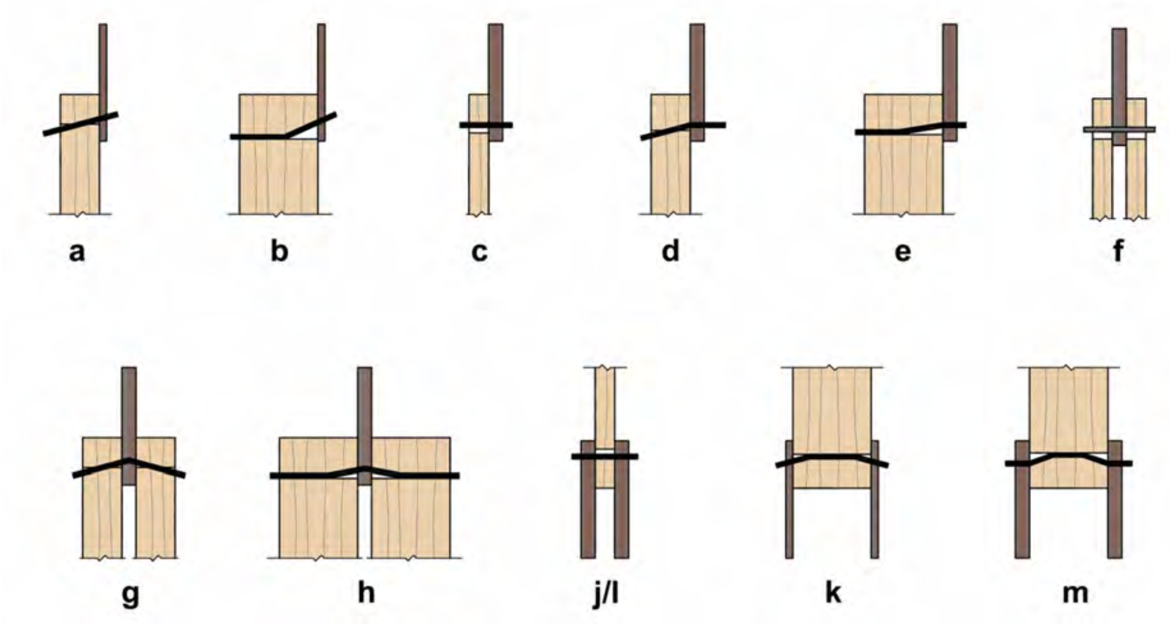

Figure 3.40 Basic failure modes of fasteners for steel-to-wood dowel type connection.

For the internal shear planes, i.e. all shear planes between the outer steel plates, the load carrying capacity per shear plane and fastener is expressed in Eq. (0.17). Note that t_2 is the thickness of the inner wooden layer. Capacity formulations like (0.16) and (0.17) are often denoted European Yield Model (EYM) and more on this may be found in (CEN 1995 2004).

$$F_{v,Rk} = \min \left\{ \begin{array}{ll} 0.5 \cdot f_{h,k} \cdot t_2 \cdot d & \text{(l)} \\ 2.3 \cdot \sqrt{\cdot M_{y,Rk} \cdot f_{h,k} \cdot d} & \text{(m)} \end{array} \right\} \tag{0.17}$$

3.5.1.4 Design of joints

The distribution of forces in a joint is dependent on the combination of shear and axial forces as well as the moment actions. One of the following failure modes usually limits the transfer of forces by rod-type fasteners:

a) the most loaded fastener relative to the directional dependent strength $F_{V,Rk}$;
b) splitting normal grain due to a resulting force component normal grain (Design check by Equation (0.14));
c) splitting along a row of fasteners parallel grain due to the rod force components acting along the row.

The design check for splitting along a row of fasteners parallel to grain is performed by a computational reduction of the number of fasteners n in the row:

$$n_{ef} = \min \left\{ \begin{array}{l} n \\ n^{0.9} \sqrt[4]{\dfrac{a_1}{13d}} \end{array} \right. \tag{0.18}$$

The effective number of fasteners in the row, n_{ef}, is dependent on the spacing along grain and the size of the fasteners (diameter d).

3.5.2 **Axially loaded fasteners**

3.5.2.1 Eurocode 5

According to EC5 (CEN 1995 2004) (for screws with $d < 12$ mm) the characteristic withdrawal capacity, $F_{ax.Rk}$, is given by (the expression is re-arranged):

$$F_{ax.Rk} = n_{ef} f_{ax.\alpha.k} d \cdot l_{ef} \tag{0.19}$$

The parameter n_{ef} is the effective number of screws and equal to $n_{ef} = n^{0.9}$, where n is the number of screws acting together in a connection. The withdrawal strength parameter, $f_{ax.\alpha.k}$, is given by:

$$f_{ax.\alpha.k} = \frac{f_{ax.90.k}}{1.2 \cdot \cos^2\alpha + \sin^2\alpha} \left(\frac{\rho_k}{\rho_a} \right)^{0.8} \quad (\alpha \geq 30°) \tag{0.20}$$

where $f_{ax.90.k}$ is the withdrawal strength parameter perpendicular to the grain which must be experimentally determined according to (CEN 2012), for the associated density ρ_a. EC5 provides no guidelines for the estimation of withdrawal stiffness.

In the technical approval of WB-T-20 rods, Z-9.1-777 (DIBt 2010), the following expression is provided for the withdrawal strength parameter (unit MPa and kg/m^3):

$$f_{ax.k} = 70 \cdot 10^{-6} \rho_k^2 \quad (45° \leq \alpha \leq 90°) \tag{0.21}$$

3.5.2.2 Analytical model

Analytical estimations can be obtained by use of the concept of the classical Volkersen theory (Volkersen 1938), applied for axially loaded fasteners (Jensen, Koizumi et al. 2001). This model has initially been developed assuming that all shear deformation occurs in an infinitely thin shear layer, while the fastener and the surrounding wood are assumed to be in states of pure axial stress. The shear stress-displacement behaviour (τ - δ) of the shear layer is approximated by a linear constitutive law, which is a reasonable approximation for glued-in fasteners.

In the case of screwed-in fasteners, however, it is more convenient to assume a bi-linear constitutive law because these fasteners are by far less brittle than glued-in fasteners and their post-elastic behaviour should not be omitted. The bi-linear constitutive law is presented in Figure 3.41. The bi-linear idealization separates the curve in two distinct domains: the linear elastic domain and the fracture domain. These domains are characterized by the equivalent shear stiffness parameters Γ_e and Γ_f, which are the slopes of the two branches of the bi-linear constitutive law. The advantage of this method is that, apart from the withdrawal capacity and stiffness, it also allows the estimation of the stress and of the displacement distribution for any given withdrawal force level. Thus, an analytical estimation of the force-displacement curve can be obtained. Note that all shear deformation is assumed to occur in a shear zone of finite dimensions. A full description of this method is given in (Stamatopoulos and Malo 2015).

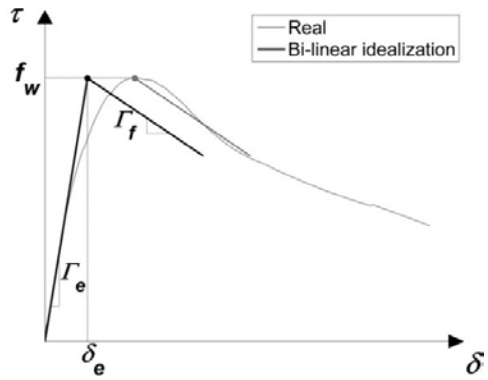

Figure 3.41 Bi-linear approximation of τ-δ curve

The withdrawal stiffness, K_w, and the characteristic withdrawal capacity, $F_{ax.Rk}$, are provided by the following expressions (Jensen, Koizumi et al. 2001, Stamatopoulos and Malo 2015):

$$K_w = \pi d l_{ef} \Gamma_e \frac{\tanh \omega}{\omega} \tag{0.22}$$

$$\frac{F_{ax.\alpha.Rk}}{d l_{ef} f_{ax.\alpha.k}} = \frac{\sin(m\omega\lambda_u)}{\omega m} + \frac{\tanh\{(1-\lambda_u)\omega\}\cos(m\omega\lambda_u)}{\omega} \tag{0.23}$$

Note that these expressions are valid for pull-push or pull-shear loading conditions, but not for the pull-pull loading condition. The parameter m has been introduced as:

$$m = \sqrt{\Gamma_f / \Gamma_e} \tag{0.24}$$

This parameter is a measure of the brittleness of the shear zone. In the limits, $m \rightarrow 0$ indicates perfect plastic post-elastic behaviour, while $m \rightarrow \infty$ indicates totally brittle behaviour. The parameters ω and β have been defined as follows:

$$\omega = \sqrt{\pi d \Gamma_e \beta \cdot l_{ef}^{\ 2}} \tag{0.25}$$

$$\beta = \frac{1}{A_s E_s} + \frac{1}{A_w E_{w.\alpha}} \tag{0.26}$$

where E_s and $E_{w.\alpha}$ are the moduli of elasticity of steel and wood (as function of α), respectively. The core cross-sectional area of the rod is $A_s = \pi \cdot d_1^2 / 4$ and A_w is the area of wood subjected to axial stress. $E_{w.\alpha}$ may be estimated by the Hankinson formula and A_w by an effective area, confer (Stamatopoulos and Malo 2015). The parameter λ_u is a dimensionless length parameter which expresses the percentage of the embedment length (at failure), in which post-elastic behaviour takes place and it can be determined by the diagram in Figure 3.42.

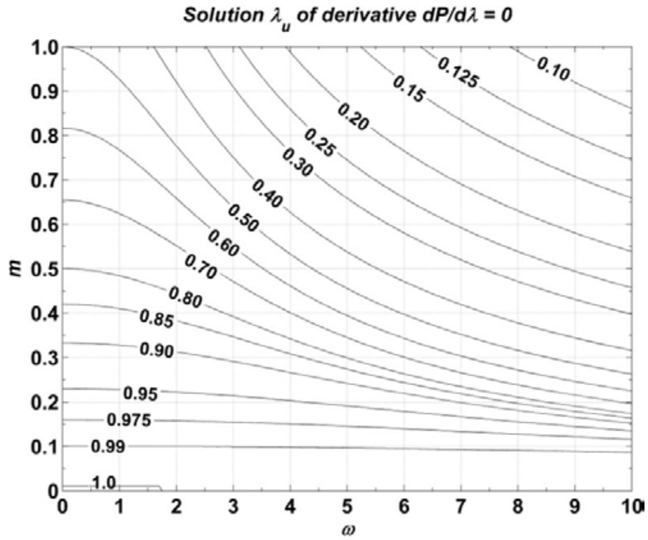

Figure 3.42 Diagram for the determination of parameter λ_u

The parameters Γe (in MPa/mm) and m are provided as functions of α, by the following expressions (Stamatopoulos and Malo 2015):

$$\Gamma_{e.\alpha} = \frac{9.35}{1.5 \cdot \sin^{2.2}\alpha + \cos^{2.2}\alpha} \tag{0.27}$$

$$m_\alpha = \frac{m_0}{(m_0 / m_{90})\sin\alpha + \cos\alpha} = \frac{0.332}{1.73 \cdot \sin\alpha + \cos\alpha} \tag{0.28}$$

Finally, $f_{ax.\alpha.k}$ can be calculated by Equation (0.20). A conservative approximation can be made by letting $\lambda_u = 1$ and the right hand side of Equation (0.23) simplifies to only the first term.

3.5.3 **Fatigue loading and resistance**

3.5.3.1 Introduction and overview of European regulations

Fatigue is the process of progressive damaging of a material subjected to repeated loading, resulting eventually in failure at stress levels smaller than the corresponding quasi-static strength. Bridges are predominantly subjected to heavy repeated traffic loading and therefore fatigue verification of their structural components is required. The fatigue strength is typically defined as the number of loading cycles N to fail at a given stress level or stress range. It is usually given on the basis of $S - \log_{10} N$ curves, which are derived by cyclic tests with constant amplitude S (where S represents a given stress level or stress range). A constant cyclic load process can be characterized by the stress range $\Delta\sigma$ and the stress ratio R, respectively defined by:

$$\Delta\sigma = \sigma_{\max} - \sigma_{\min} \tag{0.29}$$

and

$$R = \frac{\sigma_{\min}}{\sigma_{\max}} \tag{0.30}$$

The stress levels $\sigma_{\max}$ and $\sigma_{\min}$ are the numerically maximum and minimum stresses, respectively.

The fatigue life of wooden structures is largely dependent on the stress ratio R. The values of R typically range between -1 (fully reversed loading) and +1 (quasi-static loading). For wooden materials, decreasing values of R lead to decreased fatigue life. Fully reversed loading (R = -1) typically results in largest fatigue strength reduction. The stress ratio R is closely related to the mean stress and the stress range as follows:

$$\sigma_{mean} = \frac{\Delta\sigma}{2} \cdot \frac{1+R}{1-R} \tag{0.31}$$

For some materials, if the stress level, or the stress range, is below a certain limit, the fatigue life can be considered as unlimited. This stress limit is called fatigue limit or endurance limit. There is no available experimental evidence regarding the validity of endurance limits for wooden materials. On the other hand, there is not known many structural failures in wooden parts of bridges which can be related to the fatigue phenomenon. For connections in timber structures the fatigue life typically appears to be shorter than that of the base wooden materials.

Note that metal components or metal parts in timber bridge connections shall comply with the fatigue requirements for the metals.

3.5.3.2 Traffic loads on road bridges

Traffic running on bridges produces stress spectra depending on the geometry of the bridge as well as the vehicles, the axle loads, the vehicle spacing, the traffic composition and possible dynamic effects.

European standards provide five different fatigue load models for road bridges. These are specified in EN 1991-2 (CEN 2003) and intended for evaluations of stress ranges and stress range spectra. Note that these models neglect the influence of the mean stress (or the stress ratio R).

Fatigue load models 1 and 2 are described as follows:

- **Fatigue load model 1 (FLM1):** FLM1 is a reduced version of the static load model 1 (LM1) and applies a certain percentage of the characteristic static loads (70% of the concentrated axle load and 30% of the uniformly distributed load) as fatigue loading.
- **Fatigue load model 2 (FLM2):** FLM2 consists of a set of 'frequent' lorries. The maximum and minimum stresses should be determined from the most severe effects of the different lorries, separately considered. The use of FLM2 is similar to FLM1, but FLM2 is more accurate than FLM1, which is rather conservative.

The intention of both fatigue load models 1 and 2 is to check whether the fatigue life can be considered as unlimited when a constant amplitude fatigue limit (S-$\log_{10}N$ curves) is given.

There are currently (2017) no normative rules given for fatigue evaluation of timber structures in Europe. An informative Annex for the fatigue verification of timber bridges is provided by EN 1995-2 (CEN 2004). According to EN 1995-2 (CEN 2004), a simplified fatigue verification can be performed by evaluation of a stress ratio κ, defined as the ratio between the maximum stress range $\Delta\sigma = \sigma_{d,\max} - \sigma_{d,\min}$ and the fatigue design stress $f_k / \gamma_{\mathrm{M},fat}$, given by

$$\kappa = \frac{\left|\sigma_{\mathrm{d,max}} - \sigma_{\mathrm{d,min}}\right|}{\dfrac{f_{\mathrm{k}}}{\gamma_{\mathrm{M,fat}}}} \tag{0.32}$$

In Equation (0.32), $\sigma_{d,\max}$ and $\sigma_{d,\min}$ are the numerically maximum and minimum design stresses respectively, f_k is the corresponding characteristic quasi-static strength and $\gamma_{M,fat}$ is the material partial factor for fatigue loading. Either FLM1 or FLM2 should be used to evaluate $\sigma_{d,\max}$ and $\sigma_{d,\min}$.

The stress ratio κ, given in Equation (0.32), should not be greater than the limit values provided by Table 3-3 for various types of loading on details or components in order to avoid a more accurate fatigue evaluation. Actually, these limiting values imply endurance limits although there is in fact very little experimental evidence available on the existence of endurance limits for timber structures. Furthermore, the stress ratio κ is evaluated on the basis of a stress range although experiments show that the stress level might be more relevant. The evaluation of κ can only implicitly take notice of the important influence of the stress ratio R (or mean stress) by careful estimation of limiting values. The use of FLM1 and FLM2 together with endurance limits should be used with great caution.

Table 3-3 Limit values of ratio κ (CEN 2004)

Type of loading or connection	**Limit value of ratio κ**
Members in compression parallel or perpendicular to grain	0.60
Members in bending or tension	0.20
Members in shear	0.15
Connections with dowels	0.40
Connections with nails	0.10
Other connections	0.15

Fatigue load models 3, 4 and 5 are models for fatigue life assessment in combinations with available fatigue strength curves giving the constant stress amplitude fatigue limits. Briefly, their characteristics are as follows (EN 1991-2):

- **Fatigue load model 3 (FLM3):** FLM3 is a simplified model. It consists of four axles, each of them having two identical wheels. The force from each axle is 120 kN and the contact surface is 0.40x0.40 m^2.

- **Fatigue load model 4 (FLM4):** FLM4 consists of sets of standard, equivalent lorries which simulate traffic deemed to produce damage equivalent to actual traffic distribution.

- **Fatigue load model 5 (FLM5):** In FLM5 traffic loads are derived directly by recorded traffic data by use of appropriate statistical and projected extrapolations.

Fatigue load models FLM1, FLM2 and FLM3 result in constant amplitude loading, while FLM4 and FLM5, consisting of different lorries, result in varying stress amplitudes with different number of cycles. If the stress amplitude varies, the use of a damage accumulation rule is required. The simplest damage accumulation rule is the linear damage accumulation (Palmgren-Miner rule (CEN 2004)):

$$D = \sum_{\mathrm{i}} \frac{n_{\mathrm{i}}}{N_{\mathrm{i}}} \leq 1 \tag{0.33}$$

where n_i is the actual number of cycles at a given stress level or stress range, and N_i is the corresponding number of cycles at failure. Usually a statistical distribution or spectra of the exposure of cycles and stress levels or ranges should be used to evaluate the accumulated damage D .

It is usually assumed that most fatigue damage is caused by the heavy traffic on the bridges. A simplified estimation of loading cycles for load models FLM3 and FLM4 has been made by evaluating the annual number of heavy vehicles on the bridge (traffic on slow lanes). Typical patterns of traffic have been worked out, categorizing the traffic into Traffic Categories (TC). EN 1991-2 gives the recommendations stated in Table 3-4 where N_{obs} is the annual number of heavy lorries.

Table 3-4 Traffic categories and indicative N_{obs} values per year and per slow lane (CEN 2003)

Traffic Categories		**N_{obs} per year and per slow lane**
TC1	Roads and motorways with 2 or more lanes per direction with high flow rates of lorries	$2.0 \cdot 10^6$
TC2	Roads and motorways with medium flow rates of lorries	$0.5 \cdot 10^6$
TC3	Main roads with low rates of lorries	$0.125 \cdot 10^6$
TC4	Local roads with low rates of lorries	$0.05 \cdot 10^6$

By use of FLM3 a constant amplitude loading is obtained, but note that the intention behind FLM3 is to produce stress ranges and not stress levels. The use of stress ranges is suitable in cases where the mean stress (or R) has no importance like in welded steels, but is questionable for wooden structures. However, given that the constant amplitude stress levels can be estimated, a simplified fatigue verification can be performed as a stress check in the following way (according to EN 1995-2 (CEN 2004)):

$$\sigma_{\mathrm{d,max}} \leq f_{\mathrm{fat,d}} \tag{0.34}$$

where

$$f_{\text{fat,d}} = k_{\text{fat}} \cdot \frac{f_{\text{k}}}{\gamma_{\text{M,fat}}} \tag{0.35}$$

The strength reduction factor k_{fat} takes into account the strength reduction with the number of loading cycles as well as the effect of the stress ratio R and it is given by the following expression:

$$k_{\text{fat}} = 1 - \frac{1-R}{a \cdot (b-R)} \cdot \log_{10}\left(\beta \cdot N_{\text{obs}} \cdot t_{\text{L}}\right) \geq 0 \tag{0.36}$$

where:

- a and b are coefficients representing the type of the fatigue action provided in (CEN 2004) and are given in Table 3-5;
- β is a factor taking into account the consequences of damage (β = 3.0 for substantial consequences and $\beta = 1.0$ for non-substantial consequences);
- t_L is the service life of the structure according to EN 1990 (CEN 2002);
- N_{obs} is the number of constant amplitude stress cycles per year, see Table 3-4.

Equation (0.36) specifies a log-linear relationship between the strength reduction factor k_{fat} and the total number of stress cycles. It can be re-written in the following format:

$$k_{\text{fat}} = 1 - A \cdot \log_{10} N \tag{0.37}$$

where A is the slope of the fatigue resistance curve and N is the total number of load cycles. By comparison of Equations (0.36) and (0.37) we have:

$$A = \frac{1-R}{a \cdot (b-R)} \tag{0.38}$$

$$N = \beta \cdot N_{\text{obs}} \cdot t_{\text{L}} \tag{0.39}$$

The values of the slope of the fatigue curves for non-alternating loading with $R = 0.1$ are presented in Table 3-5, and the resulting fatigue resistance curves are plotted in Figure 3.43.

Table 3-5 Values of coefficients a and b (CEN 2004)

Type of loading or connections	a	b	$A(R=0.1)$
Compression parallel or perpendicular to grain	2.0	9.0	0.051
Bending or tension	9.5	1.1	0.095
Shear	6.7	1.3	0.112
Connections with dowels ($d \leq 12$ mm)	6.0	2.0	0.079
Connections with nails	6.9	1.2	0.119

The slope A of the fatigue curves are strongly dependent on the stress ratio R, see Equation(0.38), and this dependency is visualized in Figure 3.44.

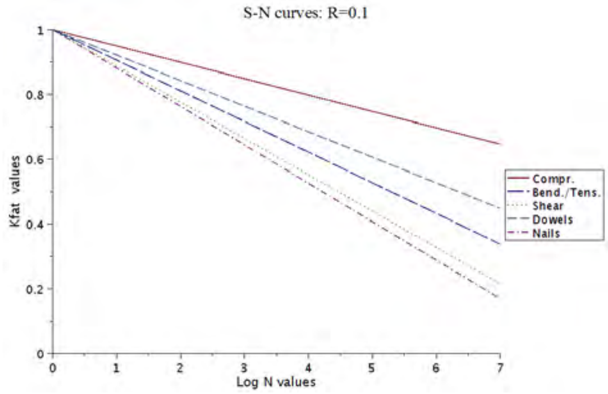

Figure 3.43 S – Log N curves for various stress types or connection types for R = 0.1

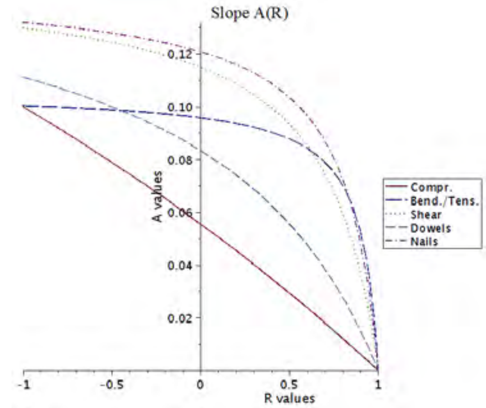

Figure 3.44 Variation of the slopes of the S – Log N curves for various R – values and stress types or connection types

3.5.3.3 Tests of joints with dowels

Joints consisting of slotted-in steel plates (gusset plates) and dowels are widely used in timber bridges. The static and fatigue performance of such joints has been investigated by Malo et al (Malo 1999, Malo 2002, Malo, Holmestad et al. 2006) on the basis of full-scale tests of glulam components with joints at both ends. This study has given experimental verification for the fatigue guidelines of dowelled connections in EN 1995-2 (CEN 2004). In these tests, the joints consisted of two slotted-in steel plates and 12 dowels arranged in a 3x4 configuration. The diameter of the dowels and the holes were 12.0 mm and 12.5 mm, respectively. The thickness of the steel plates was 9.0 mm. Glulam was made of Nordic Pine (*Pinus Silvestris*) with a characteristic bending strength of 30 MPa. The moisture content in all specimens was kept constant to approximately 12%. Tests were performed with a frequency in the range 0.5-4.0 Hz and with two stress ratios, $R = 0.1$ and $R = -1.0$. In total, 48 tests were performed. All specimens were axially loaded parallel to the grain.

The least squares method was used to fit a line on the acquired experimental results. Note that a static ultimate reference test represents only a 1/4 of a loading cycle ($N = 0.25$), and strictly in a logarithmic base 10 scale this leads to $\log_{10}N$= -0.6 for the static reference. The experimental results are plotted for $R = 0.1$ and $R = -1.0$ in Figure 3.45 and Figure 3.46, respectively.

The following log-linear equation was obtained for the stress ratio R = 0.1: $f_{max} = 0.96 - 0.066 \cdot \log_{10} N$. However, the design recommendation in (CEN 2004) is $f_{max} = 1.0 - 0.079 \cdot \log_{10} N$. The corresponding test results and design recommendations for $R = -1.0$ are $f_{max} = 0.941 - 0.098 \cdot \log_{10} N$ and $f_{max} = 1.0 - 0.111 \cdot \log_{10} N$, respectively.

Note that the stresses are not directly evaluated; the obtained results are relative to the static reference capacity of the connection and hence $f_{\max} = F_{\max} / F_{ref}$ is the ratio between load-carrying capacity F_{max} after N cycles normalized to the reference mean value of the static load-carrying capacity (F_{ref} = 410 kN).

From these tests no conclusion could be drawn about the existence of an endurance limit. If existing, the endurance limit would probably be for a number of cycles greater than 10^7.

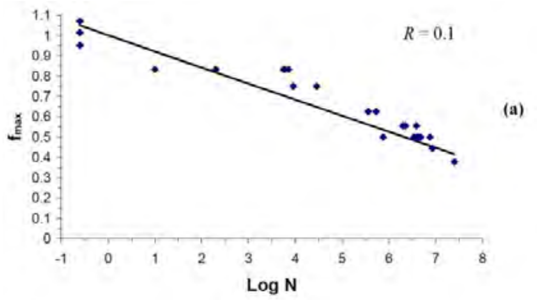

Figure 3.45 S – Log N curves for dowel connections obtained from tests with R = 0.1 (Malo, Holmestad et al. 2006)

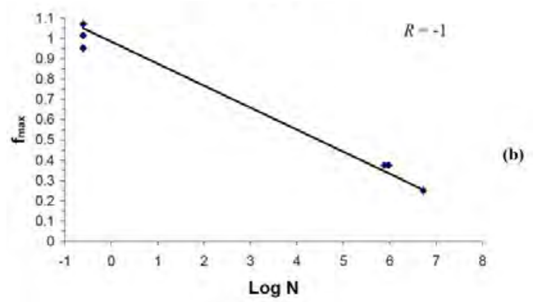

Figure 3.46 S – Log N curves for dowel connections obtained from tests with R = -1 (Malo, Holmestad et al. 2006)

3.5.3.4 Tests of axially loaded threaded rods

The load-carrying capacity and the stiffness of fasteners loaded perpendicular to their axis (e.g. dowels) are limited by the wood embedding strength and stiffness, and by the bending capacity and stiffness of the fasteners. Axially loaded threaded rods feature high withdrawal capacity and stiffness and hence they may be used to develop rigid joints for timber bridges. Stiffer joints at bridge footings can increase the sideways stability of bridges (Wollebæk 2005). Moreover, rigid joints can be used for effective splicing of timber members. Another potential application of axially loaded threaded rods could be the fastening of hangers. An example can be found in the conceptual study of the timber network arch bridge (Malo, Ostrycharczyk et al. 2013).

Today (2017) there is very limited knowledge about the fatigue performance of axially loaded threaded rods or screws. The present version of EN 1995-2 (CEN 2004) does not provide guidelines for the fatigue verification of these fasteners. Axially loaded fasteners at small angles to grain introduce mainly shear stresses along the grain in the timber element they are embedded into. It is therefore reasonable to assume that their fatigue performance depends on the fatigue properties of timber subjected to shear. No comprehensive experimental documentation is currently available although a fatigue curve for shear is given in (CEN 2004), see the continuous line on the plot of Figure 3.47. Their load-bearing capacity is also restricted by the strength of the steel in the rods. A fatigue verification of the steel should be carried out according to EN 1993-1-9 (CEN 2005).

A preliminary experimental investigation of axially loaded threaded rods has been recently carried out at NTNU (Løkken 2016). In this investigation, threaded rods with outer-thread diameter $d = 22$ mm, embedded in glued-laminated timber of strength class GL30c (CEN 14080 2013) at 45º to the grain direction, were tested. Static and fatigue withdrawal tests with stress ratio $R = 0.1$ were carried-out. Regression analysis on the experimental results resulted in the following expression:

$$f_{max} = 0.976 - 0.059 \cdot \log_{10} N \qquad (0.40)$$

where f_{max} is the ratio between the withdrawal strength after N cycles normalized to the quasi-static withdrawal strength. The obtained experimental results are plotted in Figure 3.47 together with the prediction of EN 1995-2 (CEN 2004) for shear. In this case EN 1995-2 (CEN 2004) provides a very conservative prediction of the withdrawal strength. However, further examination at different stress ranges R, lower stress levels and different angles to the grain direction is required to obtain a better insight of the fatigue performance of these fasteners.

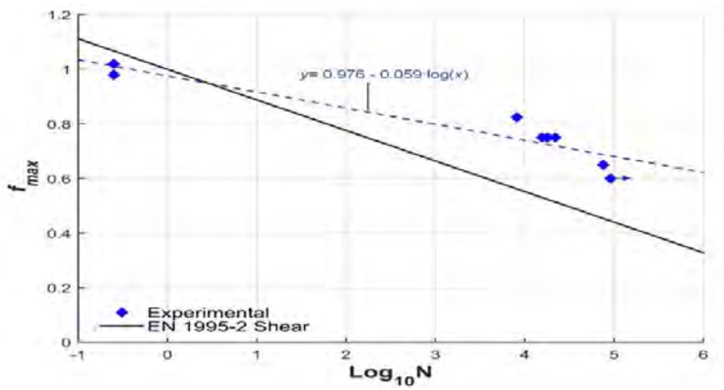

Figure 3.47 S – log$_{10}$N curves for axially loaded threaded rods (R = 0.1); experimental results compared to shear loading curve obtained from (CEN 2004).

3.6 Splicing of large wooden members

The development of glued laminated timber (glulam) enables production of timber elements with nearly unlimited cross-sectional dimensions. The fact that glulam has an excellent strength to weight ratio compared to steel and concrete enables glulam to be used in structures with large spans. However, production and transportation impose limitations on the length of timber elements. In order to obtain large spans, either truss structures or splicing of elements are necessary. Truss structures are characterised by a high number of connections, which are expensive and time consuming. Bridges are exposed to rough outdoor conditions and the connections have increased risk of decay due to moisture and dirt trapping and consequently increased exposure.

Splice joints (in some literature denoted end or butt joints) are connections used to assembly two elements end-to-end to make continuous elements. On building sites, these elements are either connected at its final location in the structure, or pre-connected on the ground and lifted in place in their entire length.

Splice joints are mostly used to carry shear and axial forces and are often considered as pinned joints in the design even though the geometry of connections introduces restriction in rotation and thus they possess a certain bending stiffness. However, it is assumed that the expected rotations are small and that the initial slip of connections allows some rotational deformation without introducing significant stresses. However, recent developments in connection design demonstrate ability to achieve both rotational stiffness and high load carrying capacity as well as ductile behaviour. Feasibility studies of glulam arches with network hanger configuration have shown that large span timber bridges can be achieved

(Bell 2010). In order to maintain stability and reduce buckling problems of the timber arches, it is crucial to incorporate flexural rigidity in the splice connections (Bell and Wollebæk 2004).

In the following, moment resisting splice joints in timber bridges are discussed. Two state-of-the-art splicing solutions are briefly presented and a novel splicing solution making use of long threaded rods is introduced.

By introducing a moment resisting splice joint in timber bridge engineering, new design possibilities can be achieved. Erection of glulam arch bridges with network hanger configuration with spans up to 100 m can be carried out, providing implementation of rotationally rigid splice joints.

3.6.1 **Requirements to moment resisting splice joints in timber bridges**

A splice joint should feature the following properties:

- Sufficient strength and stiffness without significant initial slip
- Fast, easy and reliable mounting process on site (cost competitiveness, production tolerances and quality control)
- Good durability. The joint should have a service life time corresponding to the required life time of the other members of the load bearing structure

3.6.1.1 Sufficient strength and stiffness

With regards to the Ultimate Limit State (ULS) strength verification, the joint should be designed to withstand the actions of the forces acting in the joint (see Figure 3.48). Care must be taken to changing signs of the internal forces (e.g. tension/compression or orientation of bending moments) caused by the position of traffic loads on the bridge, combined actions of wind and traffic load, as well as specific load cases during the erection phase. The compression axial force is often transmitted by direct contact of the end faces. In cases where the space between the end faces shall be filled with mortar, it must be assured that the joint can withstand the temporary loading actions during erection phase, before it is completed with mortar.

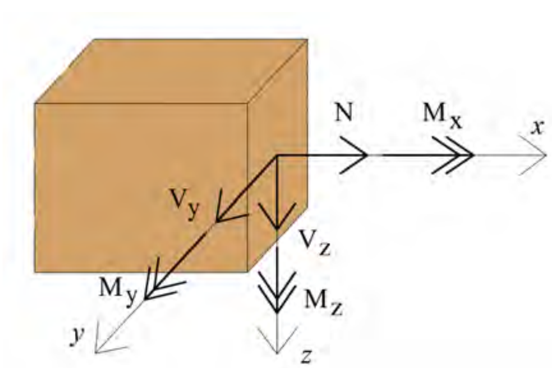

Figure 3.48 Internal forces to be considered in the splice joint design

In large timber cross sections, it may be advantageous to split the action of bending moment into tension and compression normal forces as shown in Figure 3.49 (see also example of application in Figure 3.54.). For connections with slotted-in steel plates and dowels, this leads to a reduction of force components perpendicular to grain, and thus it reduces the risk for splitting of timber. Moreover, a stiffer connection can be achieved, since the embedment stiffness of dowels (known also as foundation modulus) is approximately two times higher in the direction parallel to grain compared to the direction perpendicular to grain (Gattesco and Toffolo 2004).

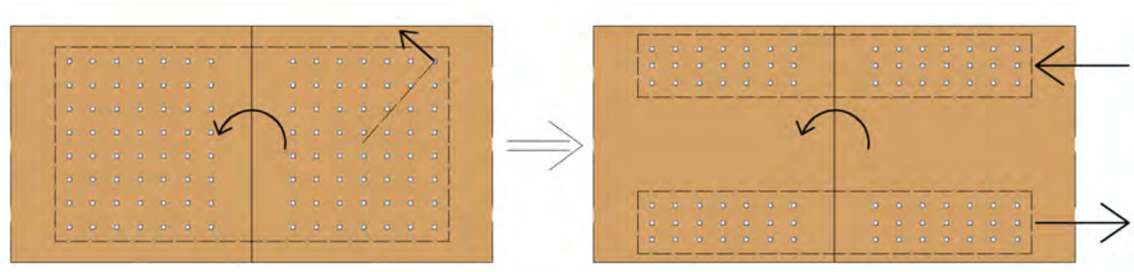

Figure 3.49 Geometry layout of moment resisting joints with slotted-in steel plates and dowels

3.6.1.2 Rotational stiffness and ductility

For statically indeterminate structures, the load distribution is affected by slip in the joints. Therefore, stiffness of the joints has to be considered also in the ULS verifications. If splice joints are placed in arches, flexural rigidity of the joints is necessary in order to maintain stability and reduce buckling problems of the timber arches. The rotational stiffness is mainly governed by a load-slip behaviour of the individual fasteners. Axially loaded fasteners (screws, threaded rods and glued-in rods) feature higher stiffness and lower initial slip compared to the dowel-type fasteners (bolts, dowels). Moreover, the prediction of the rotational stiffness for joints with axially loaded fasteners is more reliable due to absence of clearances in the holes for fasteners. An example of how to determine the rotational stiffness for joints with long threaded rods is given in Section 3.6.3.

Ductile failure modes in joints are preferred due to significant deformations before failure, and consequently visible signs of close-to-failure state occur. The brittle failure is, on the contrary, characterized by a sudden failure without “warning” before the collapse. See discussions on design provisions in Sections 3.6.2 and 3.6.3.

3.6.1.3 Detailing with respect to moisture-induced stresses

The change of moisture content in wood is associated with shrinkage and swelling deformations. Due to the anisotropy of wood, these moisture-induced deformations are typically 15-30 times larger in directions perpendicular to grain than those parallel to the grain (Thelandersson 2003). The presence of steel fasteners may restrain the moisture-induced deformations and thus cause moisture-induced stresses in the timber cross-section. Such stresses are often negligible in the direction parallel to grain, where also the strength is high. However, in the direction perpendicular to grain, the moisture-induced stresses are significantly larger, and together with the low strength in this direction, this can cause splitting in the joint area. Due to the strong moisture transport mechanism in the grain direction, joints in timber bridges are susceptible to moisture variation, being located close to the end grain. Experiments show that the load carrying capacity of joints with slotted-in steel plates and dowels is reduced due to moisture-induced stresses perpendicular to grain (Sjödin and Johansson 2007). Increased spacing between the dowels in a direction perpendicular to grain (thus increasing the joint size), resulted in a reduction of load carrying capacity and increased the occurrence of moisture-induced cracks. With reference to Figure 3.49, the geometry layout to the right is therefore superior to the layout to the left, considering moisture-induced stresses propagation.

3.6.1.4 Learning from failure – Perkolo bridge, Norway

On February 17, 2016, Perkolo bridge collapsed under the weight of a timber truck, see Figure 3.50. The bridge, a glulam truss bridge with a span of 47,5 m and a stress laminated timber deck on steel crossbeams, was an overpass bridge on a new stretch of the E6 road in Gudbrandsdalen: the main road between Oslo and Trondheim in Norway. Luckily the new stretch of the road had not yet been opened for traffic, and the truck driver came away with only minor injuries.

Figure 3.50 Perkolo bridge hours after the collapse (Photo: R. Abrahamsen)

A drawing of the bridge is shown in Figure 3.51. The top and bottom chords of the truss, which were massive glulam beams with cross sections of 575 by 630 mm, were spliced at joints 17 and 5, respectively.

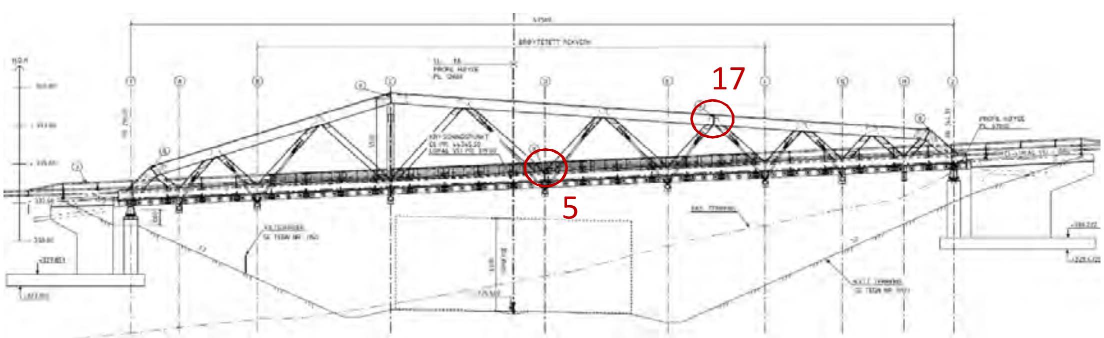

Figure 3.51 The Perkolo bridge truss – chord splices at joints 5 and 17

A grossly undersized splice joint in the bottom chord (joint 5) caused the failure. The joint consisted of four slotted in steel plates (12 mm thick) and steel dowels (12 mm diameter), see

Figure 3.52. For the used number of dowels, the joint capacity was only about 25% of the design tensile force in the chord. The bridge could in fact have failed due to dead weight only.

It appears that the design engineer misread the transfer of forces in the joint. As designed, the joint was capable of transferring only the *difference* in tension between the two parts of the chord. This collapse, which was due to human error, should of course never have happened. However, far more serious than the error itself, is the fact that it was not picked up by neither the internal, nor the external design controls.

The same mistake was also made at the splice joint in the upper (compression) chord, but here the manufacturer of the glulam truss prevented a joint failure by injecting an acrylic mortar in the gap between the two chord ends (this was not prescribed by the design engineer).

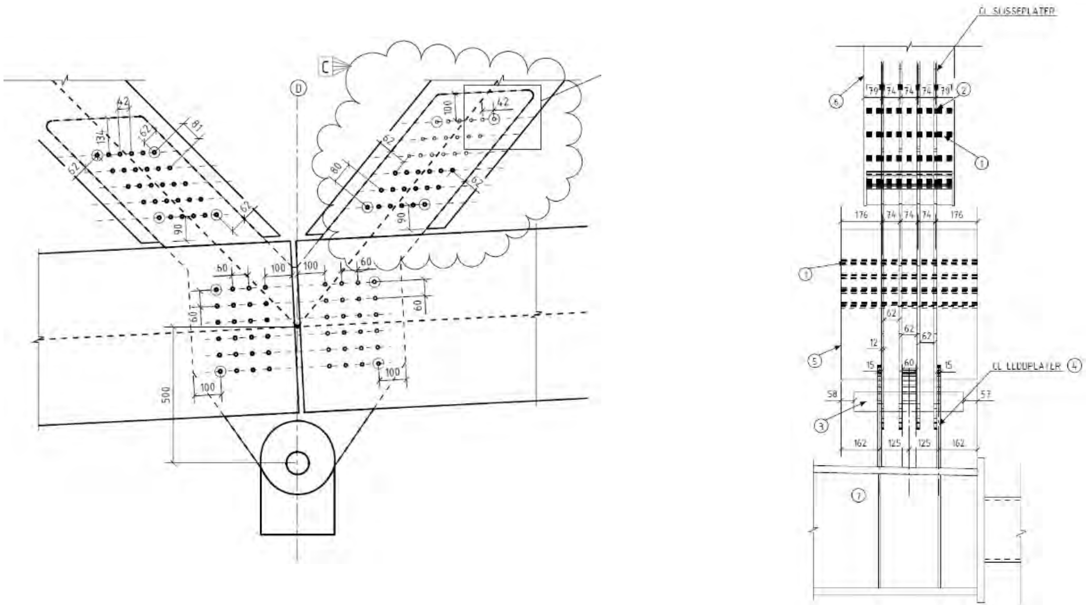

Figure 3.52 The splice joint in the bottom (tension) chord – joint number 5

So what is the lesson here? Apart from not making gross mistakes and perform proper controls, it is perhaps wise to take a closer look at the joint. The right-hand side of Figure 3.52 shows that the width of the diagonal is much smaller than that of the chord. This limits the number of steel plates to four, while the chord could easily accommodate six plates. To transfer the large tensile force in the chord with only four plates will require a very long joint. A possible alternative is to supplement with two plates just in the chord. However, this makes a more complex force transfer in the joint.

Another, and in our view better solution, is to move the splice joint in the chord away from the truss joint. This will require an extra joint, but the splice joint will be simpler and more effective (due to more steel plates), and also the truss joint will be simpler and more straightforward. Another argument in favour of this solution is that, if chosen, the bridge would probably have been standing today!

3.6.1.5 Durability

Due to moisture exposure and limited drying possibilities, connections in timber bridges present an increased risk with respect to decay. A splice joint in a large timber bridge is difficult to inspect and repair possibilities are very limited. The joint should therefore be designed to have a life time corresponding to the required life time of the members of the load bearing structure (NPRA 2016). Proper detailing is essential and attention should be paid to the following recommendations:

- The joint area should be kept dry and in case of water ingress, rapid drying through ventilation should be allowed.
- Any form of free standing water, or spaces where dirt can accumulate in contact with timber surfaces should be avoided.
- Steel parts in the connections should have anti-corrosion treatment (use properly galvanized or stainless steel).
- The upper faces of timber members should be covered (application of cladding at side faces of timber members is also favourable).
- The end faces of timber members should be well protected from leaking water, because of the strong moisture transport mechanism in the grain direction. Epoxy mortar is often used to fill the space between the timber members for timber bridges due to ease of application. However, cases with poor joint durability have been reported (Burkart 2016). Deterioration of mortar allows water leakage into gaps between timber elements, causing fast decay development and eventually joint damage. Weathering degradation and creep of acrylic mortar in joints under compression can lead to overload of the fasteners not designed to carry the full compression force (joints with dowels).
- CNC cutting machines allow very precise manufacturing of timber interface planes. A study by (Cepelka and Malo 2016) shows no reduction of the axial capacity, nor the stiffness in case of direct timber-to-timber contact of the end faces.

3.6.2 State-of-the-art splicing solutions

There are various examples of use of moment resisting splice joints in the building industry. These are mostly placed in planar structures (frames, arches) and indoor conditions. There are fewer examples of splice joints used in timber bridges. Two connection techniques with possible application for timber bridges are shortly presented herein. More details together with additional splicing techniques can be found in (Cepelka and Malo 2014).

3.6.2.1 Slotted-in steel plates and dowels

Timber elements are connected via steel plates which are mounted to timber by dowel type fasteners. Steel plates can either be placed externally (forming steel brackets) or slotted into the timber members. Steel brackets are, due to durability issues, not recommended for use in timber bridges since they give limited moisture dry-out possibilities at the interface between steel and timber. Weathering exposure of steel/timber interface is avoided by slotting steel plates inside the timber elements. Connection techniques using slotted-in steel plates and dowels have been widely used in modern timber bridge design. The joint is usually built up of several steel plates of thickness 8 or 10 mm and dowels of diameter 10, 12 or 16 mm (NPRA 2016).

The technique is commonly used to carry axial and shear forces as for example in joints in truss structures and hinges in arches. Figure 3.53 shows a splice joint used in Kjøllsæter

Bridge, Norway. This is a typical example of a joint in a truss structure transmitting axial forces by use of slotted-in steel plates and dowels. The gap between the end faces of compression members is filled with acrylic mortar which allows direct contact force transmission.

However, there are not many examples of splice joints transmitting bending moments. Figure 3.54 shows a moment resisting splice joint used in Leonardo Footbridge, Norway. Slotted-in steel plates and dowels at top and bottom edge together with a shear key placed in the middle of the sections are implemented to carry bending moments and shear force, respectively. The shear key consists of a welded steel gusset connected to the timber by a combination of transversal dowels and rods glued-in from the end face. The axial compression force is transmitted by contact of end faces where the gap between the elements was filled with acrylic mortar.

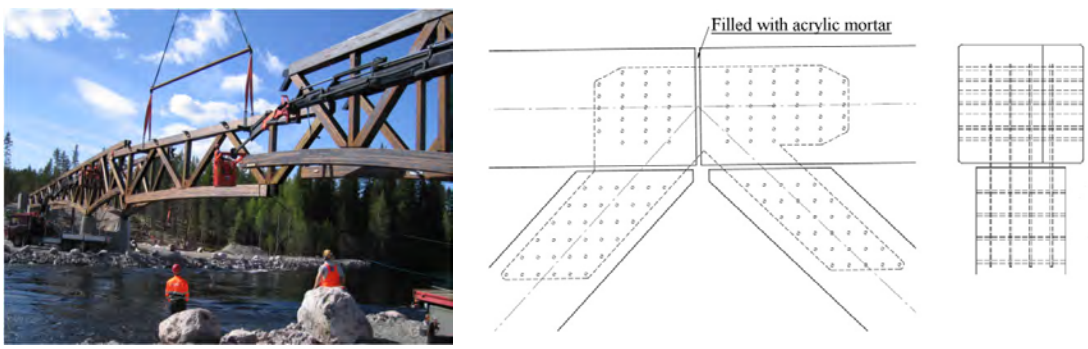

Figure 3.53 Kjøllsæter Bridge (2005), Norway, left: truss structure under assembly, centre and right: detail of connection at the top chord, source: Moelven Limtre AS and Sweco AS

When transmitting bending moments, dowel-type fasteners impose concentrated local forces in timber in an angle to the grain (Augustin 2008). The bending resistance is then governed by a combination of tension perpendicular to grain and longitudinal shear stresses – the two weakest strength properties of wood. Risk of a local failure by tension perpendicular to grain, so-called “splitting”, is related to the spacing between fasteners, the size and the number of fasteners in a row parallel to the grain, confer Section 3.5.1.4. Increasing the number of fasteners parallel to the grain increases the risk of splitting. Splitting tendency can also be initiated by shrinkage cracks. The failure mode by splitting is brittle, resulting in a low ductility of the connection. Adequate spacing and end-distances must be ensured to prevent splitting of timber. Requirements to the spacing of the fasteners often lead to large area connections and thus increase the necessary timber dimensions.

Figure 3.54 Leonardo Footbridge (2001), Norway, left: the central arch under assembly, right: visualisation of the splice joint

For moment resisting connections, stiffness and ductility play major roles in addition to capacity. Although the holes to accommodate dowels should be tight-fitting to allow for a direct contact between dowel and timber, material tolerances and requirements regarding mounting make tight-fitting difficult. Moreover, if a dowel fits too tight in its hole, splitting can be initiated. In general, a higher number of thinner plates and smaller diameter of dowels provide a smoother stress distribution and a more ductile behaviour.

Reinforcement perpendicular to grain can reduce the risk of splitting, and thus ensure ductility and reduce the required spacing of dowels. The load-carrying capacity will also increase considerably (Larsen 2003). Recent research reports show an excellent reinforcing effect of self-tapping screws placed perpendicular to grain. A highly ductile behaviour and remarkable rotation capacity of splice connections in tensile and bending tests are reported by (Brühl and Kuhlmann 2012)

3.6.2.2 Glued-in rods

Load transfer from rods embedded lengthwise in timber is characterized by a good “flow-of-forces”. Stress distribution is provided by means of shear stresses along the rods. The rods are fully embedded in timber members and thus protected. The predrilled holes are filled with epoxy resin and there is therefore no clearance between bars and wood. Initial slip is thus avoided. High strength epoxy resins are available on the market. High stiffness and pull-out capacity can be achieved. For large joints, multiple rods are necessary and the brittleness of the adhesive can lead to a progressive failure in groups of rods. Ductility is therefore an issue. A very ductile behaviour was achieved by use of low grade steel bars in experimental tests by (Gattesco, Gubana et al. 2010).

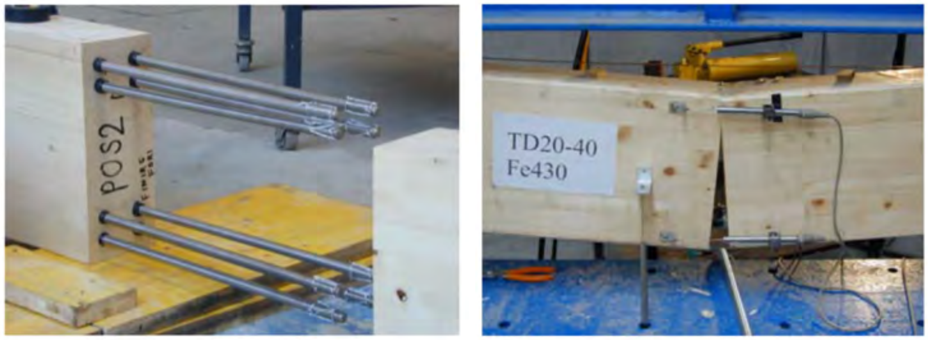

Figure 3.55 Splice joint with glued-in rods, left: rods glued into one member of the joint, right: deformation of the joint, (Gattesco, Gubana et al. 2010)

The major shortcoming associated with application of glued-in rods in load-bearing structures is the uncertainty regarding the installation of the rods. For the example shown in Figure 3.55, the rods were put into the holes using a wire guide to centre them. The epoxy was injected through holes drilled perpendicularly to each embedment hole near its end. The effectiveness of the grouting operation cannot be visually checked. Experience from investigations of failed joints shows that inadequately mixed and incorrectly applied epoxy on site are likely to happen and this therefore limits the production to climate controlled environment with quality control and skilled personnel (Tlustochowicz, Serrano et al. 2011).

A jointing technique combining glued-in bars and pinned steel connections is presented in (Gehri 2010). The principle of this so-called GSA®-technology is shown in Figure 3.56. Rods are glued to timber sections in factory conditions with welded or screwed special steel pin-joint at the end. Pinned steel-to-steel connection is thus created with very fast on-site mounting. The ductile behaviour is achieved by a combination of low-grade steel and pre-defined glue-free deformation zone of rods. Uneven distribution of forces in a group can thus be absorbed by plastic deformation of rods.

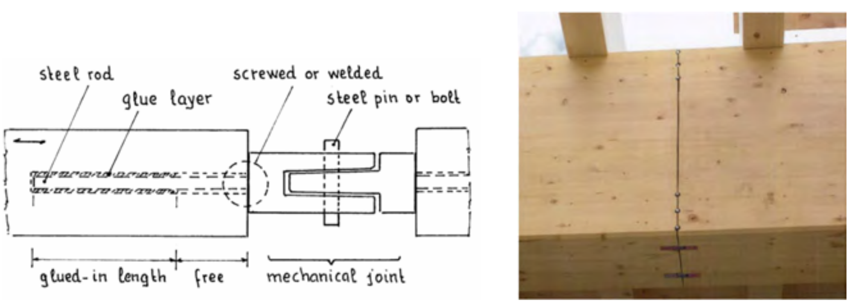

Figure 3.56 GSA®-technology, left: the principle of joint, right: moment-resisting splice joint of a beam,(Gehri 2010)

Figure 3.57 shows a splice joint by glued-in rods placed at the apex of a 2-hinged arch road bridge in Switzerland. The glulam arch was later protected by cladding applied both at the top and the sides.

Figure 3.57 Example of application of glued-in rods in the apex of an arch bridge, Kirchenbrücke, 2009, Switzerland, source: www.swiss-timber-bridges.ch

Connections with glued-in rods present complex systems with unpredictable stress distribution, since three different materials with distinctly different properties are combined. Despite many research projects, there are still issues that have not been clarified and for which common agreement has not been reached. As a result, there are still no universal design rules and technical guidelines. In 2003, it was decided to discard the Annex C in Eurocode 5-part 2 (CEN 2004), which was dealing with design of glued-in rods. There are, up to date, no design rules in the current version of Eurocode 5. The prediction of rotational stiffness and moment capacity for a splice joint with glued-in rods is given i.e. in (Jensen and Quenneville 2009).

3.6.3 A novel splicing solution by use of long threaded rods

3.6.3.1 Glue couplers

The recent research at Norwegian University of Science and Technology, NTNU, has dealt with application of long threaded rods as fasteners in timber splice connections subjected to a bending moment. The main objective of the research project has been to develop a splice that allows practical and reliable on-site splicing of large timber sections of glulam arch bridges. The dominating internal force in such structures is compression, which can be transferred by direct contact of timber end faces. Shear force can be transferred via shear keys. The design utilizes high withdrawal stiffness and has virtually no initial slip. The use of threaded rods can give rotationally stiff joints that can transfer moderate bending moments. By providing sufficient effective length, the failure mode is yielding of the steel rods. This enables a more reliable prediction of the structural properties and increased ductility of the joint.

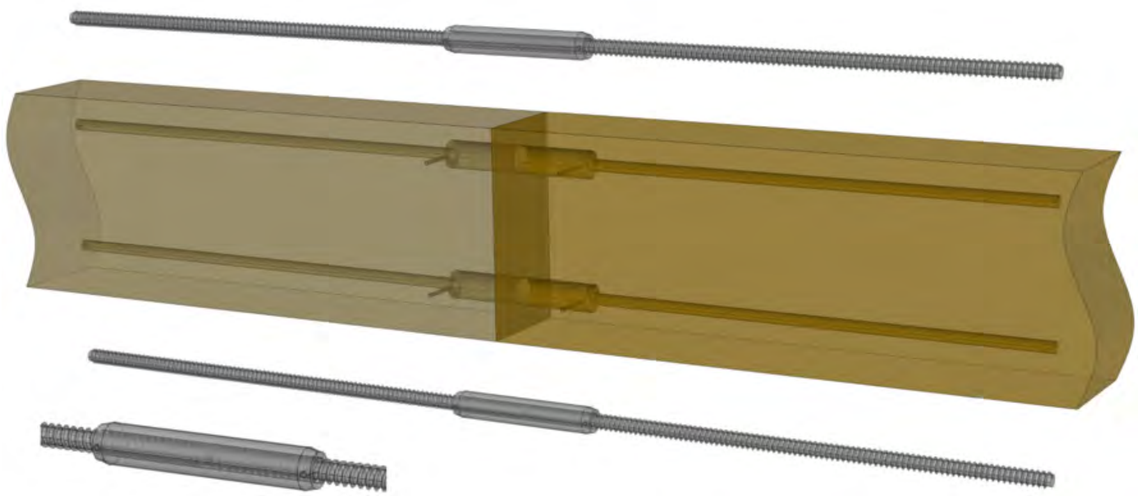

Figure 3.58 Schematic layout of splice connection with long threaded rods and grout-filled couplers

Figure 3.58 shows a prototype splice joint using long threaded rods inserted parallel to the grain. Grout-fill steel couplers (similar to systems used for reinforced pre-cast concrete) were used for a mutual connection of the long threaded rods inserted in the opposed parts of timber beams. The steel couplers were purpose-made and manufactured from common structural steel. Two-component epoxy adhesive was used for grouting. Experimental and numerical investigations were carried out in order to determine the rotational stiffness and the moment capacity of the splice joint. Based on those, analytical relations for determining the rotational stiffness and the moment capacity are proposed, and are here briefly summarized in the following. More details can be found in (Cepelka and Malo Submitted 01/2017).

In the present analytical model, the relative rotation of the end faces of the splice connection is approximated by a relative rotation of the end sections of a beam portion of length $2l_c$. Figure 3.59 shows a deformed splice connection with a relative rotation θ of the end faces caused by the bending moment M. Here h and b are height and width of cross-section respectively, a_0 is the height of wood in compression, a_i is a coordinate along z-axis of i-th row of rods determined from the upper edge of wood in compression, l_c represents an equivalent length of compression zone at each side of the connection, σ_x is normal stress in wood, K_{si} is axial stiffness of the i-th row of the rods and u_i is horizontal displacement at the the i-th row of the rods.

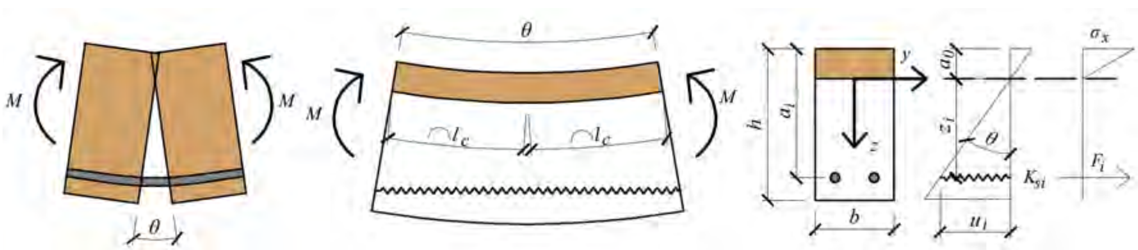

Figure 3.59 Characteristics of the analytical model

The height of wood in compression (position of neutral axis) is obtained by the following equation:

$$a_0 = \frac{-\sum_{i=1}^{n} K_{si} + \sqrt{\left(\sum_{i=1}^{n} K_{si}\right)^2 + \frac{E \cdot b}{l_c} \cdot \sum_{i=1}^{n} K_{si} \cdot a_i}}{\frac{E \cdot b}{2 \cdot l_c}} \tag{0.41}$$

E is modulus of elasticity of timber parallel to the grain.

The z-coordinate of the the i-th row of steel rods z_i is:

$$z_i = a_i - a_0 \tag{0.42}$$

The rotational stiffness of the connection k_θ is obtained as:

$$k_\theta = \frac{M}{\theta} = \sum_{i=1}^{n} K_{si} \cdot z_i^2 + \frac{E \cdot b \cdot a_0^3}{6 \cdot l_c} \tag{0.43}$$

The equivalent length of compression zone, l_c, is given by the following equation (Cepelka and Malo Submitted 01/2017):

$$l_c = 0{,}85 \cdot h + l_{cr} \cdot \frac{E}{E_{cr}} \tag{0.44}$$

where E_{cr} is crushing modulus and l_{cr} is a crushing length.

The axial stiffness of the i-th row of steel rods, K_{si}, corresponding to the layout shown in Figure 3.58, is given by Equation (0.45). K_{si} is obtained as an effective stiffness of a system of three springs representing the axial withdrawal stiffness of the threaded rods at each side of the connection, denoted K_w, and the axial stiffness of the joint of threaded rods in the rod coupler, denoted as K_{co}. The number of steel rods in one row is denoted as n_r.

$$K_{si} = n_r \cdot \frac{K_w \cdot K_{co}}{2 \cdot K_{co} + K_w} \tag{0.45}$$

The moment capacity is obtained from the moment equilibrium of compression and tension force acting at the joint:

$$M_u = \min(F_{tu}; F_{cu}) \cdot \mathrm{z}_c \tag{0.46}$$

where F_{tu} and F_{cu} are the ultimate strengths of components in tension and compression, respectively, and z_c is the lever arm of the internal forces.

The ultimate strength of the compression zone, F_{cu}, is:

$$F_{cu} = \frac{1}{2} \cdot b \cdot a_0 \cdot f_{c,0} \tag{0.47}$$

where $f_{c,0}$ is the timber strength in compression parallel to the grain.

Assuming that the joint of threaded rods, in rod couplers, has a higher capacity than the rods themselves, the ultimate strength of the tension component is found as:

$$F_{tu} = n_r \cdot \min(R_{axu}; R_u) \tag{0.48}$$

where R_u is the tensile strength of the rods (provided by the manufacturer) and R_{axu} is the ultimate withdrawal strength of threaded rods and is found by:

$$R_{axu} = R_{ax} \cdot \left(\frac{l - l_x}{l} \right) \tag{0.49}$$

where R_{ax} is the withdrawal strength of threaded rods (see Section 3.5.2 and (Stamatopoulos and Malo 2015)), l is the length of the threaded rods (length of the rod screwed in timber), whereas l_x is a free length of rod that is not contributing to the withdrawal capacity (as a consequence of the induced rotational restraint at the plane of symmetry of the joint). For rods inserted parallel to the grain l_x can be found by:

$$l_x = \frac{5}{8} \pi \cdot d_1 \cdot \sqrt[4]{\frac{\pi \cdot E_s}{k_t}} \tag{0.50}$$

where d_1 is the core diameter of the threaded rods, E_s is the elastic modulus of steel and k_t is the foundation modulus of timber transverse to the grain.

With reference to the performed experimental work as presented in (Cepelka and Malo Submitted 01/2017), the following input parameters were determined: K_w=264 kN/mm, K_{co}=299 kN/mm, E_{cr}=114 MPa, l_{cr}=3 mm, k_t = 710 N/mm^2.

3.6.3.2 Mechanical rod couplers

The orientation of the threaded rods in the grain direction enables direct force transfer in the axial direction. It also utilizes the high withdrawal stiffness of rods parallel to the grain. On the other hand, for rods inserted parallel to the grain, the withdrawal failure is rather brittle, something that can lead to a progressive failure of a group of rods. Furthermore, the development of shrinkage cracks (in the grain direction) in close proximity to the threaded rods, can lead to loss of capacity. These shortcomings can be overcome by using long threaded rods with a small inclination to the grain.

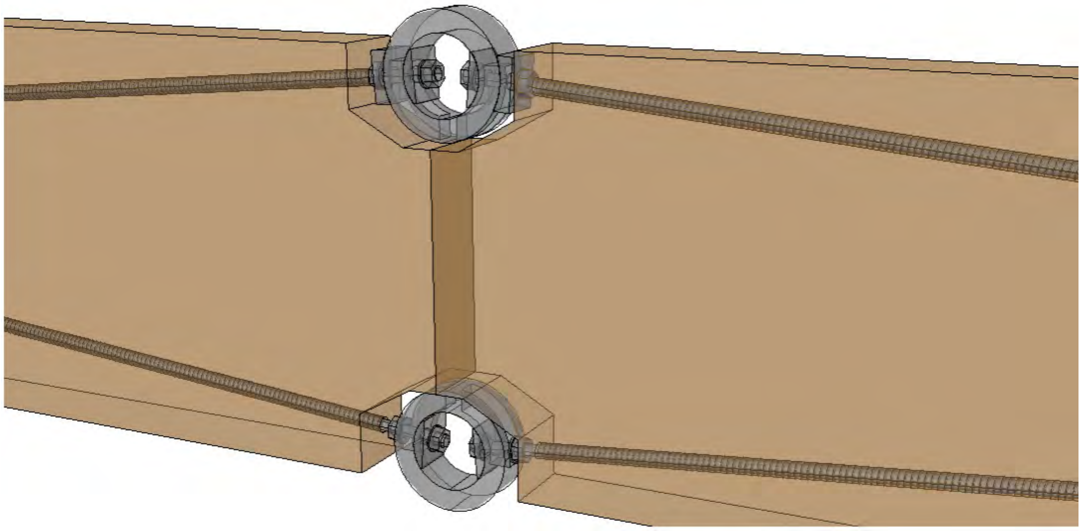

Figure 3.60 Visualization of a splice joint using long threaded rods inserted with an inclination to the grain

Figure 3.60 shows a splice joint using long threaded rods inserted with an inclination to the grain. Moreover, the threaded rods are fabricated with a metric threaded part at the end of the rods, allowing easy and fast mounting of the rod coupler. Details of a prototype splice joint are shown in Figure 3.61. The inclination of the rods was 5 degrees. A ductile tensile failure in rods (in the tension side) was achieved for rods of 1200 mm effective length (the length of the rod screwed in the timber).

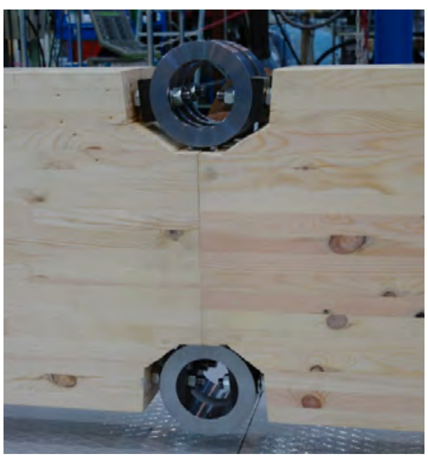

Figure 3.61 Details of the prototype splice joint with mechanical couplers

Please note that the application of the threaded rods with an inclination to the grain imposes a transverse force component at the end of the rods, which must be taken into account in the structural calculations.

3.7 References, chapter 3

Augustin, M. (2008). Ultimite Limit States – Joints, Educational Materials for Designing and Testing of Timber Structures – TEMTIS Handbook 1 – Timber Structures, Leonardo da Vinci Pilot Project CZ/06/B/F/PP/168007.

Bell, K. (2010). Structural systems for glulam arch bridges. Proceedings of the International Conference on Timber Bridges (ITCB2010). Lillehammer, Norway**:** 49–66.

Bell, K. (2010). Structural systems for glulam arch bridges. International Conference on Timber Bridges (ICTB 2010). Lillehammer, Norway.

Bell, K. and L. Wollebæk (2004). Large, mechanically joined glulam arches. WCTE 2004. Lahti.

Brunn, B. and F. Schanack (2003). Calculation of a double track railway network arch bridge applying the european standards. Graduation thesis Article, Dresden University of Technology.

Brühl, F. and U. Kuhlmann (2012). Connection Ductility in Timber Structures Considering the Moment-rotation Behavior. WCTE 2012. Auckland.

Burkart, H. (2016). Learning Experiences from Timber Bridge Inspections. NPRA reports, Statens Vegvessen (Norwegian Public Roads Administration).

Ceccotti, A. (1995). Timber-concrete composite structures. Timber engineering, Step 2: Design, details and structural systems. P. A. H. Blass, B. Choo, R. Görlacher, et al. The Netherlands, Centrum Hout**:** E13/11-E13/12.

Ceccotti, A. (2003). Composite Structures. Timber Engineering. S. T. H. J. Larsen. Chichester, John Wiley & Sons Ltd.**:** 409-427.

CEN 1990, European committee for standardization (2002). EN 1990:2002: Eurocode - Basis of structural design. Brussels, Belgium.

CEN 1991-1-4, European committee for standardization (2002). EN 1991-1-4:2005+A1:2010: Eurocode 1 Actions on structures, parts 1-4: General action - Wind actions. Brussels, Belgium.

CEN 1991-2, European committee for standardization (2003). Eurocode 1: Actions on structures - Part 1-2: Action on structures Traffic load on bridges. Brussels, Belgium.

CEN 1991, European committee for standardization (2002). EN 1991-1-x:2002-2006: Eurocode 1 Actions on structures, parts 1 to 7. Brussels, Belgium.

CEN 1991, European committee for standardization (2003). EN 1991-1-5:2003: Eurocode 1: Actions on structures - Part 1-5: General actions - Thermal Actions. Brussels, Belgium.

CEN 1992, European committee for standardization (2003). EN 1992-1-1:2004/AC:2010: Eurocode 1: Design of concrete structures - Part 1-1: General rules and rules for buildings. Brussels, Belgium.

CEN 1995-2, European committee for standardization (2004). EN 1995-2:2004: Design of timber structures. Part 1-2: Bridges. Brussels, Belgium.

CEN 1995, European committee for standardization (2004). EN 1995-1-1:2004+A1:2008+A2:2014: Design of timber structures. Part 1-1: General-Common rules and rules for buildings. Brussels, Belgium.

CEN 14080, European committee for standardization (2013). EN 14080-2013: Timber structures- Glued laminated timber and glued solid timber - Requirements. Brussels, Belgium.

CEN (2004). EN 1995-2: 2004: Design of timber structures. Part 2: Bridges

Brussels, European committee for standarization.

CEN, European committee for standardization (2002). EN 1990:2002: Eurocode-Basis of structural design. Brussels, Belgium.

CEN, European committee for standardization (2003). EN 1991-2:2003/AC:2010: Eurocode 1: Actions on structures - Part 2: Traffic loads on bridges. Brussels, Belgium.

CEN, European committee for standardization (2004). EN 1995-2:2004: Design of timber structures. Part 2: Bridges. Brussels, Belgium.

CEN, European committee for standardization (2005). EN 1993-1-9:2005: Eurocode 3 - Design of steel structures -Part 1-9: Fatigue Brussels, Belgium.

CEN, European committee for standardization (2012). EN 14592:2008+A1:2012: Timber structures- Dowel type fasteners- Requirements. Brussels, Belgium.

Cepelka, M. and K. A. Malo (2014). Review on on-site splice joints in timber engineering. COST-Timber Bridges Conference 2014. Biel/Bienne.

Cepelka, M. and K. A. Malo (2016). Experimental study of end grain effects in timber joints under uniaxial compression load. CD-ROM Proceedings of the World Conference on Timber Engineering (WCTE 2016), August 22-25, 2016. W. W. J. Eberhardsteiner, A. Fadai, M. Pöll. Vienna, Austria, Vienna University of Technology, Austria, ISBN: 978-3-903039-00-1.

Cepelka, M. and K. A. Malo (Submitted 01/2017). "Moment resisting splice of timber beams using long threaded rods and grout-filled couplers – Experimental results and predictive models." Submitted for publication in Construction and Building Materials.

DIBt, Deutsches Institut für Bautechnik (2010). SFS intec, GmbH., Gewindestangen mit Holzgewinde als Holzverbindungsmittel, Allgemeine bauaufsichtliche Zulassung Z-9.1-777.

Eilertsen, M. and D. E. Haddal (2016). Long span network arch bridges in timber Master's Thesis, Norwegian University of Science and Technology.

Fragiacomo, M. (2006). "Long-Term Behavior of Timber-Concrete Composite Beams II: Numerical Analysis and Simplified Evaluation." Journal of Structural Engineering **132**(1): 23-33.

Gattesco, N., A. Gubana and M. Buttazi (2010). Cyclic behaviour of glued-in joints under bending moments. WCTE 2010. Riva del Garda.

Gattesco, N. and I. Toffolo (2004). "Experimental study on multiple-bolt steel-to-timber tension joints." Materials and Structures/Materiaux et Constructions **37**(266): 129-138.

Gehri, E. (2010). High Performing Jointing Technique Using Glue-in Rods. WCTE 2010. Riva delGarda.

Jaaranen, J. (2016). Timber concrete composite bridges Diploma Thesis, Aalto University, Finland.

Jensen, J. L., A. Koizumi, T. Sasaki, Y. Tamura and Y. Iijima (2001). "Axially loaded glued-in hardwood dowels." Wood Science and Technology **35**: 73-83.

Jensen, J. L. and P. Quenneville (2009). Connections with glued-in rods subjected to combined bending and shear actions. CIB-W18/42-7-9 International council for research and innovation in building and construction working commission W18 -Timber structures.

Johansen, K. W. (1949). Theory of timber connectors. Bern, Switzerland

International Association of Bridges and Structural Engineering. **Publication No. 9:** pp. 249-262.

Jutila, A. and L. Salokangas (2010). Wood-Concrete Composite Bridges - Finnish Speciality in the Nordic Countries. Proceedings of the International Conference Timber Bridges ICTB2010. Lillehammer, Norway.

Kleppe, O. (2010). Durability of Norwegian timber bridges. Proceedings of the International Conference on Timber Bridges (ITCB2010). Lillehammer, Norway**:** 157-168.

Larsen, H. J. (2003). Fasteners, Joints and Composite Structures. Timber Engineering. S. Thelandersson and H. J. Larsen, Wiley.

Løkken, N. (2016). Fatigue of Threaded Rods Subjected to Axial Load Master's Thesis, Norwegian University of Science and Technology.

Malo, K. A. (1999). Fatigue Tests of Dowel Joints in Timber Structures. Nordic Timber Bridge Project. Sweden, Stockholm, Nordic Timber Council AB.

Malo, K. A. (2002). Fatigue Tests of Dowel Joints in Timber Structures, Part II: Fatigue Strength of Dowel Joints in Timber Structures. Nordic Timber Bridge Project. Sweden, Stockholm, Nordic Timber Council AB.

Malo, K. A., Å. Holmestad and P. K. Larsen (2006). Fatigue strength of dowel joints in timber structures. Proceedings of WCTE 2006 - World Conference on Timber Engineering, Portland, OR, USA.

Malo, K. A., A. Ostrycharczyk, R. Barli and I. Hakvåg (2013). On development of network arch bridges in timber. Proceedings of the International Conference Timber Bridges (ICTB2013). Las Vegas, USA.

Nielsen, O. F. (1929). Foranderlige Systemer med anvendelse på buer med skraatstillede Hængestenger ('Discontinuous systems used on arches with inclined hangers', in Danish) Ph.D. Thesis.

NPRA (2016). Trebruhåndboken - Preliminary version, Statens Vegvessen (Norwegian Public Roads Administration).

Ostrycharczyk, A. W. and K. A. Malo (2017). Comparison of network patterns suitable for timber bridges with crossbeams. ICTB17 3rd International Conference on Timber Bridges 2017. Skellefteå, Sweden.

Ostrycharczyk, A. W. and K. A. Malo (2017). "Parametric study of radial hanger patterns for network arch timber bridges with a light deck on transverse crossbeams." submitted to Engineering Structures.

Pipinato, A. (2016). Innovative Bridge Design Handbook, Butterworth-Heinemann for Elsevier

Pousette, A. and K. Sandberg (2010). Outdoor tests on beams and columns. Proceedings of the International Conference Timber Bridges (ICTB 2010). Lillehammer, Norway**:** 169–178.

Rodrigues, J., A. Dias and P. Providência (2013). "Timber-concrete bridges: State-of-the-art review." BioResources **8**(4): 6630-6649.

Ryall, M. J., G. A. R. Parke and J. E. Harding (2000). The manual of bridge engineering. London, Thomas Telford.

Schanack, F. (2008). Puentes en Arco Tipo Network, (Network Arch Bridges). Doctoral Thesis, Department of Structural Engineering and Mechanics, Technical College of Road, Channel and Port Engineering, University of Cantabria, Spain.

Sjödin, J. and C.-J. Johansson (2007). "Influence of initial moisture induced stresses in multiple steel-to-timber dowel joints." Holz als Roh- und Werkstoff **65**(1): 71-77.

Stamatopoulos, H. and K. A. Malo (2015). "Withdrawal capacity of threaded rods embedded in timber elements." Construction and Building Materials **94**: 387-397.

Stamatopoulos, H. and K. A. Malo (2015). "Withdrawal stiffness of threaded rods embedded in timber elements." Submitted to Construction and Building Materials.

SWECO NORGE AS Brosjyre om trebruer ('Brochure about timber bridges', in Norwegian), available from http://www.sweco.no/no/Norway/Markedsomraader/Infrastruktur/Bruer/.

Thelandersson, S. (2003). Wood as Construction Material. Timber Engineering. S. Thelandersson and H. J. Larsen, Wiley.

Tlustochowicz, G., E. Serrano and R. Steiger (2011). "State-of-the-art review on timber connections with glued-in steel rods." Materials and Structures **44**(5): 997-1020.

Tveit, P. (1959). Bogebruer med skrå krysstilte hengestenger ('Arch bridges with inclined intersecting hangers', in Norwegian) Ph.D. Thesis, Tech. Univ. of Norway.

Tveit, P. (1966). "The design of network arches." The Structural Engineer **44**(7): 249-259.

Tveit, P. (1987). "Considerations for Design of Network Arches." Journal of Structural Engineering **113**(10): 2189-2207.

Veie, J. and R. B. Abrahamsen (2013). Steien Network Arch Bridge. Proceedings of the International Conference Timber Bridges (ICTB2013), Las Vegas.

Volkersen, O. (1938). "Die nietkraftverteilung in zugbeanspruchten nietverbindungen mit konstanten laschenquerschnitten." Luftfahrtforschung **15**: 41-47.

Wollebæk, L. (2005). Analyses of geometrical nonlinearities with applications to timber bridges Ph.D. Thesis, Norwegian University of Science and Technology.

4 Wooden bridge decks

Wooden bridge decks are often built as stress-laminated decks in Sweden and Norway. Wooden decks can also be made as spike-laminated decks or longitudinal glulam decks which is sometimes used in Finland and USA.

Wooden stress-laminated, spike-laminated and glulam decks are usually covered with asphalt layers on the top to prevent the erosion of the wooden surface (see Figure 4.1).

For more heavily loaded larger road bridges, concrete deck slabs can be used. By using shear connectors to wooden beams, composite action is achieved, see also chapter 3.

Figure 4.1 Asphalt cover on the timber deck

Wooden short span pedestrian bridges are quite common especially in parks and cities. Wooden plank decks are used on many smaller pedestrian timber bridges. Different forms and layouts are easily constructed by using nailed plank decks. Planks can be positioned into transversal, longitudinal or diagonal direction (see Figures 4.2 and 4.3). However, a thin deck requires quite dense supporting layer under the wooden surface.

Figure 4.2 Longitudinal nailed plank deck

Figure 4.3 Diagonally nailed plank deck

4.1 Stress-laminated timber decks

Stress-laminated timber decks have become popular due to their light weight and high lateral stiffness. The system consists of parallel timber laminations that are held together by pre-stressed rods, usually made of high-strength steel, inserted into pre-drilled holes (see Figure 4.4a). By allowing the use of prescribed butt-joint pattern in the timber laminations, continuous spans are unlimited in length.

The pre-stressing of the stress-laminated decks is of utmost importance for a sustainable function of the decks, and creep and moisture movements must be controlled. Durability of wooden stress-laminated decks is depending on the moisture content in the deck. Waterproof covering and good design of details can prevent moisture ingress.

The pre-stressing generates lateral stress between laminations which then work as a plate due to the friction between the lamellas, giving a better distribution of loads. However, there is a reduction of longitudinal stiffness due to the presence of butt joints of the lamellas. They extend the laminations in longitudinal direction but they cannot transfer bending moment so the full flexural capacity is reached only at a certain distance from the butt joints. In order to avoid weak sections the timber lamellas are displaced lengthwise relative to each other, spreading the butt joints (see Figure 4.4a), Malo (2016).

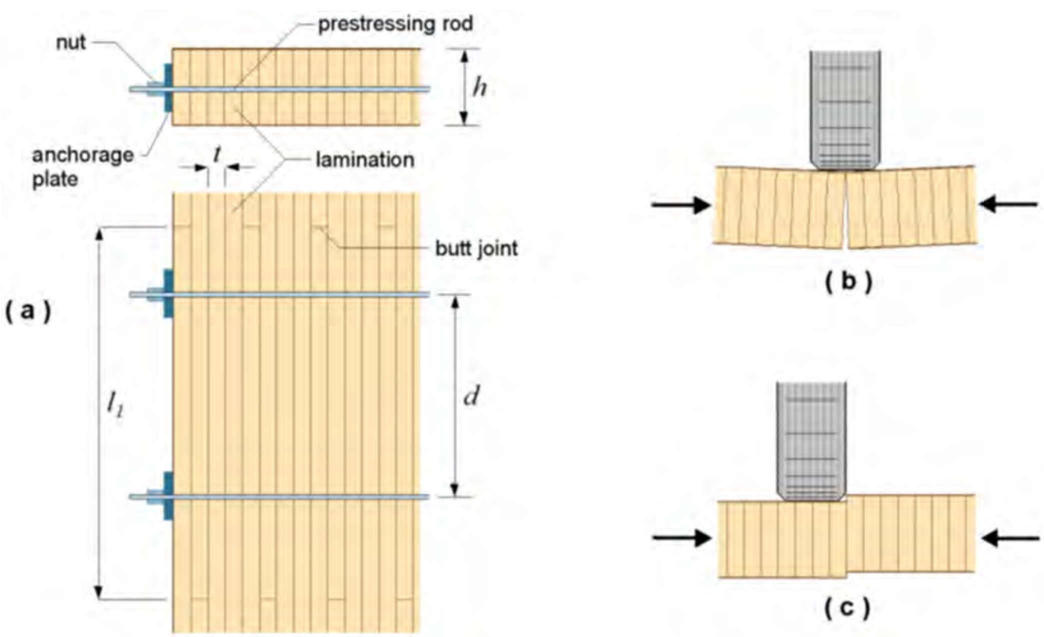

Figure 4.4. Stress-laminated timber deck plate (drawing: K. Bell)

Stress-laminated timber decks work as plates due to the lateral stress between the lamellas created by the pre-stressing force. Such force must be able to prevent vertical slips due to concentrate wheel loads (see Figure 4.4c) and to avoid gaps between the lower portion of the laminations due to transverse bending moment (see Figure 4.4b). Ritter (1992) suggested the necessary pre-stressing force F_p can be evaluated according to Equation (4.1).

$$F_p \geq 6\frac{M_T}{h} \quad ; \quad F_p \geq \frac{V_T}{\mu} \tag{4.1}$$

In Equation (4.1) M_T is the transverse moment given by the loads, h is the height of the timber deck, V_T is the shear acting on the deck and μ is the friction coefficient.

However, the pre-stressing force cannot be higher than the compression strength perpendicular to grain of timber under the anchorage plate.

Moreover, EN 1995-2, CEN (2004b) prescribes a minimum long term pre-stressing stress of 0.35 MPa. The dimensional change of timber due to long term moisture and load exposure is the reason for the losses of pre-stress in the pre-tensioned rods and therefore in pre-stressed timber decks. Thus, the rods are commonly re-stressed after some months as well as after about 25 years to guarantee the stiffness of the deck.

4.1.1 Long term deformations (Creep)

Creep with respect to perpendicular-to-grain compressive loading is induced by highly tensioned pre-stressing rods in stress-laminated decks. Creep is usually defined as the delayed deformation that occurs after the initial elastic deformation when a material is subjected to loads. The delayed deformation of timber is not only affected by the duration of the load, but also by the variations of moisture content in the material while exposed to loading.

Therefore, we can distinguish between *viscoelastic creep* and *mechano-sorptive creep*, whereas the first one is the time-dependent deformation (under constant load), and the second is moisture-dependent creep deformation, see Figures 4.5 and 4.6.

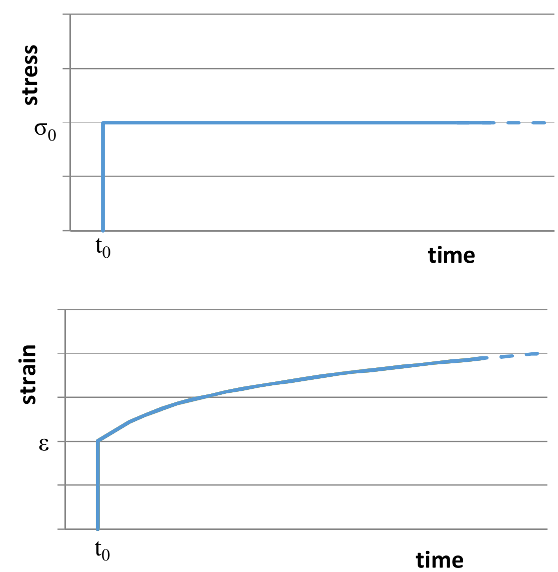

Figure 4.5. Viscoelastic creep: Strain vs. time during constant stress

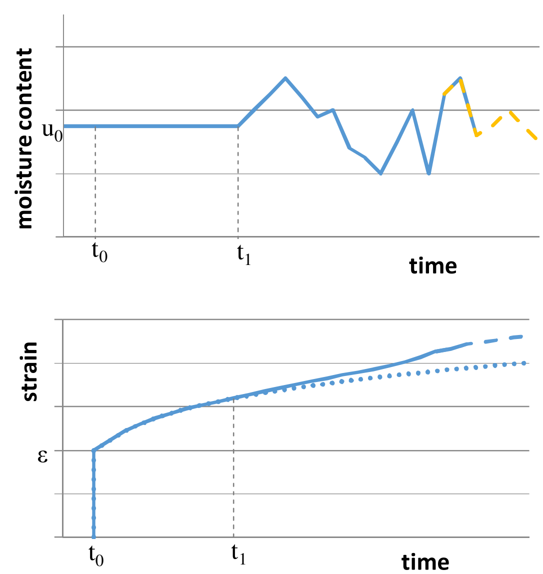

Figure 4.6. Mechano-sorptive creep: Strain vs. time during constant stress and variable moisture content

4.1.2 Creep in Eurocode 5 (EN 1995)

EN 1995-1-1, CEN (2004) introduces the concept of service classes in order to take into account the environmental conditions where a timber structure is located. Eurocode 5 defines three service classes each referring to a different range of relative humidity of the air and therefore to a different expected moisture content (MC) in the timber elements of the considered structure.

Table 4.1. Service classes of EN 1995-1-1

Service class	**1**	**2**	**3**
T [°C]	20	20	-
max RH in the surrounding air [%] *	65	85	-
Approximate average MC in softwoods [%]	< 12	< 20	> 20
k_{def} [-] **	0.6	0.8	2.0
* The max RH can be exceeded for few weeks per year ** Values for solid timber and glued laminated timber Note: National Annexes might have additional or different information			

EC5 considers the reduction of the mechanical properties due to creep through the introduction of the factor k_{def}. The value of the factor k_{def} is dependent on the service class which the timber structure belongs to, as shown in Table 4.1. The mean value of the modulus of elasticity E_{mean} is reduced according to Equation (4.2) in order to obtain its long-term value $E_{mean,fin}$.

$$E_{mean,fin} = \frac{E_{mean}}{1+k_{def}} \tag{4.2}$$

Therefore, the long term deformation considered by EC5 is at least equal to 1.6 times, and up to 3 times, the initial elastic deformation, in serviceability analysis. This way of proceeding does not take into account the influence of the mechano-sorptive creep. Indeed a timber element operating in an environment where the relative humidity is constant at 65% will have a smaller deformation than if the relative humidity decrease to 50% before returning back to 65%. Even if both the environments match the requirements of the service class 1, the elements will have quite different behaviour.

More information about the factor k_{def} can be found in Section 2 and Section 3 of EN 1995-1-1.

4.1.3 *Analytical model*

A more detailed evaluation of the delayed deformations can be performed by use of an analytical model. The model suggested by Toratti (1992) and updated in Svensson and Toratti (2002) is shown in Equation (4.3) in strain-rate form.

$$\dot{\varepsilon} = \dot{\varepsilon}_s + \dot{\varepsilon}_{ve} + \dot{\varepsilon}_{ms} \tag{4.3}$$

In Equation (4.3) the total strain rate $\dot{\varepsilon}$ is expressed as the sum of the shrinkage-swelling strain rate $\dot{\varepsilon}_s$, the viscoelastic strain rate $\dot{\varepsilon}_{ve}$ and the mechano-sorptive strain rate $\dot{\varepsilon}_{ms}$.

The elastic strain vector ε_e is obtained by multiplying the stress vector σ with the inverse of the stiffness matrix C.

$$\varepsilon_e = \boldsymbol{C}^{-1}\sigma \tag{4.4}$$

The hygroscopic expansion/shrinking ε_s is proportional to the variation of moisture content through the coefficient of hygroscopic expansion α.

$$\Delta\varepsilon_s = \alpha\,\Delta u \tag{4.5}$$

The coefficient α is a scalar and is dependent on angle to grain.

The visco-elastic strain ε_{ve} is related to the elastic strain through the viscoelastic creep parameter Φ and increases with the time. Indeed, $\Phi(t)$ is a function of the time.

$$\varepsilon_{ve} = \Phi\,\varepsilon_e \tag{4.6}$$

The mechano-sorptive strain ε_{ms} consists of a recoverable part $\varepsilon_{ms,r}$ and an irrecoverable part $\varepsilon_{ms,i}$.

$$\varepsilon_{ms} = \varepsilon_{ms,r} + \varepsilon_{ms,i} \tag{4.7}$$

The recoverable part is function of the moisture content variation through the mechano-sorptive creep coefficient $m(u)$. The irrecoverable part exists only in presence of moisture content never reached before by the timber element.

$$\varepsilon_{ms,r} = m\,\varepsilon_e \tag{4.8}$$

$$\varepsilon_{ms,i} = m_i\;\Delta U\;\sigma \tag{4.9}$$

In Equation (4.9) m_i is a material parameter independent of moisture, and U is a moisture content value not previously reached during the load history of the material.

4.1.4 Re-stressing of rods

The analytical model described above has been calibrated through experiments performed at NTNU (Norwegian University of Science and Technology) in Trondheim, Norway. Figure 4.7 shows the results of a long term numerical analysis performed on a section of a pre-stressed timber deck consisting of timber laminations (Norwegian spruce). The model takes into account an annual change of the moisture content (MC) between 12% and 16% modelled as a sinusoidal MC change with period of one year. The choice of the MC numbers was made on the basis of measurements of MC in stress-laminated decks of some instrumented Norwegian bridges. Figure 4.7 displays a 20% decrease of the tension in the rods during the first year of life of the deck. Subsequently, the necessary time is almost 20 years in order to get the same level of stress loss as in the first year.

It is common to accept a loss of 40% of the initial stress before re-stressing the rods and therefore the practice of re-stressing them after about 20 years agrees with the results shown in Figure 4.7. However, it should be kept in mind that the moisture change over the years might be larger than the quantities measured and used in this simulation.

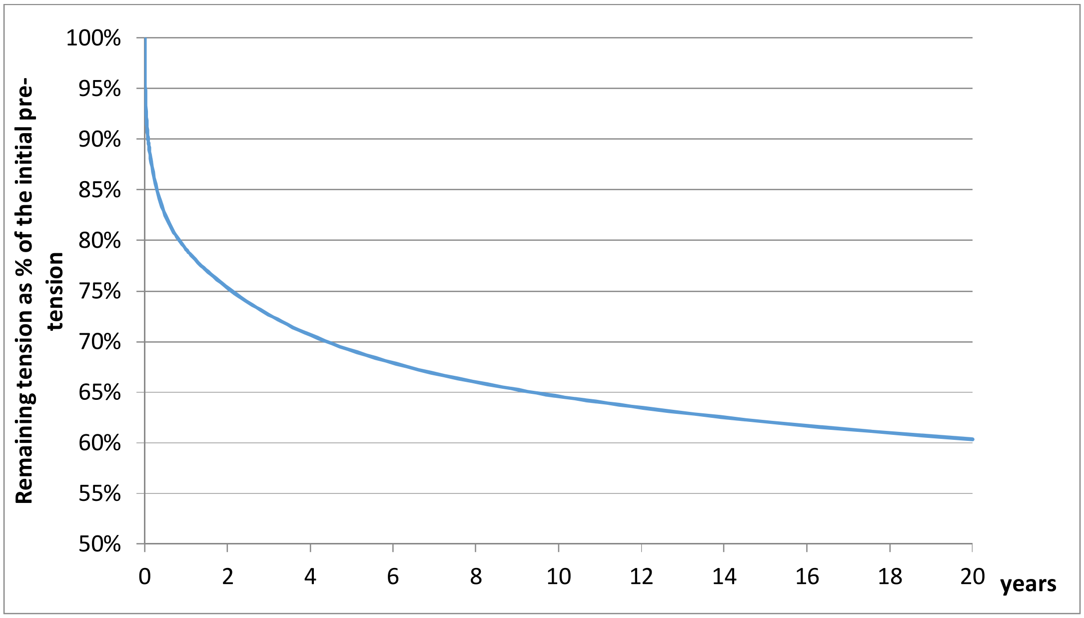

Figure 4.7. Tensile stress in the rods as percentage of the initial pre-stress

4.1.5 Compression orthogonal to grain

The pre-stressed rods cause a compression stress in the timber deck that is higher in proximity of the edge and become constant after a diffusion length L_d (see Figure 4.8).

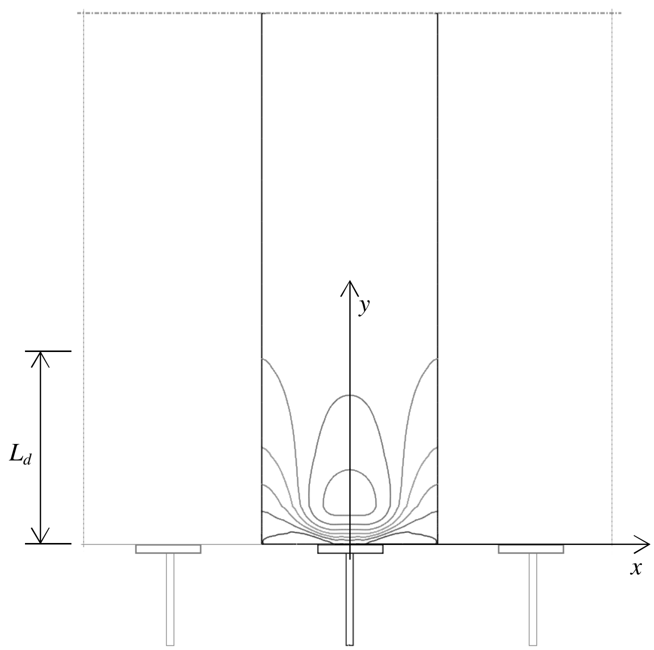

Figure 4.8. Diffusion of compression stress in section of a pre-stressed deck (plane section of a deck: the x-direction is the longitudinal to grain direction)

Numerical analyses have been performed on a pre-stressed timber deck (Norwegian spruce) with height of 450 mm where the dimensions of the circular anchorage plate (radius *R* and thickness *T*) have been varied. The simulations show that a too small plate does not allow a good distribution of the stresses. The results of the analyses using plates with radius R of 150, 175, and 200 mm and with thickness T of 10, 20, 30, and 40 mm are shown in Figure 4.9 to Figure 4.15. In the plots, the value 100% corresponds to the stress reached after passing the diffusion length L_d using the biggest plate described in the figure, respectively the plate T10R200 in Figure 4.9, T20R200 in Figure 4.10 and so on.

It is evident that the use of plates with radius 150 mm achieves a lower compression stress after L_d than using plates with bigger radius (see Figure 4.9Figure 4. to Figure 4.12). This trend recurs analysing the effect of different thicknesses. Indeed, the use of the plate with only 10 mm thickness cannot achieve the same compression as the other analysed plates due to the bending deformations of the plate (see Figure 4.13 to Figure 4.15).

4.1.6 Recommendations

It is recommended to re-stress the rods after few months in order to recover the loss of pre-stress occurred in the initial period, and thereafter again after 20 years.

It is important that the anchorage system allows the spread of the compression stresses. A small radius of the load plate, e.g. 150 mm, can lead to high compression stresses under the plate, but too low compressive stresses in the timber deck, only between the 65% and 85% of the stress reached using plates with larger radii. Similarly, thicker plates allow the achievement of higher pre-stress.

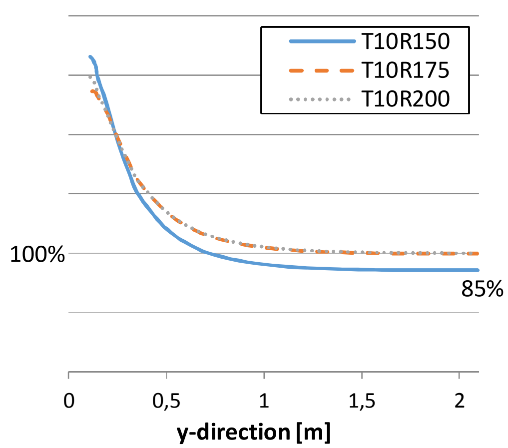

Figure 4.9. Development of compression stress along the y direction (transversal): anchorage plates thickness 10 mm

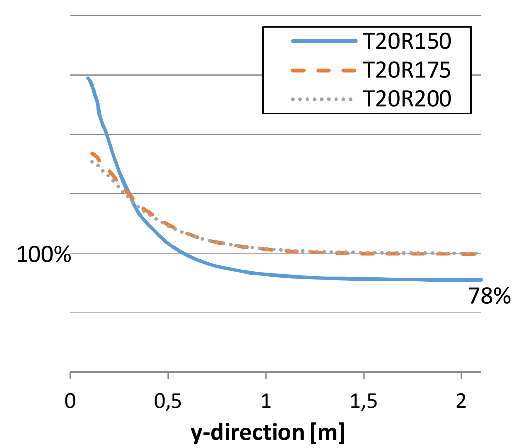

Figure 4.10. Development of compression stress along the y direction (transversal): anchorage plates thickness 20 mm

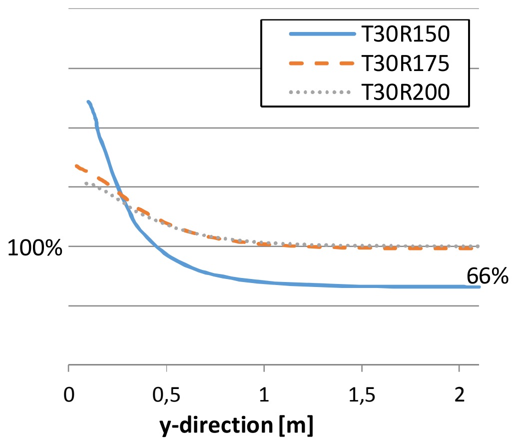

Figure 4.11. Development of compression stress along the y direction (transversal): anchorage plates thickness 30 mm

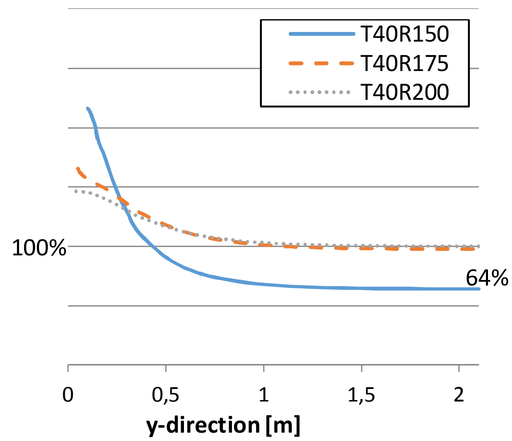

Figure 4.12. Development of compression stress along the y direction (transversal): anchorage plates thickness 40 mm

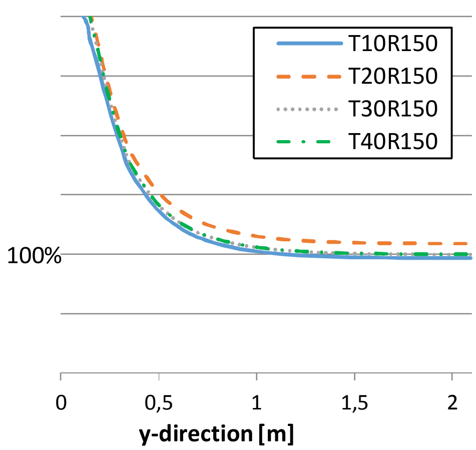

Figure 4.13. Development of compression stress along the y direction (transversal): anchorage plates radius 150 mm

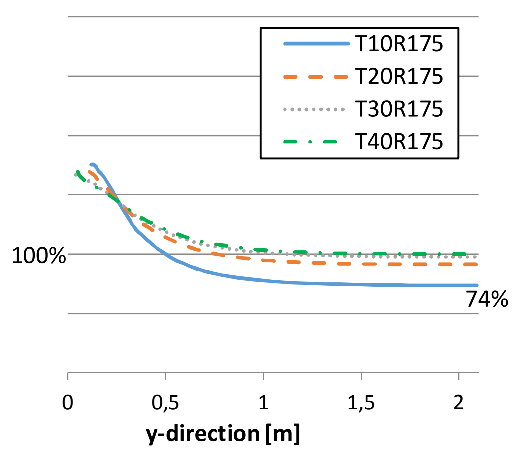

Figure 4.14. Development of compression stress along the y direction (transversal): anchorage plates radius 175 mm

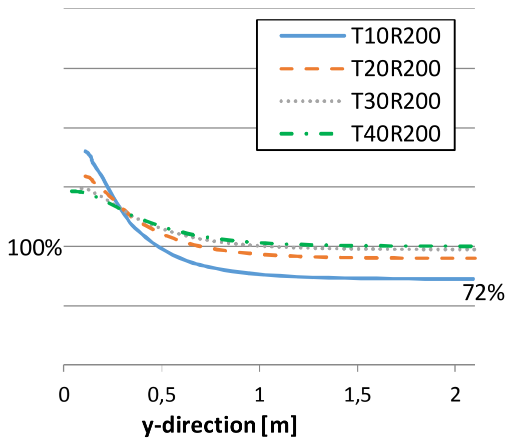

Figure 4.15. Development of compression stress along the y direction (transversal): anchorage plates radius 200 mm

4.2 Waterproofing and edge details of stress-laminated decks

Low moisture content in stress-laminated decks is important; moist wood gets softer and the anchor plates can get pressed into the wood at the edges, and moist wood during long periods can lead to decay. Consequently the waterproofing and edge details are of great importance to keep the function of the decks.

Demands for impregnation and waterproofing of wooden stress-laminated decks vary between countries. For example creosote impregnated wood is used in Norway to protect against decay while in Sweden creosote is not allowed in bridges. The wooden bridge decks in Sweden are built of spruce without any wood preservatives and this means a big challenge and high demands on constructive wood preservation and especially the design at the edges is important to prevent moisture ingress.

4.2.1 Decks of creosote impregnated wood

According to the Norwegian Public Roads Administration, Vegdirektoratet (2015), service class 2 may be used for decks with the outer lamellas treated with creosote and a waterproof protection. Usually creosote impregnation is used; at least the outer lamellas are treated with creosote. Creosote impregnation should be performed after all the processing of wood is made and for block glued laminated parts double impregnation is recommended (lamellas are salt impregnated before gluing and creosote impregnation after bonding). The Norwegian timber bridge decks should have at least two asphalt layers and full moisture protection of deck. Waterproofing is made with 12 mm Topeka 4S, and according to the Norwegian Public Roads Administration, Vegdirektoratet (2015b), a mastic asphalt should be used between creosoted wooden deck and Topeka 4S. The mastic asphalt is a protective layer to prevent creosote from affecting the waterproofing and is laid directly on dry and cleaned deck without the use of adhesive.

This protective layer is used because the main problem with the asphalt layers has been the reaction to creosote sweating from the deck, which weakens or liquefies the membrane and also the wearing course. Topeka 4S is a bitumen membrane that during summer time weakens and to some extent acts self-healing by sealing gaps. When it has been further liquefied by the creosote, large wheel tracks have sometimes been found. Creosote sweating is not fully understood, but overpressure or lack of vacuum pressure after impregnation process is thought to be the main cause. Other causes might by internal pressure by damping from creosote or the deck being pressed together because of creep.

The waterproofing on bridges in Norway without edge beams or kerbing shall be brought to the outer edge of the bridge deck about 50 mm in on the waterproofing and with inclination to full height. On bridge decks with edge beams or kerbing on the waterproofing there should be a board between the edge beam and the wearing course while laying the wearing course. It is afterwards removed and the gap is filled with Topeka. Stress-laminated decks can have drains through the deck with lamellas and butt joints designed for the drain locations and dimensions. Constructive protection should ensure that surface water cannot come into contact with the edge faces of the deck or anchor plates of pre-stressing rods (see Figure 4.16).

Figure 4.16. Creosote impregnated deck edge

4.2.2 Decks of untreated spruce

In Sweden the stress-laminated decks for road bridges and pedestrian bridges are built of glulam beams of untreated spruce. Since the spruce wood has no impregnation against rot the moisture content of the wood is very decisive for the durability and the well-designed details are very important to ensure that water cannot penetrate into the wood.

Wooden decks with waterproof bitumen sheets and asphalt layers on top and wooden cladding on the sides are protected from direct influence of precipitation and can be considered to be "under a roof". Rain water should be drained away from the bridge surface as soon as possible and the waterproofing must protect the wood from remaining water in the asphalt layer. The edge of the waterproofing layer at the deck edges is a critical detail to ensure that it is waterproof and durable, see Figure 4.17. Timber bridge manufacturers often produce pre-fabricated bridges or bridge parts and after installation at the construction site the bridges are paved with asphalt. Several actors are involved in the construction process of a bridge and clear instructions for all actors are important for a good result.

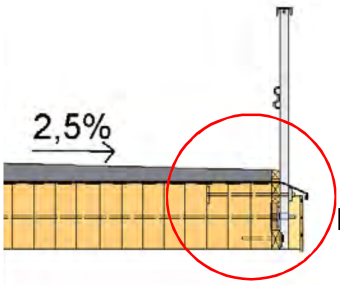

Figure 4.17. Example of stress-laminated timber deck (from TräGuiden)

4.2.3 Asphalt surfacing on decks of untreated spruce

The stress-laminated decks in Sweden usually have a bitumen primer on the wood surface, a waterproof bitumen sheet, and asphalt layers adapted to the traffic type, Trafikverket (2016), Trafikverket (2013). The 5 mm waterproof bitumen sheet is welded to the wooden deck which is pre-treated with bitumen primer to increase the adhesion. Asphalt is applied in several layers; on road bridges there is a protection layer, a binding layer and a wearing layer.

Sometimes blisters can be seen on the asphalt surface of bridges. Blistering of the paving means that the waterproof sheet rises slightly from the wood to form a blister while resulting in reduced adhesion to the deck. The adhesion is important to cope with the braking forces from vehicles. Experience is that the blistering problem is different for timber bridges than for concrete bridges. For concrete bridges the blisters can occur throughout the lifetime, while for timber bridges any blisters are mainly reported in connection with the asphalt works of the first layer. Adhesion of waterproof bitumen sheet to timber deck has been tested, Pousette (1997b), Pousette (2016), and blistering has been studied, Edwards (2002). The experience is that the blisters usually disappear and do not come back if the first asphalt layer is cooled before putting on the next layer. The final result is then usually no blisters during the lifetime.

4.2.4 Edge details of decks of untreated spruce

The waterproof bitumen sheet on untreated wooden decks must be very carefully connected to the bridge edge so that it becomes sealed. A system with edge strips and edge steel angles is described in Figures 4.18, 4.21 and 4.22.

A strip of waterproofing sheet with a minimum width of 300 mm should be mounted along the edges before the waterproofing bitumen sheet is installed. On longer bridges the strip must be spliced because they are typically manufactured in 8-10 m long pieces. To secure a waterproof splice there should be an underlying smaller splice overlap sheet mounted on the wooden deck. The splice overlap sheet is preferably mounted in a recess in the deck to get a horizontal surface for the edge steel angle, see Figure 4.18.

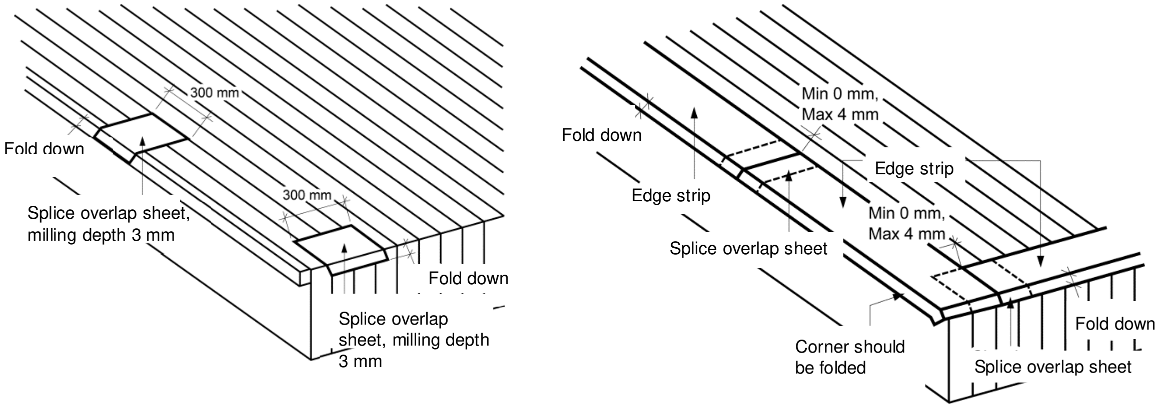

Splice overlap sheets

Edge strip of waterproof bitumen sheet

Figure 4.18. Edge strip of bitumen sheet. (Illustrations from AMA (2017))

The edge steel angle should be mounted with perforated leg on the edge strip, see Figure 4.21. The steel angle should be cleaned before installation to ensure adhesion and the edge strip should be heated at installation so that bitumen can flow up through the holes. Tests with steel angles have showed good adhesion; see Figure 4.19 and Figure 4.20, Pousette (2016). The steel angle should also be fastened to the deck with nails or screws for additional security, see also Figure 4.21.

Figure 4.19. Steel angle with perforations in horizontal leg

Figure 4.20. Test of welding the waterproof bitumen sheet on edge steel angle

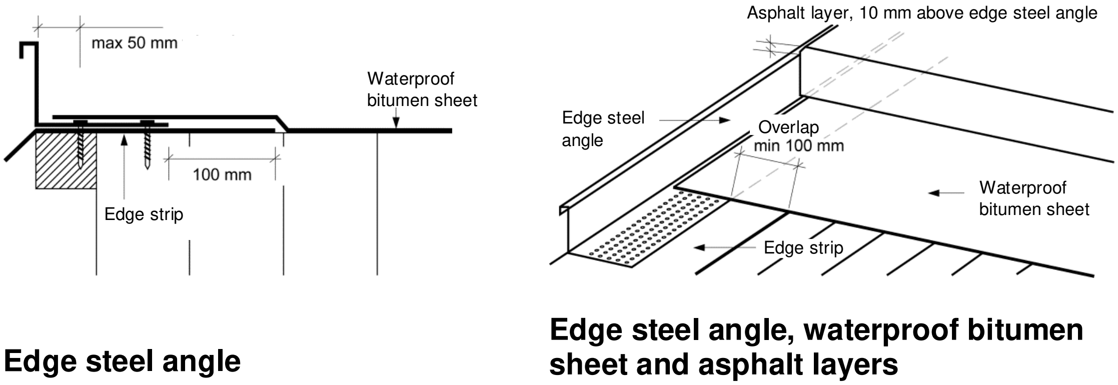

Figure 4.21. Edge steel angle. (Illustrations from AMA (2017)

Drip plates should be performed with solid supports and can optionally be fixed with fixing brackets at certain centre distances, see Figure 4.22. Penetrations of the drip plate for the railing posts must be carefully sealed. This is an important detail where leakage has been observed on quite a lot of timber bridges, Pousette and Fjellström (2016). Drip edge of the drip plate should end beyond the cladding to be protected.

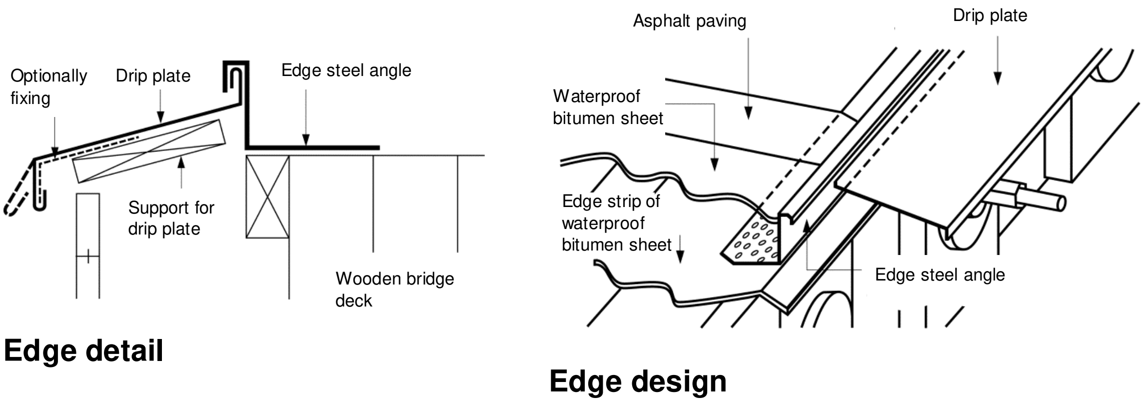

Figure 4.22. Edge design of stress-laminated decks. (Illustrations from AMA (2017)

Drains through decks of untreated spruce should be avoided. The drainage of water on the waterproof bitumen sheet can be performed via openings/drains at certain distances at the bottom of the vertical leg of the angle.

4.3 Cupping of stress-laminated decks

The phenomenon of cupping in stress laminated timber decks refers to the bending of cross section of timber deck, originated from the moisture content differences between the upper viable surface and lower surface of the structure. Due to the environmental conditions and mainly to the moisture effects, the bottom surface tends to expand increasing the risk of fractures and water infiltration, and consequently decreasing the useful life of the bridge. Moreover, cupping generates a vertical translation of the deck edges causing a visible uplift of the resistant structure of the bridge with respect to the supports on the ground. Several examples of cupping phenomena in Swedish bridges can be found in Pousette and Fjellström (2016).

The structural integrity and serviceability of stress-laminated decks depends on the compressive stress maintained among the lumber laminations Ritter et al. (1991). For acceptable performance, this compression must be sufficient to prevent vertical slip because of shear and opening between the laminations due to transverse bending. This initial compressive stress is based on the assumption that 40 to 60% of the stress will be lost over the life of the structure because of wood stress relaxation and minor changes in wood moisture content. Studies have shown the importance of the slip between the laminations due to the reduction of the interlaminar compression Ritter et al. (1991), Ritter and Wacker (1995), Carlberg and Toyib (2012).

4.3.1 Numerical evaluation of cupping and bar force losses

The single-Fickian approach for moisture transport described in detail in Chapter 5, coupled with the three-dimensional orthotropic-viscoelastic-mechanosorptive model for wood, has been used in the present work to calculate the moisture induced cupping in timber decks. The models allow also the calculation of bar force losses during time. However, in this work the computational models do not take into account the slip between laminations.

Cupping of deck specimens tested within the Nordic Timber Bridge project

The purpose of the tests with deck specimens, Pousette (1997), was to study the influence of different climates on stress-laminated timber deck plates in the Nordic countries. Test specimens were placed outdoor (in contact with the external environmental conditions) in Skellefteå, Oslo, Copenhagen and Helsinki. For each test specimen measurements of moisture content, forces in the pre-stressed bars and cupping/uplift of wood deck were measured monthly, from the 1.5.1995 to 1.8.1996.

Four timber deck specimens were manufactured at Trätek in Skellefteå. They had a length of 2.94 m, width of 0.8 m, height of 0.36 m and were made of laminations of glulam beams, of dimensions 140 × 360 × 800 mm and strength class L40. Each lamella had dimensions140 × 45 × 800 mm (eight lamellas per each glulam beam). The glulam beams were stressed together with two steel bars Dywidag 15.1 mm anchored with steel plates (200 × 200 × 43.25 mm) with a force of 144 kN, which gives a compressive stress of 1.0 MPa between laminations. An insulating mat was put on top of the deck plate and down on the edges. On top there was also a 25 mm thick layer of asphalt paving. The underside of the specimen was coated with two applications of penetrating stain.

The measuring equipment was installed and one deck specimen was then placed in a test yard at Trätek in Skellefteå. The other test specimens were sent to the Norwegian Institute of

Wood Technology in Oslo, to the Danish Technological Institute in Copenhagen, and to the University of Technology in Helsinki for measurements during one year.

Figure 4.23 shows the scheme of tested specimen and the phenomenon of cupping and the measured uplift (X).

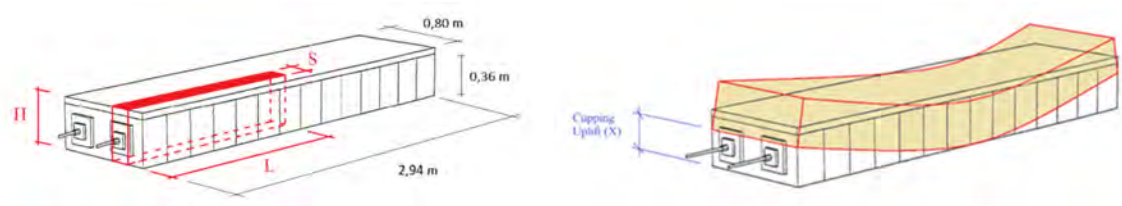

Figure 4.23. Left: sketch of the specimen tested within the Nordic Timber Bridge project and slice analysed in Abaqus (in red). Right: sketch of the cupping phenomenon and measured uplift.

The test specimens were placed outdoor on a frame on stands at a height above ground of about 0.8 m. The frame had two supports for the deck plate with a centre distance of 1800 mm. The first reading was taken after the deck was installed and then readings were taken during one of the first days every month. One load cell was installed on each bar to measure the steel bar forces. Measurements of moisture content were made in three locations with electrical resistance measuring equipment. Readings were taken for every 25 mm through the deck plate, from level 1 to level 11, where level 1 represents the closest level at the top of the deck plate and level 11 was placed 51 mm from the underside.

The cupping of deck was determined by measuring the vertical distance between the edges and a point on the bottom surface of the specimen; the value is the difference between the deformed configuration (originated by environmental humidity changes) and the undeformed shape taken at the beginning of the tests.

Abaqus analysis
In order to decrease the duration of calculation without compromising the quality of the analysis, the geometry model used in Abaqus, for all the cases explained in the following, is a smaller portion but nonetheless representative of the specimens that were actually tested. The slice geometry has a width of 0.082 m and the half length of the specimen (Figure 4.23, left). A global coordinate system with vertical axis along the tangential direction of wood (RTL) was considered in the analyses. The elastic properties listed in Table 3 and the other material properties proposed in Fortino et al. (2009) are used. The steel bar is connected to the wooden deck by using the contact TIE of Abaqus code (Figure 4.24, left).

The weather data for the cities of Copenhagen, Hesinki, Oslo and Skellefteå were taken from the European ECMWF website (ECMWF) referring to the airport locations, see Figure 4.25 for the city of Skellefteå. The results in terms of distribution of vertical displacements are drawn in Figure 4.24 (right). The cupping and moisture content (MC) during time is presented in Figure 4.26 that shows the increase of cupping during wetting and its decrease during drying. The numerical bar force losses are evaluated as average along the steel bar and show a decrease of bar losses during the whole period of analysis and this trend was observed for all studied cases. However, a force loss during a time step corresponds to a drying step while a gain of force corresponds to a wetting step.

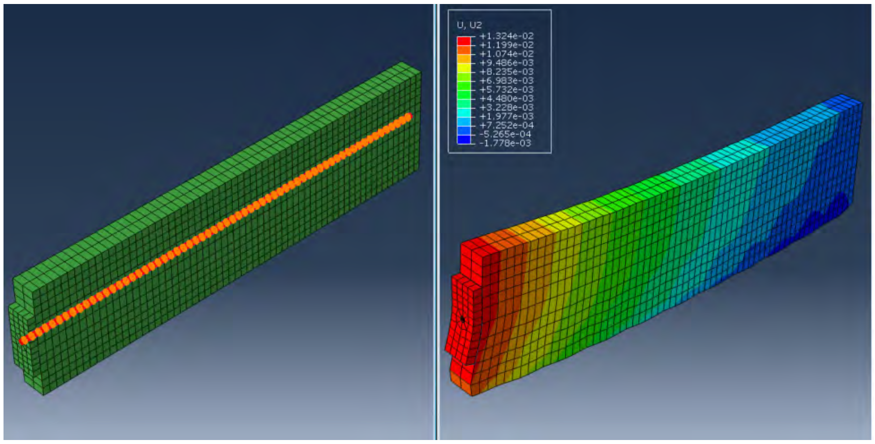

Figure 4.24. Left: Abaqus model (steel bar in red). Right: vertical displacements (right) for the specimen tested in Skellefteå.

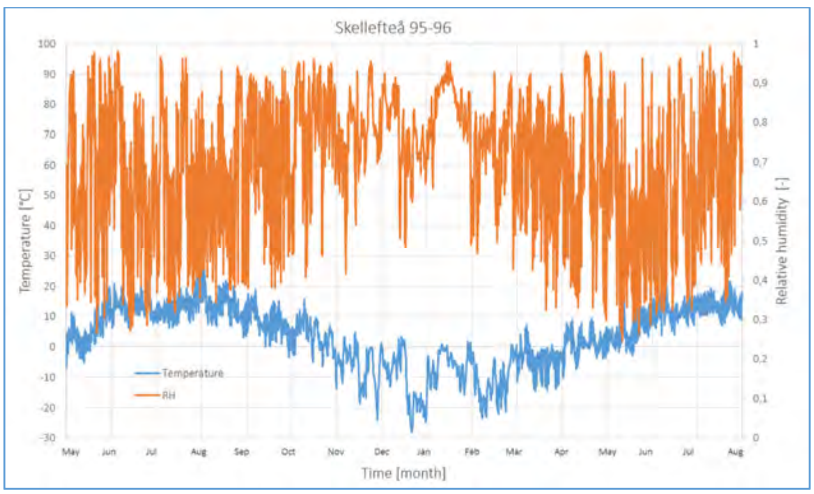

Figure 4.25. Weather data for the city of Skellefteå, Sweden (1.5.1995-1.8.1996).

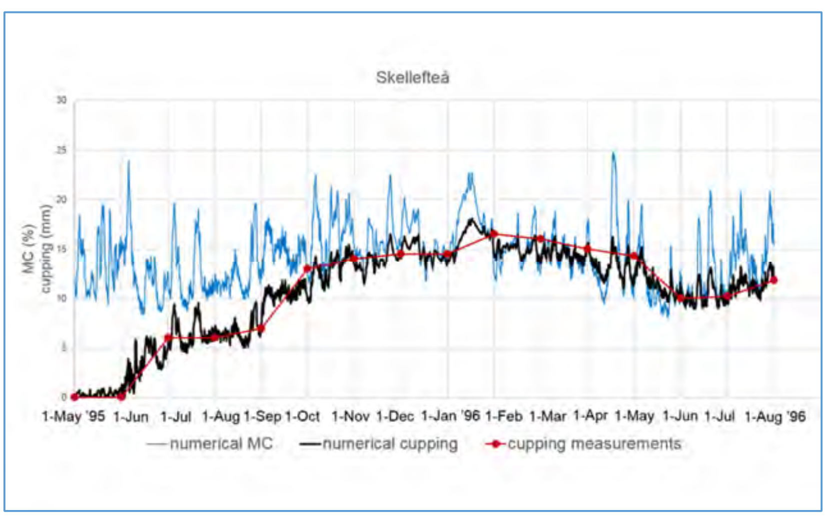

Figure 4.26. Numerical moisture content (MC), measured and numerical cupping in Skellefteå, Sweden (May 1995-Aug 1996).

4.3.2 Cupping of deck, case-study: Bridge in Umeå, Sweden

SP Technical Research Institute of Sweden inspected during 2011-2015 more than hundred Swedish timber bridges built during 1990-2015. The inspections were made on behalf of the Swedish Transport Administration, local authorities or engineering consultants.

Among the inspected bridges, the bridge in Umeå (Figure 4.27) showed similar characteristics as the specimens tested within the Nordic Timber Bridge project described in 4.3.1 and, due to this; it was selected for a numerical analysis. It is a pedestrian bridge over water with a stress-laminated glulam deck. The deck has a width of 3875 mm, a depth of 360 mm and the span is 10720 mm. It is composed of 21 glulam beams of spruce in class L40 (corresponds to GL30), with section 94.5 × 360 mm each, compressed by Dywidag steel bars, diameter ø 20, see Pousette and Fjellström (2016) for the details.

Figure 4.27. Pedestrian bridge with SLT deck, Umeå, Pousette and Fjellström (2016).

The climate data have been taken from the European ECMWF website (ECMWF) referring to the real bridge position for the year 2013 during which the *in situ* measurements were carried out. The initial moisture content (MC) in the glulam was about 12.5% when the bridge was constructed (year 2010). Since the presence of the river induces a higher concentration of moisture in the air around the bottom surface of the bridge compared to other areas, the MC under the waterproof membrane is still around 12.5% but the underside of deck has a MC around 18% (end of year 2013). Winter cold temperatures lead to freezing of condensed moisture on the underside. The cupping at the inspection was found to be 15-30 mm in the corners of the bridge deck (Figure 4.28).

Figure 4.28. Cupping in every corner of the deck, Pousette and Fjellström (2016).

The material properties used for the Abaqus analysis are the same as the ones adopted for the deck specimens in the previous sections. The analysis provides results in terms of cupping, moisture content and stress in pre-tensioned bar. The measurements of tensions in the bars are not reported in Pousette and Fjellström (2016). However, it is possible to compare the numerical results in terms of cupping and moisture content at the point on the lower surface of deck in line with the steel bar.

Numerical result of moisture content starts from 12.5% as initial condition imposed in Abaqus and increases up to 18% in the last months of the year. For the top surface of deck, where the lamellas are insulated from the external atmosphere due to the road paving and the waterproof membrane, MC remains stabilized at 12.5%. These values are in agreement with the measured *in-situ*; in fact the measurements show MC values of 12% for the surface on top and about 20% for the lower surface of the bridge. The cupping versus time is shown in Figure 4.29. The numerical cupping values appear to be in agreement with the measured cupping since, after a transition time at the beginning of the analysis; these values are in the range of 15-30 mm, as stated in Pousette and Fjellström (2016).

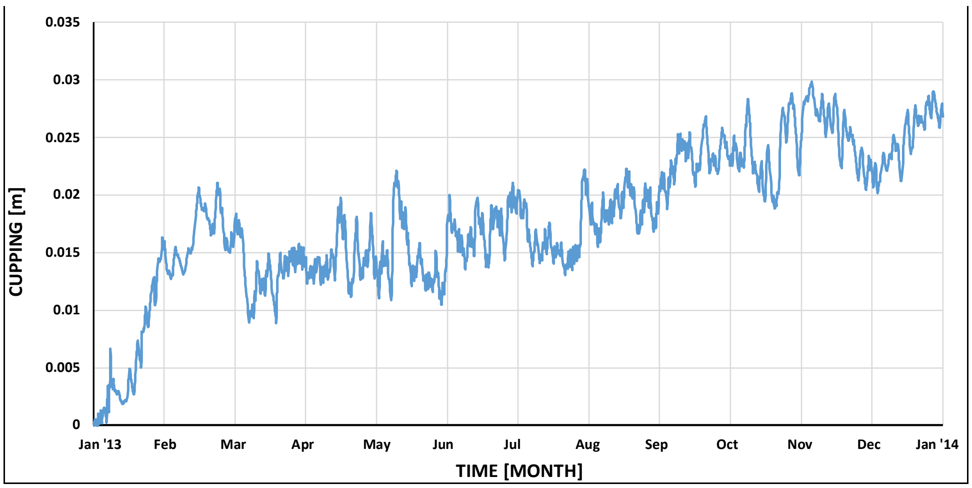

Figure 4.29. Cupping trend at the underside of deck.

4.3.3 Summary

Table 4.2 shows all results in terms of cupping and bar force losses obtained for the deck specimens of the Nordic Timber Bridge project and for the deck of the Umeå bridge. It can be observed that the loss of bar forces after 15 months of analysis is about 33-34% for all studied cases.

The maximum cupping is found during the month of January for all the studied cases. This corresponds to the high peaks of relative humidity coupled with low peaks of temperature in winter. It is recommended to check the conditions of deck during the autumn before the eventual peak of cupping in January or other winter months.

Table 4.2. Summary table for calculated cupping and bar force losses

City and period of analysis	MC_{ini} (%)	MC_{avrg} (%) (bottom deck)	MC_{avrg} (%) (middle deck)	MC_{avrg} (%) (top deck)	Max cupping (mm) (peak in January)	Bar force loss (%)
Helsinki (15 months)	12	16.86	13.24	12.00	17.00	34
Copenhagen (15 months)	12	17.16	14.67	12.00	21.60	33
Oslo (15 months)	12	15.65	12.96	12.00	19.40	33
Skellefteå (15 months)	12	14.36	12.59	12.00	18.10	33
Umeå (12 months)	12.5	17.58	13.57	12.5	27.0	34

4.4 Spike-laminated decks

Spike-laminated decks consist of a series of full-span deck panels placed onto the bridge supports to form a slab-type, longitudinal deck superstructure. Each individual deck panel is prefabricated using sawn lumber laminations (100 mm thick and up to 400 mm wide) that are laminated together with 8 mm diameter steel nail spikes that are hydraulically driven into pre-bored holes following an alternating top-to-bottom and repetitive pattern. The partial width panels are interconnected together using a ship-lap joint and drive-spike fasteners along the span length.

In addition, transverse stiffener beams are placed at regular intervals and through-bolted to the deck underside to assist with distribution of lateral loads. A waterproof asphalt wearing surface is added to protect the deck against deterioration from moisture. Also, a crash-tested rail and curb system is most applications in accordance with national roadside safety guidelines.

The key advantages of this spike-laminated deck system are its constructability. It is easy and quick to assemble with prefabricated deck panels and future widening is straight forward. The disadvantages of this spike-laminated deck system are the availability of sawn lumber laminations in longer lengths and bigger widths, which mean these bridge decks are used for simple span lengths up to 12 m. Longer crossings are typically achieved with a series of simple spans in a trestle-like arrangement. Also, these dowel-type mechanical fasteners tend to loosen which decreases the efficiency of the deck system over a period of time.

Figure 4.30. Example of a Spike-laminated deck bridge in Minnesota (USA).

4.5 Longitudinal glulam decks

Longitudinal glulam decks consist usually of a series of 1.2 m wide glulam panels that are placed adjacent to each other on the bridge supports and transversal beams. They are typically butted together along the edges without any interconnections, except for continuity provided by the transverse stiffener beams bolted to the deck underside. Longitudinal glulam deck panels are manufactured with a multiple-piece layup (deeper section) configuration to achieve longer span lengths.

The main advantages of the longitudinal glulam deck system are that they can be manufactured to greater panel depths and for multiple continuous span configurations ranging up to 30 m total. Its constructability is similar to the spike laminated deck and is very rapid installation of the prefabricated deck panels. It also nearly eliminates the need for field cuts and borings which can result in a more durable deck from a better envelope of preservative protection. The glulam panels can easily bend during construction to follow slight vertical curvature of the bridge geometry if necessary. A disadvantage of the longitudinal glulam deck system is that moisture-accumulated distortions can occur in some cases when inadequate waterproofing and drainage details are employed.


Figure 4.31. Example of a longitudinal glulam deck bridge in New York (USA).


Figure 4.32 Longitudinal glulam deck.

4.6 References, chapter 4

AMA (2017). AMA Anläggning 17, Svensk Byggtjänst, 2017 (in Swedish), https://byggtjanst.se

Carlberg J., Toyib B. (2012). “Finite Element Modelling of Interlaminar Slip in Stress-Laminated Timber Decks”, Sweden. Master Thesis.

CEN (2004). Eurocode 5: Design of timber structures – Part 1-1: General rules and rules for buildings, Comité Européen de Normalisation 2004.

CEN (2004b). Eurocode 5: Design of timber structures – Part 2: Bridges, Comité Européen de Normalisation 2004.

ECMWF, European Centre for Medium-Range Weather Forecasts, ERA Interim Daily, http://apps.ecmwf.int/datasets/data/interim-full-daily/levtype=sfc

Edwards, Y. (2002), Tätskikt och beläggning på träbroar, Vägverksprojektet ”State of the art 2002”, KTH 2002

Fortino S, Mirianon F, Toratti T. A (2009). 3D moisture-stress FEM analysis for time dependent problems in timber structures. Mech Time-Depend Mater 13(4):333–56, 2009.

Malo, K. A. (2016). Chapter 11 - Timber bridges. Innovative Bridge Design Handbook. A. Pipinato. Boston, Butterworth-Heinemann, pp. 273-297, 2016.

Pousette, A. (1997). Nordic Timber Bridge Project, Influence of different climates on moisture content, bar forces and cupping. Trätek (1997)

Pousette, A. (1997b), Wearing surfaces for timber bridges, Nordic Timber Bridge Project, 1997, ISBN 91-89002-12-1

Pousette A. (2016) Tätskikt och kantlösningar på tvärspända brobaneplattor av trä (in Swedish), SP Rapport 2016:90, SP Technical Research Institute of Sweden, Borås, 2016

Pousette, A., Fjellström, P.-A. (2016), Experiences from timber bridge inspections in Sweden – examples of influence of moisture, SP Technical Research Institute of Sweden, SP Rapport 2016:45, ISBN 978-91-88349-49-1, 2016

Ritter, M. A. (1992). Timber bridges: design, construction, inspection, and maintenance. Washington DC, U.S. Department of Agriculture, Forest Service, 1992.

Ritter M.A., Geske E.A., , McCutcheon W.J., Moody R.C., Wacker, J.P., Mason L.E. (1991) Methods for assessing the field performance of stress-laminated timber bridges. In: Proceedings of the 1991 International timber enigneering conference; 1991 September 2-5; London. London:TRADA; 1991:3.319-3.326. Vol. 3.

Ritter M.A., Wacker J.P. (1995). Field Performance of Stress-Laminated Timber Bridges on Low-Volume Roads, In Proceedings of the 6th International conference on low-volume roads; 1995 June 25-29; Minneapolis, MN. Washington DC: National Academy Press; 1995. Vol 2. 1995.

Svensson, S., Toratti T. (2002). Mechanical response of wood perpendicular to grain when subjected to changes of humidity, Wood Science and Technology, vol. 36(2), pp. 145-156, 2002.

Toratti, T. (1992). Creep of timber beams in a variable environment. Espoo, Helsinki University of Technology - Laboratory of Structural Engineering and Building Physics, 1992.

Trafikverket (2013). TDOK 2013:0531, Tätskikt på broar, Version 1.0, 2014-07-01, Trafikverket, 2013 (in Swedish)

Trafikverket (2016). TDOK 2016:0204, Krav Brobyggande, Version 1.0, 2016-10-03, Trafikverket, 2016 (in Swedish)

TräGuiden, Skogsindustrierna (in Swedish), www.traguiden.se

Vegdirektoratet (2015). Håndbok N400, Bruprosjektering, Prosjektering av bruer, ferjekaier og andre baerende konstruksjoner, , Statens vegvesen, Vegdirektoratet, 2015 (in Norwegian)

Vegdirektoratet (2015b). Håndbok R762 (2015), Processkode 2, Standard beskrivelse for bruer og kaier, Hovedprocess 8, Statens vegvesen, Vegdirektoratet, 2015 (in Norwegian)

5 Design for long service life

5.1 Design for long service life – good design and bad details

The design and execution of details is extremely important for a long life of timber bridge components. The bridges are exposed to impact from traffic and weather. Experiences from timber bridges which failed on the design of some details leading to deterioration and damages have led to new knowledge of how to develop the bridge designs. To secure a long life of wood, the first step is to study the constructive requirements to avoid risks, which includes the general design and the choice of materials and constructive requirements of well adapted details. Poor detailing has often been the reason for high moisture contents and damages in timber bridges.

The building of timber bridges should as far as possible favor untreated wood, which is a good material with respect to health and the environment. Untreated wood is easy to use in sheltered buildings but a timber bridge generally needs very careful constructive wood protection and carefully designed details. Subjected directly to climatic factors, like rain and sun, untreated wood has a limited lifespan. Treatments and impregnations are needed for a long life.

Chemical preservation with biocide products are used to eliminate damages of fungi, mold and insects which can grow on wet wood. Other damages like cracks and weathering are though not always affected by this impregnation. New wood modification techniques for exterior durability have been developed in recent years. However, even with impregnation or other treatment, the durability is best if wood is kept dry by good detailing.

Wooden bridges with good design that are properly executed are likely to have low maintenance costs. They may even be lower than for other bridges, as bridges of steel and concrete in many locations have maintenance costs due to contamination, corrosion, carbonation etc. because of moisture, pollutants and salting.

5.2 Examples of details

This chapter describes some good and bad examples that can provide support in the design of timber bridges.

The examples show details from bridges that have been built. The assessment is based on experiences from inspections where these types of details have been given annotations. Some mistakes are easy to repair in place; others require greater renovations in the bridge.

Bridges and details should be possible, and preferably easy, to inspect and maintain to give the bridges a long service life.

5.2.1 Foundations, in contact with ground, bushes, sills, etc.

Plants and trees preserve and emit moisture that locally increases the moisture level of the wood. This is part of the natural degradation process of wood. Measure to avoid this is good and solid ground covering around bridges to ensure a drier climate.

Figure 5.1. Bad detail, too much vegetation.

Figure 5.2. Good design, ground has good covering to avoid vegetation.

Figure 5.3. Bad detail, too much vegetation near the bridge end.

Figure 5.4. Good design, ground is covered with gravel (and the grass is cut).

Figure 5.5. Bad detail, new bridge with risk of gravel and dirt to be collected on the abutment.

Figure 5.6. Good design, new bridge with good ventilation at abutment.

A sill beam protruding outside the bridge deck will accumulate water, dirt, and snow. The water collected on the protruding sill beam moistens up to the deck. The sill should be built shorter than the deck width.

Figure 5.7. Bad detail, sill beam protrudes outside deck.

Figure 5.8. Good design, sill beam is drawn in under the deck, but still foundation ledge protrudes.

5.2.2 Stress-laminated decks

Stress-laminated decks are common for both road bridges and pedestrian bridges, and are sometimes used in combination with other structural elements, for example trusses or arches.

The edge details are important as bad details can lead to high moisture contents along the deck edge. A good design should have moisture protection and large enough plates to introduce the pre-stressing force into the deck. Bad design at railing posts can result in drainage water running down the posts causing high moisture contents at the edges of the decks. Bad design of cross-beams under the deck can also contribute to high moisture contents in the deck.

Asphalt coatings ensure a good surface for motor vehicle and cycle traffic. It is important that the waterproofing layer covers the entire deck surface and that it connects well along the edges so that water can drain off in a good way to prevent damage to the structure.

Any cable ducts and cable ladders should be placed in a protected place that is appropriate for wood protection, maintenance and appearance, preferably under the bridge deck.

Figure 5.9. Bad detail, high moisture contents, the leakage came from inadequate execution at the edge and the rail posts.

Figure 5.10. Good design, only small amounts of water follows the railing posts but it does not affect the moisture content in the deck.

Figure 5.11. Bad detail, running water under the deck because edge detail does not work, possibly due to a joint.

Figure 5.12. Good design, a small drip nose prevents water coming on the side of the deck to drain further under the deck. Drip nose and pulled in cross-member can reduce moisture invasion in deck.

Figure 5.13. Bad detail, cables mounted afterwards are placed on the outside of the wooden deck without regard to the structure and they will moisten the wood.

Figure 5.14. Good design. Cable duct laid over transverse beams between longitudinal beams for the sidewalk.

Figure 5.15. Bad detail, many constructions are problematic to inspect both due to accessibility and to installations attached afterwards, for example cables on the outside of deck panel that make it very difficult to control bar forces.

Figure 5.16. Good design, the cladding can easily be removed to control the bar forces and optionally for restressing the bars.

5.2.3 Beams

A solution to prevent water on load-bearing beams is to cover the lateral faces with panel and the horizontal surfaces with a protective plate or hood.

The panel on lateral faces can be made of boards of wood arranged horizontally or vertically. Good ventilation between the boards and the beams must be ensured. The covering will also prevent cracks due to solar aggression and humidity gradients.

Protective coverings of stainless steel, copper or aluminum may be installed to protect horizontal wood surfaces. The use of different metals for protection is to be avoided because of the risk of galvanic corrosion. The end wood of the beams must be protected to avoid water infiltration in wood end grain. The wood should be protected by a metallic protective covering or boarding.

Joints between two pieces of wood should have a minimized contact surface and sufficient spacing of the wood to facilitate the wood to dry quickly after humidification.

Figure 5.17. Bad detail, beam without cladding, with typical cracks on unprotected and weather exposed surfaces.

Figure 5.18. Bad design, large salt-impregnated glulam beams of pedestrian bridge without cladding, with typical cracks and delamination.

Figure 5.19. Bad detail, no cover of end grain and typical cracks and delamination.

Figure 5.20. Good design, steel cover on horizontal surface and end grain of glulam crossbeam.

 

Figure 5.21. Good design. Left: Painted glulam beam with painted cladding of ventilated horizontal wood panel on vertical battens on the outside. Right: The outside of the cladding and on top of the beam is a ventilated steel plate.

Wires, cable ducts and cable ladders should be placed in a protected place that is appropriate for maintenance and appearance. It is quite common for a district heating pipeline to be located under a bridge. During new construction it may be planned for a good location below or next to the bridge. When installing at a later stage it is important to consider wood protection and the opportunity to inspect different parts. Simple installation should be sought and bridge bearing capacity must be checked. See also cables mounted on stress-laminated bridges, Figures 5.13-5.15.

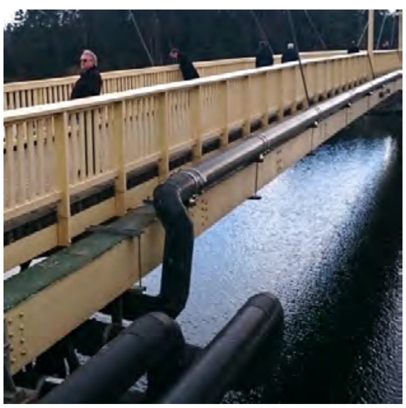

Figure 5.22. Acceptable design, the tube is installed afterwards, in this case on top of the beam.The risk is moisture from the tube to the beam and problem to inspect the covering on top of the beam.

Figure 5.23. Good desing, tube and cables are installed under the deck, protected from moisture and will not moisten the beams.

5.2.4 Columns

Direct contact between wood and concrete should be avoided because the concrete is likely to be wet. This can lead to humidification of the wood and difficulty of drying since it is not ventilated. The solution consists of separating the wood (from the concrete) using a spacer part for example a metal part, making the humidification by the concrete no longer possible. The metal part supporting the column should be smaller (at least 10 mm for each side) to avoid water traps by capillarity. The solution can be further improved by creating a drip groove under the wooden column.

Figure 5.24 shows that water is concentrated to a slot because of water runoff into the connection between the columns. Water flows on the upper side of the inclined columns and down to the slot between the columns. In Figure 5.25 the joining of the columns is attempted sealed with sealant. Immediately after applying the sealant it looks good, but over time a vapor pocket is created between the wood and sealant. Instead it should be constructed with fittings as shown in Figure 5.26. The fittings are slit into the wood to lead the water away from the slot.

Figure 5.24. Bad detail, water can be concentrated to a slot between columns.

Figure 5.25. Bad detail, sealant creates moisture pocket after some years.

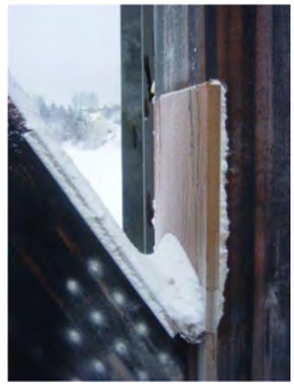

Figure 5.26. Good design, metal fitting protects the slot.

5.2.5 Arches

Arches should have good protection on top and on the sides. The largest risk is at the bottom part, where water can run down along the arch and be collected at the foundation. The steel details at the mechanical connections to abutment must be protected from influence and deterioration of water.

A

B

C

Figure 5.27 Arch bridges. In A the arch was unprotected but painted and had several cracks. In B the top of the arch was protected with a steel cover, but the sides were still unprotected. In C the sides were covered with a ventilated cladding of painted plywood sheets. The growth of cracks should then be significantly reduced and water cannot penetrate into the cracks.

Figure 5.28. Good design with cladding. Moisture sensors have been installed for control at the bottom part of the arch where there is the largest risk of moisture.

Figure 5.29. Good design with cladding of untreated wood and steel cover on top.

Figure 5.30. Bad detail, copper ions from copper fitting runs down to the underlying joint and corrodes the zinc coating.

Figure 5.31. Good design, water from copper fitting is taken out to the side before it reaches the bottom section.

5.2.6 Railings

Railings are weather-exposed parts and replacement of the railing is often necessary during the life of the bridge. However, with good material and execution, the railing can have a relatively long life. The impact of the railing on the durability of the bridge main structure is mainly from attachments of rail posts to beams or deck plates. With distances and drip noses the water should be drained off and not be collected in slots or spaces.

Figure 5.32. Bad detail, railing with no constructive protection, and water flows along diagonal and decay has occurred in lower part.

Figure 5.33. Bad detail, railing with some constructive protection (covering of horizontal parts), but connections between parts prevent adequate ventilation.

Figure 5.34. Bad detail, railing post is designed so that water is directed towards the deck edge.

Figure 5.35. Good design, railing post is extended so that the lower part serves as a dripping nose.

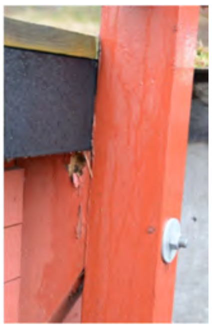

Figure 5.36. Bad detail, railing post attachment, sheet metal cladding is missing and wooden distance have severe decay damage.

Figure 5.37. Good design, sheet metal between bridge deck and railing post protecting from water and no decay in wooden distance or in railing post.

Figure 5.38. Bad detail, railing panel of spruce, one layer of primer with fungicide, two layers of paint, severe decay in the lower part due to water trap between pickets and lower panel rail.

Figure 5.39. Good design, railing panel of treated pine, NTR class A, two layers of primer with fungicide, two layers of paint, paint erosion on all parts but no visible signs of decay.

5.3 Wood coatings or cladding protection measures to reduce effects of moisture intrusion and UV exposure

5.3.1 Generalities and needing of numerical methods

The use of wood in unsheltered structures, such as bridges, is rather limited due to their exposure to the harsh climate conditions. Designers and structural engineers are mostly worried about the service life of load-carrying structures which is recommended to be one hundred years for bridges and fifty years for common buildings in Europe (CEN 2002).

While in the literature it is widely proved that rheological behaviour of wood as well as its mechano-sorptive creep in timber elements can cause large deflections in service conditions (Metelli et al. 2015), further research studies are needed to investigate the effect of moisture content on the peak values of the stresses which can cause premature brittle failure of timber elements or joints (Fragiacomo et al. 2011). The situation has become more challenging in recent years with the increasing demands on load-carrying capacity of structures (e.g. allowed vehicle weight on road bridges was increased from 60 t to 76 t in Finland) and stricter control of the environmental performance of wood treatment (e.g. creosote is likely to be banned in the near future). Therefore, an accurate knowledge of wood moisture behaviour is essential for planning new durable structures and for the assessment of the existing ones (Hradil et al. 2016).

The effects of moisture content *MC* in wood influence the durability, serviceability and safety of timber structures. The moisture accumulated in wood for longer periods may cause, in combination with certain temperatures, conditions suitable for biodegradation of the primary material. The risks for durability in wooden members exposed to variable climates can increase because of the annual variations of relative humidity RH that enlarge the moisture penetration depth (Svensson et al. 2011). In addition, high daily variations of moisture at high levels of relative humidity can cause large moisture gradients near the external surfaces of timber members with development of the so called moisture induced stresses (MIS) and possible increase of crack risk (Fragiacomo et al. 2011), (Fortino et al. 2013)). These stresses can produce cracks in wooden components as, for example, glulam (Jönsson 2005) and cross laminated timber (Gereke and Niemz 2010). As discussed in (Fragiacomo et al. 2011) the MIS perpendicular to grain may exceed the tensile and compressive strength of wooden members also in the absence of external mechanical loads. Improved design of wooden structures accounting for possible moisture effects caused by significant variations of RH is important for their serviceability and safety in order to prevent structural failures related to the design phase (Frühwald et al. 2007).

The moisture-related degradation of timber structures during their service life has been an important topic within the COST Action E55 ('Modelling of the performance of timber structures') along with the development of computational methods aiming at evaluating moisture gradients and MIS. The numerical methods for simulation of moisture transport in timber elements subjected to continuously variable climates are finalized to a more accurate knowledge on the distribution of moisture content (MC) in wood. The numerical approach is particularly useful for the hygro-thermal analysis of bridge elements exposed to outdoor climates along with sensor-based monitoring (Fortino et al. 2013). Furthermore, the numerical methods are useful to evaluate the effects of moisture content MC on specific moisture-driven deformations of timber elements as, for example, the cupping in timber decks (Pousette 2016).

The classical approach for numerical modelling of moisture transport is based on a single-Fickian theory in which the only variable is the moisture content MC (Fortino et al. 2009) while the temperature in wood is assumed equal to the air temperature. On the contrary, the so-called multi-Fickian theory, particularly developed in the last decade (Frandsen 2007) allows a more realistic representation of the moisture transport in wood by simulating the diffusion of water vapour in the cell lumens, the sorption of bound water, and the diffusion of bound water in the cell walls. The multi-Fickian differential problem is characterized by two variables: the bound water concentration and the water vapour concentration. In non-isothermal cases, also the temperature T must be taken into account as a variable of the moisture transport problem while both the relative humidity and the temperature of the air are considered as loads on the wooden structure. In the presence of natural environmental conditions, a model for hysteresis of wood is also needed which uses at least two sorption isotherms to describe the phenomena of adsorption and desorption in wood. A multi-Fickian model with wood hysteresis for timber structures subjected to continuously varying climates was implemented and tested for glulam beams of timber bridges under Southern European climates (Fortino et al. 2013) and, more recently, under Northern European climates (Fortino et al. 2016).

In the following, the single-Fickian and multi-Fickian models for moisture transfer in wood material used in the earlier literature are described and some examples of applications are provided for exploitation in the engineering practice. The models are implemented in user subroutines of Abaqus finite element code (Hibbit et al. 2014).

5.3.2 Single-Fickian method for moisture transport in wood

The so-called single-Fickian theory of moisture transport in wood is based on the three dimensional Fick equation (Fortino et al. 2009):

$$\frac{\partial MC}{\partial t} - = \nabla \bullet (\mathbf{D}\nabla MC) \tag{5.1}$$

where MC is the moisture content of wood and $\mathbf{D}$ the diffusion tensor of moisture transfer. This form of the Fick equation can be used when the density of wood (ρ) is constant. For varying density, the variable concentration $c = \rho MC$ instead of MC should be considered (where c represents the concentration in kg/m^3). In the literature the assumption of isotropic diffusion is usually made and only the diagonal coefficients of the corresponding matrix are considered to be nonzero. The moisture flow through the surface is given by the following equation:

$$q_n = \rho S(MC_{air} - MC_{surf}) \tag{5.2}$$

where q_n is value of the flow across the boundary, ρ_0 represents the wood density in absolute dry conditions, S is the so-called surface emissivity (that can take into account also eventual protective coatings), MC_{surf} is the moisture content on the wood surface and MC_{air}, also known as sorption isotherm, represents the equilibrium moisture content of wood corresponding to the air humidity. The expression for the sorption isotherm used in (Fortino et al. 2009) is:

$$MC_{air} = 0.01\left(\frac{-T\ln(1-RH)}{0.13(1-T/647.1)^{-6.46}}\right)^{\frac{1}{110T^{-0.75}}} \tag{5.3}$$

where T is temperature of the air and RH the relative humidity of the air. Expressions for diffusion and surface emission parameters are provided in (Fortino et al. 2009). A review on the material parameters for moisture transfer used in the literature is given by (Angst 2012). Very recently the described model has been further developed for cases of MC above the fibre saturation point (FPS) in water traps by using a permeability tensor in place of the diffusion tensor, see (Musci 2016).

5.3.3 Multi-Fickian method for moisture transport in wood

According to (Fortino et al. 2013), the multi-Fickian differential equations governing the hygro-thermal behaviour of wood are the following:

$$\frac{\partial c_b}{\partial t} = \nabla \cdot \mathbf{D}_b \nabla c_b + \dot{c} \tag{5.4}$$

$$\frac{\partial c_v}{\partial t} = \nabla \cdot (\mathbf{D}_v \nabla c_v) - \dot{c} \tag{5.5}$$

$$c_w \rho \frac{\partial T}{\partial t} = \nabla \cdot \mathbf{K}_H \nabla T + \nabla \cdot (\mathbf{D}_b \nabla c_b) h_b + \nabla \cdot (\mathbf{D}_v \nabla c_v) h_v + \dot{c} h_{vb} \tag{5.6}$$

where (5.4) and (5.5) are the transport equations and (5.6) represents the equation of energy conservation. The variables of the problem are the concentration of bound water in cell walls c_b, the concentration of water vapour in cell lumens c_v and the temperature T. $\mathbf{D}_b$ and $\mathbf{D}_v$ are the diffusion tensors for bound water and vapour water and $\mathbf{K}$ the thermal conductivity tensor. The coupling term dot c represents the sorption rate, c_w the specific heat and ρ the dry density. In Equation (5.6) h_b and h_v represent the specific enthalpies of bound and vapour water while $h_{vb} = h_b - h_v$ is the specific enthalpy of the transition from the bound water phase to the water vapour. According to (Frandsen 2007) the sorption rate in terms of concentrations is defined as

$$\dot{c} = H_c (c_{bl} - c_b) \tag{5.7}$$

in which H_c is the so-called moisture-dependent reaction rate and $c_{bl} = \rho_0\, m_{bl}$ represents the bound water concentration in equilibrium with a given relative humidity according to a suitable sorption isotherm m_{bl}. All expressions of the above material parameters can be found in (Fortino et al. 2013).

Boundary conditions

The following homogeneous Neumann boundary conditions for bound water concentration, water vapour concentration and temperature are used on the protected surfaces:

$$\nabla c_b = 0, \quad \nabla c_v = 0, \quad \nabla T = 0 \tag{5.8}$$

while the surface in contact with air assumes only bound water concentration:

$$\nabla c_b = 0 \tag{5.9}$$

The flux of the water vapor is expressed as

$$-\mathbf{n}\cdot\mathbf{D}_v\nabla c_v = k_v\left(c_{1v} - c_v^a\right) \tag{5.10}$$

and the heat flux is:

$$-\mathbf{n}\cdot\mathbf{K}\,\nabla T = k_T\left(T - T^a\right) \tag{5.11}$$

where c_v^a and T^a are ambient water vapour concentration and temperature of the surrounding air, k_v and k_T represent the surface emission coefficients for water vapour and temperature, respectively, and $c_{1v}=c_v/\varphi$ is the concentration of vapour divided by the porosity φ.

The used surface emission coefficient for temperature in boundary conditions (14) is $k_T = 20$ W $m^{-2}K^{-1}$.

Considering the surface emission for the uncoated wood and the coefficient for coating the whole resistance to the humidity exchanges between wood and the surrounding environment is calculated as in (Fortino et al 2016).

5.3.4 Models for sorption isotherms

In the literature the following Hailwood – Harrobin isotherm is often used (Frandsen 2007):

$$m_{bl} = \frac{RH}{f_1 + f_2 RH + f_3 RH^2} \tag{5.12}$$

where the relative humidity RH is calculated as the ratio between vapour pressure p_v and saturated vapour pressure p_{vs} that is temperature-dependent and for the thermal ranges above the freezing point is defined by the following semi-empirical Kirchhoff equation:

$$p_{vs} = \exp\left(53.421 - \frac{6516.3}{T} - 4.125\ln(T)\right) \tag{5.13}$$

Additionally, the temperature dependency in the subfreezing range is described with the following equation fitted by Teten for ice:

$$p_{vs} = 100\times 10^{9.5(T-273.15)/(T-7.65)+0.7858} \tag{5.14}$$

The values of parameters f_i fitted on the measurements by Ahlgren (see Frandsen 2007) and used in the applications are reported in Table 5.1.

Table 5.1. Shape parameters for adsorption and desorption isotherms fitted on Ahlgren's measurements (1972).

α	$f_{1\alpha}$ [-]	$f_{2\alpha}$ [-]	$f_{3\alpha}$ [-]
a	1.804	13.63	-12.12
d	1.886	7.884	-6.526

To take into account the varying temperature, the following Anderson-McCarthy model for sorption isotherms is available:

$$m_\alpha = \ln\left(\frac{\ln(1/RH)}{f_{1\alpha}}\right); \quad \alpha = a, d \tag{5.15}$$

where $f_{i\alpha}$ are shape parameters defined as functions of the current temperature and represented as polynomials $f_{i\alpha} = b_{i0\alpha} + b_{i1\alpha}T + b_{i2\alpha}T^2 + \ldots + b_{in\alpha}T^n$, i=1,2. The subscripts a and d refer to adsorption and desorption, respectively. The used parameters $b_{ij\alpha}$, calibrated for temperatures above and below zero, are extrapolated from the measurements of Hedlin on Norway spruce (see references in Fortino et al 2016) and reported in Table 5.2.

Table 5.2. Shape parameters for the temperature-dependent adsorption and desorption functions fitted on Hedlin's measurements (1967)

α	n	$b_{10\alpha}$ [-]	$b_{11\alpha}$ [K^{-1}]	$b_{20\alpha}$ [-]	$b_{21\alpha}$ [K^{-1}]
a	1	7.719	-0.011	5.079	0.04577
d	1	9.7397	-0.017	-13.419	0.1002

As shown in the earlier literature, the use of an algorithm of sorption hysteresis allows taking into account the dependency of the equilibrium bound water concentration on the history of variations in relative humidity. The reader is referred to (Frandsen 2007) for the description of the algorithm. To make the analysis faster, the multi-Fickian model used in the present Guidelines does not include the algorithm of hysteresis for wood but considers a temperature dependent sorption curve which is the average between the adsorption and desorption curve of Table 5.2.

5.3.5 Orthotropic-viscoelastic mechanosorptive model for wood

The calculation of moisture induced stresses (*MIS*) is based on the orthotropic-viscoelastic-mechanosorptive material model proposed in (Fortino et al. 2009). The model is composed of five deformation mechanisms in series which provide a decomposition of strain into elastic response, hygroexpansion, viscoelastic creep, recoverable mechanosorption and mechanosorptive irrecoverable creep. Both the viscoelastic and the mechanosorptive recoverable creep are described through Kelvin type elements. The derivation of all stresses and strains and the matrix form of the viscoelastic $\mathbf{C}_i^{ve}$ and mechanosorptive $\mathbf{C}_j^{ms}$ elemental tensors as well as the material parameters of the model can be found in (Fortino et al. 2009). In particular, the elastic strain of the model is form is defined as

$$\boldsymbol{\varepsilon}^{e} = \boldsymbol{\varepsilon} - \boldsymbol{\varepsilon}^{u} - \sum_{i=1}^{p} \boldsymbol{\varepsilon}_i^{ve} - \sum_{j=1}^{q} \boldsymbol{\varepsilon}_j^{ms} - \boldsymbol{\varepsilon}^{ms,irr} \tag{5.16}$$

being the $\boldsymbol{\varepsilon}$ the total strain, $\boldsymbol{\varepsilon}^{u}$ the hygroexpansion strain, $\boldsymbol{\varepsilon}_i^{ve}$ and $\boldsymbol{\varepsilon}_j^{ms}$ the viscoelastic and mechanosorptive elemental creep strain and $\boldsymbol{\varepsilon}^{ms,irr}$ the irrecoverable mechanosorptive strain tensor. The elastic moduli of the model are expressed as functions of density, temperature and moisture content.

5.3.6 Moisture gradients and moisture induced stresses in protected glulam beams of bridges

Suitable paints on the wooden surfaces together with cladding panels on the outside surfaces are protective systems for glulam beams of timber bridges largely used in Sweden.

5.3.7 Glulam beams protected by paints and cladding. Case-study: Älsvbacka bridge.

As a case-study, the hygro-thermal response of a glulam beam of pedestrian and bicycle Älsvbacka bridge (Figure 5.40) is studied by using the multi-Fickian method for moisture transport. The beam has a cross section of 645×1100 mm^2. The 130 meter long cable-stayed bridge passes over the river in Skellefteå. It is a slender and complex structure taken into use in late summer 2011. The beams and pylons of the bridge are painted with an opaque wood stain in a yellow colour. Furthermore, the pylons and the outer surfaces of the beams are coated with one coat of paint and covered by painted panels. The used wood is Norway spruce (Picea abies). The top of the beam is protected by a roof construction of wood with wood cladding covered by a roof underlay membrane and flat steel sheeting. The inner surfaces and the ends are treated with an oil primer and two coats of paint (see (Pousette et al 2014) for the details).

Long-term monitoring of moisture content *MC* and temperature *T* of the beam was performed in a previous research by SP Wood Building Technology by using wireless sensors from Omnisens (Pousette et al 2014). Several sensor systems were installed to monitor the long-term behaviour of the bridge. The data have been collected since 2011 with some interruptions and the moisture measurements are still on-going. The same wireless system was also tested in other projects. The sensors were activated once an hour and the monitored data were sent to a gateway placed in a control box at one of the foundations. The sensors were mounted with screws but were not insulated. Due to this, they were able to measure the highest moisture content from the surface to about 25 mm into the beam but the precise location of the registered measurement is not known. The moisture content and temperature were registered every hour. From the beginning of measurements there was interference with another gateway in a nearby wooden house. Due to this, from October 2012 there were no measurements for the bridge for a few hours each afternoon.

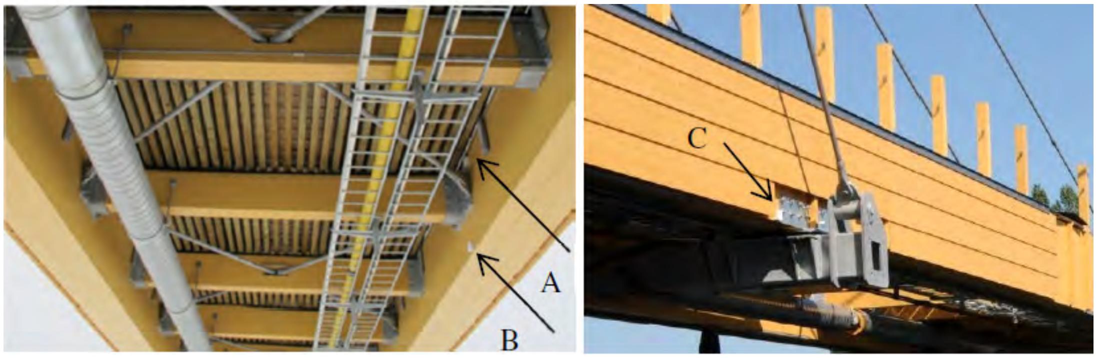

Figure 5.40. Älsvbacka bridge. Sensors A and B in the internal part of the beam (top) and sensor C on the outside beam protected by cladding (bottom).

Air temperature, relative humidity, wind speed and direction, barometric pressure, rainfall intensity and duration were measured *in situ* with a weather station located on top of the roof of the building of SP Wood Building Technology about 900 m from the bridge in westerly direction and about 10 m above ground and at a distance from the river of about 300 m. The measured data showed an interesting difference between the moisture contents at the outside and inside of the bottom of the monitored beam (see the positions of sensors in Figure 5.40). In particular, the moisture content on the inside bottom registered very different moisture variations in summer and winter seasons due to the fact that the sensors are not insulated.

Information on the values of the surface resistance or permeance of the used paints and oils are not available. However, according to SP, these values could be considered in the range of the alkyd oil paints, acrylate paints or varnishes (Berge 2009). These permeance values are reported in Table 5.3 together with the values for a weaker paint (glue paint). The related numerical results are considered as references to be compared with the measurements.

Table 5.3. Permeance and resistance values of the reference paints

Paint	**Permeance** [kg/ m^2 s Pa]	**Resistance** [Pa m^2 s/kg]
alkyd oil paint/linseed oil paint	4E-10	2.5E+9
acrylate oil paint/varnish	1E-9	1E+9
glue paint	5E-9	2E+8

In the present study, the moisture gradients and moisture induced stresses of the glulam beam are studied for 20 months of service life (1.3.2012 – 31.10.2013), see Figure 5.41. After this date the monitoring weather station was changed.

In the following Probe A (inside at 250 mm from the top) and Probe C (outside at 25 mm from the bottom) indicate locations between the external wood surface and 25 mm depth (Figure 5.43).

To model the hygro-thermal response of the inside beam (Probe A), the average temperature dependent sorption model is adopted. To simulate the hygro-thermal response in the presence of cladding (outside beam, Probe C), characterized by lower levels of *MC*, the temperature dependent adsorption curve of the sorption model is used.

5.3.8 Results and recommendations

Figure 5.42 shows the moisture content *MC* during time at the wood surface and the average *MC* between the surface and 25 mm for Probe A and Probe C, respectively. Figure 5.43 shows the numerical values of temperature and relative humidity on the wood surface compared to the same values measured in a sensor out of the wood for the case of weaker coating, the glue paint. The envelopes of maximum and minumum values of moisture content along a path from the external surface to 250 mm for locations Probe A and Probe C are presented in Figure 5.44. The envelopes show that in the bottom corner with cladding the penetration depth along the width and the height of the beam is much larger than the one of the location close to the inside top. This is due to the two moisture fluxes acting on the bottom and lateral surface at the corner location.

Within the studied period (01.3.2012 – 31.10.2013) the moisture gradients and moisture induced stresses (*MIS)* are checked during seasonal periods corresponding to spring (Mar-May), summer (Jun-Aug), autumn (Sept-Nov) and winter (Dec-Feb). Figures 5.45 shows that the maximum and minimum values of surface *MIS* are found in correspondence of the maximum and minimum values of moisture gradients calculated as $(MC_{\Delta L} - MC_{surf})/\Delta L$ where $MC_{\Delta L}$ is the moisture content at a distance ΔL=12.5 mm from the external surface and MC_{surf} is the moisture content on the surface.

The *MIS* are calculated for two ideal configurations with rectangular coordinates having 1) the horizontal direction equal to the radial direction of wood (configuration RTL) and 2) the horizontal direction equal to the tangential direction of wood (configuration TRL). The used elastic properties are listed in Table 5.3 and refer to mean values for spruce wood (Mirianon et al. 2008). The other material properties are taken from (Fortino et al. 2009).

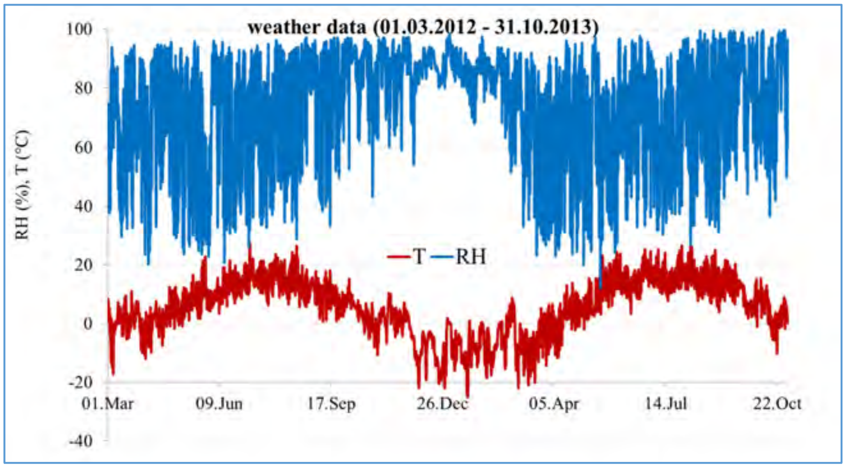

Figure 5.41 Outdoor temperature and relative humidity

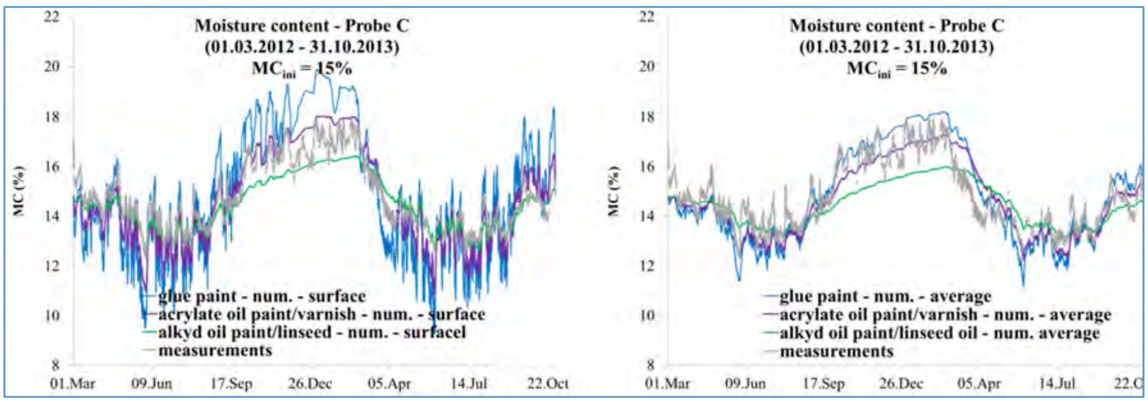

Figure 5.42. MC versus time for different coatings on the beam surface at the outside bottom with cladding (Probe C).

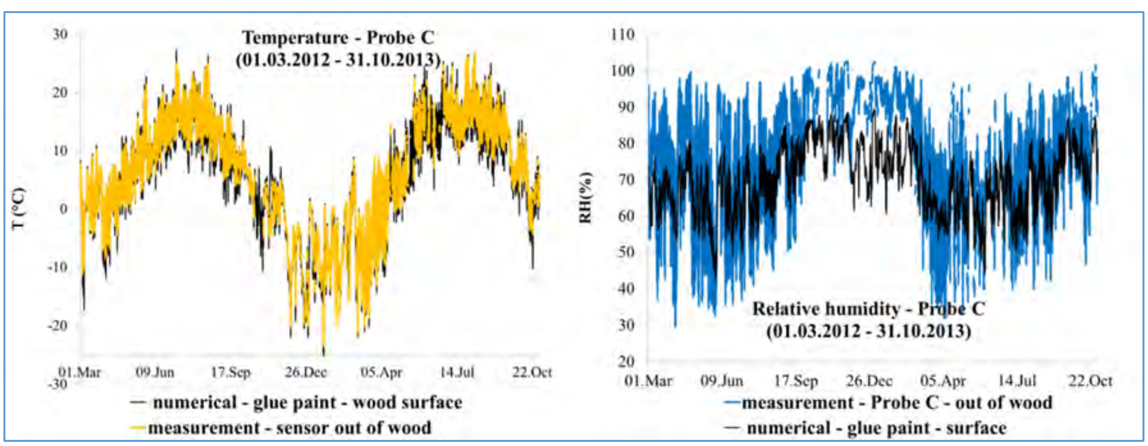

Figure 5.43. Temperature (left) and relative humidity (right) versus time for different coatings at the outside bottom with cladding (Probe C) on the wood surface.

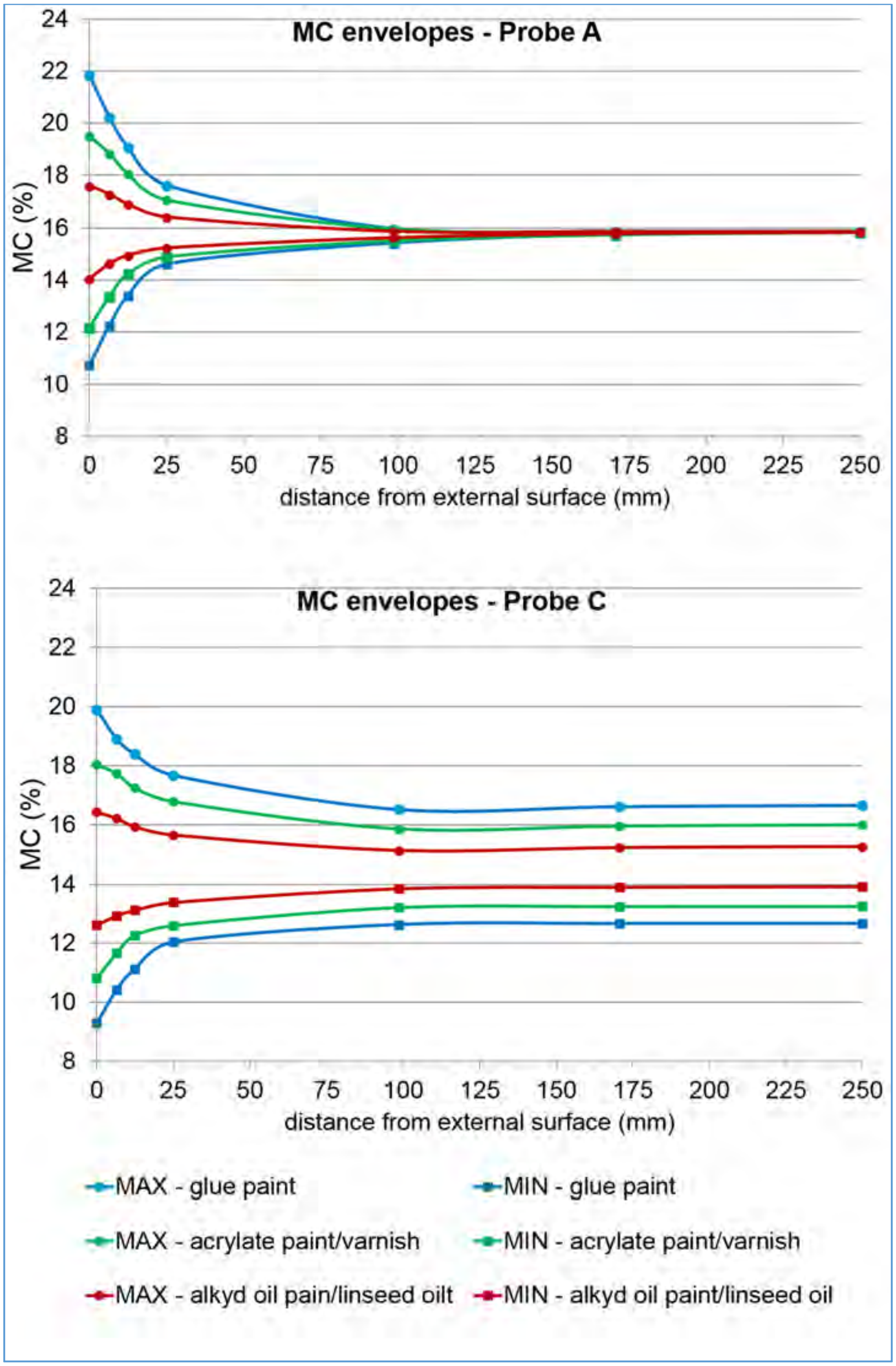

Figure 5.44. Envelopes of maximum and minimum moisture contents (MC) for different coatings at Probe A (top) and Probe C (bottom).

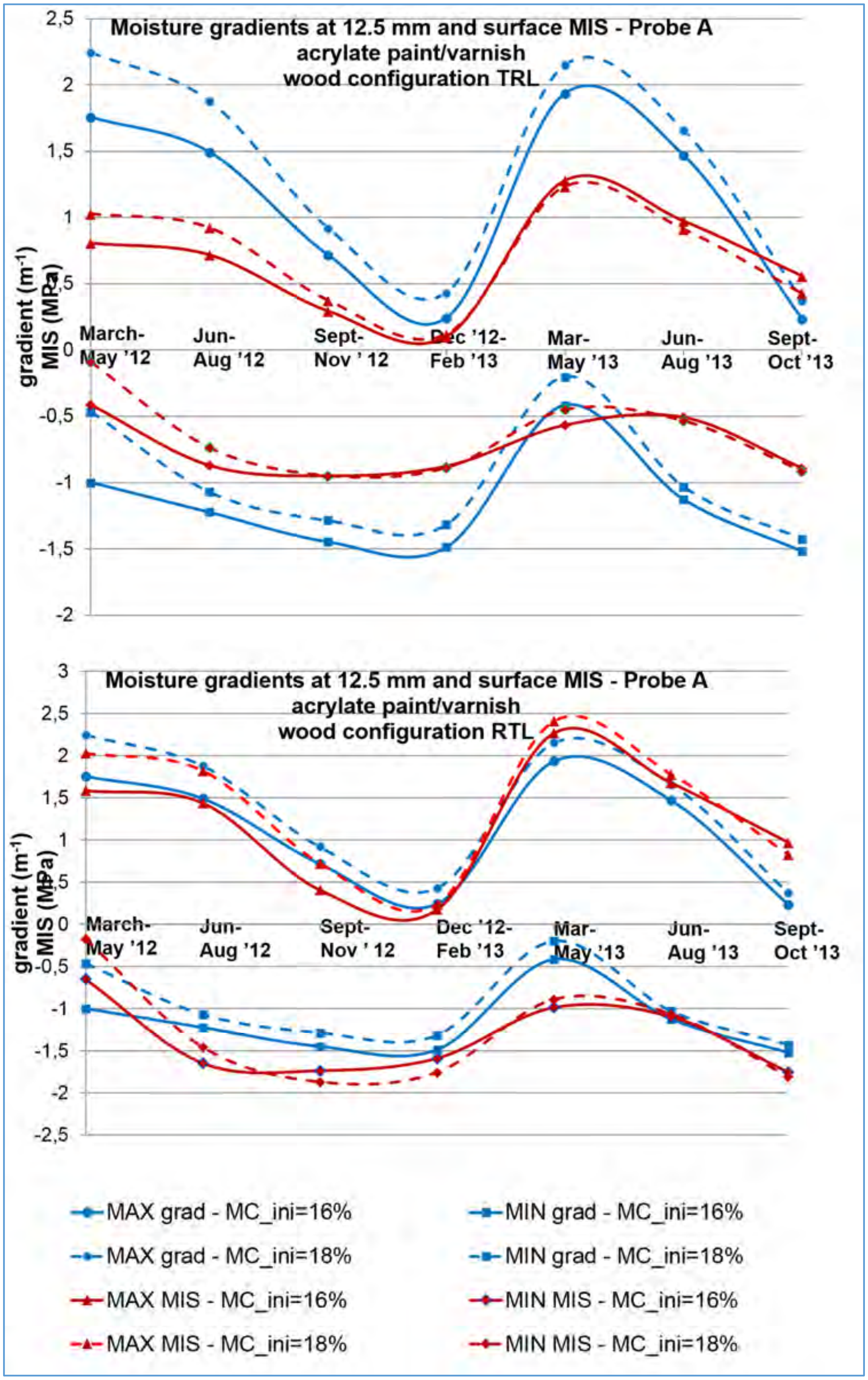

Figure 5.45. Probe A. Moisture gradients at 12.5 mm and surface MIS for different initial moisture contents (MC_ini) in the case of configuration TRL (top) and RTL (bottom).

The moisture gradients at 12.5 mm from the surface and surface moisture induced stresses are found to be larger at the top inside of the beam than at the outside bottom in correspondence of cladding where the peaks of moisture content are lower (Figure 5.44). The influence of initial moisture content (MC_{ini}=16% and MC_{ini}=18%) on the evaluation of moisture gradients and *MIS* in Probe A is shown in Figure 5.45 for the case of acrylate paint/varnish. The major effect is found at the beginning of the analysis but the peaks of gradients and *MIS* are very similar in the two studied cases. It is found that the MIS are larger in the configuration RTL (see Figure 5.45). For both configurations the maximum MIS are found in the seasonal periods with the maximum moisture gradients, i.e. end of May 2013. The results in terms of maximum *MIS* found during March-May 2013 are listed for different different reference coatings for Probe A (Table 5.4) and Probe C (Table 5.5).

Table 5.4. Elastic properties used for the MIS analysis.

E_R (MPa)	**E_T** (MPa)	**E_L** (MPa)	**G_{RT}** (MPa)	**G_{RL}** (MPa)	**G_{TL}** (MPa)	**ν_{RT}**	**ν_{RT}**	**ν_{RT}**
600	600	12000	40	700	700	0.558	0.038	0.015

Table 5.5. Protection by paint. March-May 2013 (Probe A). Moisture induced stresses (MIS) perpendicular to grain at the outside bottom. Initial moisture content= 16%.

Reference paint	**Surface resistance** [Pa m^2 s/kg]	**TRL** max tensile [MPa]	**TRL** max compr. [MPa]	**RTL** max tensile [MPa]	**RTL** max compr. [MPa]
alkyd oil/linseed oil	2.5E+9	0.70637	-0.38662	1.38044	-0.75966
acrylate paint/varnish	1E+9	1.28099	-0.56475	2.26608	-0.98292
glue paint	2E+8	1.52685	-0.71969	2.97891	-1.41915

Table 5.6. Protection by paint and cladding (Probe C). March-May 2013. Moisture induced stresses (MIS) perpendicular to grain at the outside bottom. Initial moisture content=15%.

Reference paint	**Surface resistance** [Pa m^2 s/kg]	**TRL** max tensile [MPa]	**TRL** max compr. [MPa]	**RTL** max tensile [MPa]	**RTL** max compr. [MPa]
alkyd oil/linseed oil	2.5E+9	0.36243	-0.14591	0.54804	-0.20919
acrylate paint/varnish	1E+9	0.59670	-0.507243	0.89186	-0.38072
glue paint	2E+8	0.88980	-0.44406	1.38438	-0.85331

From Tables 5.5 and 5.6 it can be observed that the maximum (positive) and the minimum (negative) moisture gradients increase with decreasing value of surface resistance of the paint. In all locations the maximum tensile *MIS* for both configurations RTL and TRL are found in correspondence of the maximum moisture gradients that appears in the presence of drying at the end of Spring (end of May). Due to this, for a good maintanance and eventual repair of the protective system, it it recommended to check the conditions of paints and claddings at the beginning of summer.

5.4 References, chapter 5

AMA (2017). AMA Anläggning 17, Svensk Byggtjänst, 2017 (in Swedish), https://byggtjanst.se

Carlberg J., Toyib B. (2012). "Finite Element Modelling of Interlaminar Slip in Stress-Laminated Timber Decks", Sweden. Master Thesis.

CEN (2004). Eurocode 5: Design of timber structures – Part 1-1: General rules and rules for buildings, Comité Européen de Normalisation 2004.

CEN (2004b). Eurocode 5: Design of timber structures – Part 2: Bridges, Comité Européen de Normalisation 2004.

ECMWF, European Centre for Medium-Range Weather Forecasts, ERA Interim Daily, http://apps.ecmwf.int/datasets/data/interim-full-daily/levtype=sfc

Edwards, Y. (2002), Tätskikt och beläggning på träbroar, Vägverksprojektet "State of the art 2002", KTH 2002

Fortino S, Mirianon F, Toratti T. A (2009). 3D moisture-stress FEM analysis for time dependent problems in timber structures. Mech Time-Depend Mater 13(4):333–56, 2009.

Malo, K. A. (2016). Chapter 11 - Timber bridges. Innovative Bridge Design Handbook. A. Pipinato. Boston, Butterworth-Heinemann, pp. 273-297, 2016.

Pousette, A. (1997). Nordic Timber Bridge Project, Influence of different climates on moisture content, bar forces and cupping. Trätek (1997)

Pousette, A. (1997b), Wearing surfaces for timber bridges, Nordic Timber Bridge Project, 1997, ISBN 91-89002-12-1

Pousette A. (2016) Tätskikt och kantlösningar på tvärspända brobaneplattor av trä (in Swedish), SP Rapport 2016:90, SP Technical Research Institute of Sweden, Borås, 2016

Pousette, A., Fjellström, P.-A. (2016), Experiences from timber bridge inspections in Sweden – examples of influence of moisture, SP Technical Research Institute of Sweden, SP Rapport 2016:45, ISBN 978-91-88349-49-1, 2016

Ritter, M. A. (1992). Timber bridges: design, construction, inspection, and maintenance. Washington DC, U.S. Department of Agriculture, Forest Service, 1992.

Ritter M.A., Geske E.A., , McCutcheon W.J., Moody R.C., Wacker, J.P., Mason L.E. (1991) Methods for assessing the field performance of stress-laminated timber bridges. In: Proceedings of the 1991 International timber enigneering conference; 1991 September 2-5; London. London:TRADA; 1991:3.319-3.326. Vol. 3.

Ritter M.A., Wacker J.P. (1995). Field Performance of Stress-Laminated Timber Bridges on Low-Volume Roads, In Proceedings of the 6th International conference on low-volume roads; 1995 June 25-29; Minneapolis, MN. Washington DC: National Academy Press; 1995. Vol 2. 1995.

Sétra (2007). Timber Bridges. How to ensure their durability. Technical Guide. © 2007 Sétra - Reference: 0743A - ISRN: EQ-SETRA--07-ED40--FR+ENG, This document is available and can be downloaded on Sétra website: http://www.setra.equipement.gouv.fr

Statens Vegvesen (2016) Inspeksjonserfaring på trebruer, Learning Experiences from Timber Bridge Inspections, Statens Vegvesen Rapporter, Nr. 468, Januar 2016

Svensson, S., Toratti T. (2002). Mechanical response of wood perpendicular to grain when subjected to changes of humidity, Wood Science and Technology, vol. 36(2), pp. 145-156, 2002.

Toratti, T. (1992). Creep of timber beams in a variable environment. Espoo, Helsinki University of Technology - Laboratory of Structural Engineering and Building Physics, 1992.

Trafikverket (2013). TDOK 2013:0531, Tätskikt på broar, Version 1.0, 2014-07-01, Trafikverket, 2013 (in Swedish)

Trafikverket (2016). TDOK 2016:0204, Krav Brobyggande, Version 1.0, 2016-10-03, Trafikverket, 2016 (in Swedish)

TräGuiden, Skogsindustrierna (in Swedish), www.traguiden.se

Vegdirektoratet (2015). Håndbok N400, Bruprosjektering, Prosjektering av bruer, ferjekaier og andre baerende konstruksjoner, , Statens vegvesen, Vegdirektoratet, 2015 (in Norwegian)

Vegdirektoratet (2015b). Håndbok R762 (2015), Processkode 2, Standard beskrivelse for bruer og kaier, Hovedprocess 8, Statens vegvesen, Vegdirektoratet, 2015 (in Norwegian)

6 Maintenance and inspections

Maintenance and inspection of existing timber bridges is important to ensure their safety and maximize service life. Owners and managers of bridges must maintain the bridges and inspect them regularly in order to meet the design service life. In addition, it may sometimes be necessary to improve bridges due to increasing loads or other changes which alter the technical requirements, but they are actions beyond normal maintenance.

6.1 Maintenance

Timber bridges, like bridges of other materials, should during the entire lifetime be maintained to be safe and meet the requirements for the intended traffic they were built for. Maintenance activities can include cleaning of dirt and other debris that can degrade the quality of the wood. For protection of the timber structure any paint or covering sheets should be maintained and asphalt and waterproofing may need replacement a few times during the lifetime. Guardrails which are no longer safe for crashes or rust should be replaced.

There are many incidents affecting bridges and a good balance between preventive and corrective maintenance minimizes costs during the planned lifespan of the bridges. Normally, a preventive maintenance is the most cost effective. This will prevent the occurrence of large damages that may impair the operation of the bridge. If damage occurs however, there should be a plan for corrective measures to maintain the structural integrity of the bridge.

6.1.1 Service life

The required service life of timber bridges varies between countries. This service life assumes that the bridges are regularly inspected and maintained.

In Finland the required life is 100 years according to EN 1990 (2002) unless otherwise agreed on a project basis. Wooden bridge superstructure life is basically 50 years, as compatible with most of the wooden bridges. The Transport Administration may require a longer lifetime of e.g. highway wooden bridges. Longer life is the subject of weather protected wooden structures in service class 2. The life of individual structural parts may be less than 50 years, provided the structural elements are designed to be easily replaceable. For example, a plank deck design service life can usually be 25 years.

In Norway the requirement is also a lifetime of 100 years for bridges and other load-bearing structures. Bridge parts and equipment that have a lifetime less than 100 years should be replaceable and the structure must be designed to take into account the planned replacement work. Reduced lifetime is possible for new bridges that are part of existing road sections, where a 50-year design lifetime can be considered.

Bridges in Sweden should be designed and dimensioned for a technical life of 40, 80 or 120 years. The requirements for wooden bridge superstructures are 40 or 80 years with different demands on the wood protection. A wooden bridge with a design life 80 years must have an operating and maintenance plan that includes at least pre-stressing and anchorage devices for this, connections, moisture contents of main structure, wood protection operation and maintenance needs, and guidelines for the inspection and maintenance of the surface treatment.

In the USA, service life requirements are not well codified in the current AASHTO-LRFD bridge design specifications. Most bridge engineers utilize 75-years as a target design life, which is required by AASHTO-LRFD primarily for substructure components. For timber bridges, many bridges have been shown to provide acceptable service life of 50-75 years, depending upon the environmental exposure and timeliness and effectiveness of maintenance. Timber bridge durability in the USA is predicated on the use of preservatives by pressure treatment methods. National efforts led by the Federal Highway Administration are focused on design practices that can achieve 100-plus year bridge service lives. Also, as part of the National Long-term Bridge Performance Monitoring program, hundreds of bridges have been instrumented and are being actively monitored to improve bridge deterioration modeling and service life predictions for a variety of bridge superstructure types.

6.1.2 Preservative treatments

Modern techniques and preservative chemicals can protect timber bridges from deterioration and prolong the life. Also exposed bridge parts made of spruce with no impregnation are at-risk structures, because untreated spruce can begin to rot within only a few years with adequate moisture. Wood preservatives can be applied by brushing, spraying, dipping or by impregnation. Impregnation is the most effective.

Copper-based salt impregnation

Pine wood is mainly used for impregnation, and it is the easily treated sapwood that can take up the waterborne agents. The heartwood has in itself a certain natural protection against decay by the content of various resins, but cannot compete with impregnated sapwood in terms of biological resistance. Impregnation is carried out industrially and the impregnated wood is divided into different wood preservation classes depending on the amount of supplied agents and penetration depth. The waterborne agents (salts) contain copper and sometimes additional agents such as boron or chromium, however chromium is not allowed in Sweden. Impregnation can have an impact on corrosion of metal components which must be considered. Impregnated wood can be painted with common paints, provided the wood is dry with moisture content of about 16%. Kiln drying or drying in timber yard is used after impregnation; the impregnated wood is often quite wet at delivery (MC $\geq$ 20%). The best is to order wood that is dried to the proper moisture content. Salt impregnation will not protect against splitting and checking, and glulam members should also be protected by design and surface treatment. In Norway lamellae are pressure treated with a waterborne copper-based preservative, then fabricated into glulam beams, cut to final lengths and prepared with holes etc. for joints, and finally the bridge components are pressure treated with creosote.

Creosote impregnation

Wood impregnation with creosote oil can last for up to 100 years depending on the amount of creosote used. Creosote impregnated wood is considered very durable and the wood surfaces require little maintenance. Creosote is a complex mixture including more than one hundred chemical compounds, mainly of polycyclic aromatic hydrocarbons, and also phenolic and aromatic nitrogen and sulphur compounds. This product is an excellent preservative but has also disadvantages from the toxicological and practical point of view. Creosote is therefore not allowed for use in timber bridges in Sweden. Creosote treated timber cannot be painted with regular paint, but can be finished with various oil products. Creosote sweating has sometimes been a problem on bridges but differs a lot between bridges and depends on different amounts of creosote in the timber, variances in the wood materials, design and climate conditions. Creosote sweating can cause dripping of creosote and be a problem if there is a road beneath the bridge, especially problematic are hot summer days. But the problem can be fixed with protective metal plates on the underside of the bridge. Migration of creosote can also affect the wearing course on the bridge leading to deformation or cracks, and a protective layer is important to avoid this. With heat and long pressure periods, creosote can be penetrating even fairly difficult to treat wood species. Creosote treatment does not accelerate the rate of corrosion of metal fasteners relative to untreated wood.

New substitutes for creosote
Creosote is an effective wood preservative but because of its toxicity there is a planned ban of creosote in Europe. Research is now ongoing to find substitutes, Newsletter (2015). Solutions based on tall oil are now examined if they have similar biocide characteristics and water repellent properties. Tall oil is a by-product of the pulp and paper industry and currently used as energy in this industry or as a resin in different industries. The research work includes studies of durability, leaching and impregnation process as well as physical, mechanical and environmental properties of the treated wood.

6.1.3 Paint

Weather exposed load bearing glulam parts of spruce or pine (without creosote treatment) should normally be fitted with a cladding, for example ventilated exterior wood panel or sheet metal cladding. A paint can also provide some protection against humidification and drying of an exposed wood surface. Note that paint only works if wood is untreated or treated with copper-based solutions, not with creosote.


Figure 6.1. Arch protected with ventilated cladding of boards on the sides and steel hood on top, arch and cladding painted red (Gislaved, Sweden). Right: Underside of arch at support.

Figure 6.2. Cross beam painted red (Falun, Sweden)

Figure 6.3. Painted beam bridge (Vaxholm, Sweden)

Wood that is untreated or surface treated with a non-pigmented treatment (for example colorless wood oil) becomes gray after a period of outdoor exposure. A good protection against UV-radiation is obtained with a pigmented coating and the higher the pigment content the better the protection. An untreated wood or poorly maintained surface treatment can be humidified by rain, wet snow, melting or splashing water, which will in time cause discoloration and cracking.

Deformations and cracking can be reduced with a coating, but the changes between rain and sunshine put great pressure on weather exposed surfaces. In sunlight, a surface can quickly get high temperature and a dark surface can reach up to 70 °C. This provides extensive drying of the wood and movements of the surface which gradually begins to crack. Smaller cracks are generally not of any major problem but larger cracks can provide water to penetrate into the inner parts of the wood. They can also collect moisture-holding debris and dirt that can induce microbial growth.

Exposed painted wood need maintenance in order to obtain a sustainable surface. Repainting of exposed parts is normally required for most paint systems every 10-15 years and about every 25 years for weather protected parts. The paint must match the existing paint system and the recommendations and instructions of the paint manufacturer should be followed. If any part is damaged and the paint is scratched off it should be repaired as soon as possible.

6.1.4 Preventive maintenance

Preventive maintenance includes the actions to keep bridges in a good condition. Maintenance companies should check the bridge, clean up and make sure that plants growing near the bridge are trimmed and do not disturb the traffic. To plan maintenance carefully, the Road Authorities usually have some kind of supporting bridge management system where information on the bridges are stored. Bridge maintenance is a long term work that requires qualified personnel.

Condition based maintenance is preventive maintenance that consists of regular inspecting and monitoring the state of a bridge with regard to its function and capacity, and the resulting need for actions. Actions are taken when the state is becoming unacceptable. In addition, bridges should be checked annually. A general inspection of the bridge should be made to find visible errors and deficiencies, for example collision damages, dirt on abutments, vegetation close to the bridge, loose parts, vandalism and other things that has happened and should be corrected as soon as possible.

Vegetation

The vegetation around the bridge should be kept away, in an area of about two meters from the bridge through an annual clearing or as needed. It is important that the vegetation does not grow up near the bridge so that it prevents the wood to dry out after rain.

Cleaning

A minimum maintenance is required to ensure correct operation of wood structures and care should be taken not to allow accumulation of organic matter in contact with wood. The planned preventive maintenance should include cleaning once or twice a year or as needed of the following bridge parts: deck, drains and gutters, expansion joints, bearings, abutments and railings. The aim is to remove moisture-holding debris and dirt that can contribute to microbial growth. The most important is to keep the wood dry.

Painting
Damages to the surface treatment should be repaired before the paint starts to peel off.

Figure 6.4. Painted glulam beam with some cracks

Figure 6.5. Dirt and old leaves on the concrete foundation

6.2 Inspection techniques

Inspections are the basis for the planning of maintenance in the shorter and longer term, and to assess whether the bridge meets the standards as a part of the transport system. The frequency of detailed inspections varies between countries; usually it is about 2-6 years. Inspection intervals may also depend on design and treatment. Serious damages occur most often in very old bridges where inspections should be performed more often.

Inspections require qualified personnel that know where to inspect and how to inspect different parts of a bridge. A number of tools exist for the diagnosis of deterioration and the decisions for maintenance actions. The inspection methods vary in the amount of experience required for reliable interpretation, ease of use and cost. These inspections should be performed at an arm’s length and include a careful examination of each bridge component. Notes should strive to include a high level of detail along with photographs so that future inspectors have sufficient background information.

Diagnostic load testing or load rating of in-service bridges can be an important maintenance inspection activity to ensure the safety of a bridge structure. The distribution of a load in the structure can be measured by installing strain and deflection sensors on primary structural members. Responses are recorded while a load is applied, for example a truck with specified load passing across the bridge. To evaluate the overall stiffness of timber bridge superstructures a dynamic testing with a forced vibration method can be used.

6.2.1 Visual inspection

A general visual inspection can give a quick qualitative assessment of the bridge. Color changes, fruiting bodies of fungi, corrosion, cracks, and deformations should be noted, see Table 6.1 and Figures 6.6 and 6.7.

Rot decay can occur if the wood moisture content exceeds 20% for a long time and at suitable temperatures ranging from 15 to 30 °C. Rot can be recognized by the fruit-body of the fungi causing rot (not always present or visible), the mycelial cords (not always visible), discoloration, a fibrous or cubic structure and a resulting considerable loss of strength.

Protection against moisture from precipitation is very important as dry wood is a prerequisite for long life. Precipitation shall be kept away from bearing components as far as possible or shall be quickly drained.

The following basic principles should be checked at inspections:

– Water is kept away, e.g. by roofing, covers, claddings, protection against splash water;

– Water can quickly drain away from the structure, e.g. by bevels, drip edges, drainage;

– Water traps are avoided, e.g. wood-on-wood contact surfaces, holes, cracks.

Table 6.1. Some visible signs of deficiencies

Deficiencies	**Visible signs**
Brown-rot decay	Wood is dark brown and brittle with cubical appearance, structural failure, crushed wood, sunken faces
White-rot decay	Wood is bleached and whiter than normal, initially no cracking or deformation
Soft-rot decay	Wood is soft at the surface, but firm immediately beneath the surface
Staining	Discoloration on the surface from mold, stain fungi, or rust from metal indicates that the wood has been subjected to water
Checks	Longitudinal separations (cracks) in the wood
Splitting	Crack at the end of board through the cross-section from face to face
Weathering	Ultraviolet (UV) degradation, chemical reaction causing grey color and erosion on the wood surface
Swelling	Can cause deformations in wood around connectors, inclined members
Shrinkage	Checks on the surface, can cause untied bolts, movements of members
Plant or moss growth	Growth in splits and cracks indicates that the wood has been at a relatively high moisture content
Loose parts, fasteners	Indicate shrinkage or movements in structure
Flaking paint	Can point to high moisture content in wood

Figure 6.6. Growth of moss at connection

Figure 6.7. Rot in lower part of railing

Visual inspections are also important to localize failures and look for overall signs of damages. Excessive defection, sagging members, is never a good sign for any type of bridge.

For example, for girder systems it is important to look near midspan tension-side for bending failures and near the girder ends for shear failures along the neutral axis or diagonally. And, of course, beam crushing at the beam supports. For stress-laminated deck systems, localized failures may include vertical slip or horizontal slip of deck laminations, indicative of low prestress. Crushing or significant creep of the outer laminations near the bar anchors is the leading cause of bar force losses, and should be carefully examined. Careful inspection of the wearing surface for stress-laminated decks for any longitudinal cracking is important as that likely is an indication of lamination slip action. Inclined rails on the bridges may mean that the moisture content of the deck is changed.

6.2.2 Equipment

Special equipment is used for conducting in-depth inspections of timber bridge elements. Basic inspection equipment is tape measure, pick hammer, knife, awl, and cordless drill. Equipment for assessment of properties is moisture meter and resistance micro-drill. Construction equipment that may be needed is trailer mounted aerial platforms, crane trucks, ladders, scaffolding, or boat.

Moisture content
Moisture measurements in wood members are usually taken with a hand-held electrical-resistance moisture meter with slide hammer and two metal pin probes that are driven into the wood, see Figure 6.8. This method is fast, easy, relatively accurate and almost non-destructive. Temperature and wood species is needed and some experience is needed for choosing measuring points in the bridge in order to detect any problems. Moisture content greater than 20 % indicates that the wood is affected by water and the cause should be investigated to avoid any growth of rot fungi. Copper or salt-based preservatives may interfere with this electrical.-resistance relationship when the moisture content is high and may become unreliable. So other moisture content measurement methods should be utilised.

Probes can also be permanently installed sensors for resistance measurement in strategic places in the bridge. The measurements are made with hand-held instruments in accessible sockets. For the monitoring over a longer period, the measuring points can be equipped with instruments that automatically measures and stores moisture values.

Figure 6.8. Moisture meter with slide hammer

Sounding and probing

A hammer can be used to strike the wood surface and based on the tone it is possible to differentiate a hollow sound of decay from the sound of solid wood. Some experience is needed for reliable interpretation.

Probing with an awl or a knife can locate decay near the wood surface. Decay is indicated by softness of wood and lack of resistance to probe penetration and the breakage pattern of the wood.

Macro-Drilling

Drilling may be necessary to confirm the presence of interior decay and to estimate the amount of sound timber that remains. The objective is to identify and measure defects for assessment purposes. An ordinary drill is the most common method but the shavings can be difficult to interpret.

Coring removal

Drilling equipment that produces an undisturbed core is recommended. Drilling should be at locations where decay is likely to occur. Unnecessary drilling must be avoided and boreholes must be treated with preservative and sealed with treated plug similar in performance to the member. Increment cores can be visually examined for signs of deterioration and may be submitted to a laboratory for biological and/or chemical analysis for the presence of decay organisms (i.e. brown rot). This can be accomplished either by hand operated coring devices (figure 6.10) or with the assistance of portable drills and specialized coring bits.

Micro-Drilling Resistance

Micro-drill resistance devices record the resistance required to drill through a piece of wood. The amount of torque resistance of the drill bit is related to the density of the wood in that particular area and can be used to determine if deterioration exists. The degree of degradation within the cross-section of the location at the location of drilling can be well defined and the procedure is almost non-destructive due to the small diameter of the drill bits.

Stress Wave timing

This technique can be used on thick timbers or glulam members where hammer sounding is not effective. However, access to both sides of the member is required and the speed of wave propagation varies with grain direction. The presence of decay can significantly affect stress wave transmission time in wood, especially in the transverse direction. For the transverse direction, the annual ring orientation and the existence of checks and splits should be considered when evaluating data. Suspected decay should be verified through techniques like resistance micro-drilling or coring.

Stress-laminated decks

The tension force in the pre-stressing rods of stress-laminated decks should be checked regularly. The force can be measured with a calibrated load cell and indicator and by using a hand-operated hydraulic jack with pressure gauge and a special steel yoke, see Figure 6.11. The measured values should be compared with the original pre-stress and the minimum design value to decide if re-stressing the entire bridge is necessary.

Figure 6.10. Core drilling

Figure 6.11. Load cell measuring tension force in bars

6.3 Repairs

Structural repairs will depend on the cause of the damage and the function of the component and any damage requires specific assessment and experienced judgement.

6.3.1 Connections

Timber connections can become loose. They need to be kept tight and any corroded components replaced. Retightening can be necessary after some time after installation if the wood dries out and shrinks. Care must be taken to not overtighten connections for glulam members at installation, as this will cause crushing of the wood if swelling occurs during the first year in-service. It is important to have sufficiently large washers at screw connections to avoid crushing.

6.3.2 Wood members

Due to reduced strength, it is necessary to remove any parts with rot or replace the entire component. The presence of decay fungi and fruiting bodies indicate that the member has high moisture content, usually above 28-30%. The source of dampness should be identified and eliminated. If wood moisture content below 20% cannot be ensured permanently, the new wood to be installed should be treated with a wood preservative corresponding to the expected moisture content.

Many factors need to be considered in deciding the best solution of repair. There is little information available to correlate the extent of decay with strength loss, and the decision to replace must be evaluated in relation to the stresses on the member. When a decayed member is removed, the adjacent members should be checked to ensure that decay has not spread. It is required to remove at least 300 mm in the grain direction of the sound wood if repair involves cutting out decayed sections of a member. Cut faces of the wood remaining in place shall be treated with a preventive anti-fungal wood preservative.

6.3.3 Reinforcement

If it is not practical to replace some decayed wood members it can sometimes be possible to reinforce with a parallel member or other bracing. Steel or preservative-treated wood can be used. It is important to analyze the structure to ensure the capacity of the repair and the load distribution to members.

6.4 References and Additional sources of information, chapter 6

Brashaw B., Dahlberg J., Hosteng T., Wacker J. 2015. Advanced Timber Bridge Inspection, Field Manual for Inspection of Minnesota Timber Bridges, University of Minnesota and Minnesota Department of Transportation. http://www.dot.state.mn.us/bridge/pdf/insp/timber-bridge-inspection-manual.pdf

Dahlberg J., Phares B., Klaiber W., (2015). Cost-Effective Timber Bridge Repairs: Manual for Repairs of Timber Bridges in Minnesota, Bridge Engineering Center and National Center for Wood Transportation Structures, Research Project, Final Report 2015-45B, Iowa State University and Minnesota Department of Transportation. http://www.dot.state.mn.us/research/TS/2015/201545B.pdf

EN 1990 (2002). Eurocode - Basis of structural design. European Committee for Standardization, Bruxelles, Belgium, April 2002.

EN 1995-1-1 (2004). Eurocode 5: Design of timber structures – Part 1-1: General – Common rules and rules for buildings/incl Amendment A1, European Committee for Standardization, Bruxelles, Belgium, November 2004/2008.

EN 1995-2:2004 Eurocode 5: Design of timber structures – Part 2: Bridges, European Committee for Standardization, Bruxelles, Belgium, November 2004.

EN 335 (2013). Durability of wood and wood-based products – Use classes: Definitions, application to solid wood and wood-based products. European Committee for Standardization, Bruxelles, Belgium, March 2013.

EN 350-2 (1994). Durability of wood and wood-based products – Natural durability of solid wood – Part 2: Guide to natural durability and treatability of selected wood species of importance in Europe. European Committee for Standardization, Bruxelles, Belgium, May 1994.

EN 460 (1994). Durability of wood and wood-based products – Natural durability of solid wood – Guide to the durability requirements for wood to be used in hazard classes. Committee for Standardization, Bruxelles, Belgium, May 1994.

Newsletter (2015). WoodWisdom-Net, Newsletter September 2015, p. 8, Creosub, www.woodwisdom.net

Pousette, A., Fjellström, P.-A., (2004). SP Trätek, Broinspektion – träbroar, SP Sveriges Provnings- och Forskningsinstitut, SP RAPPORT 2004:41, ISBN 91-85303-19-4 ISSN 0284-5172 (In Swedish)

Ritter, M.: (1990). Timber Bridges, Design, construction, inspection and maintenance. US Department of Agriculture, Washington DC, USA, 944 p. http://www.woodcenter.org/docs/em7700_8--entire-publication.pdf

Sétra (2007). Timber Bridges. How to ensure their durability. Technical Guide. © 2007 Sétra - Reference: 0743A - ISRN: EQ-SETRA--07-ED40--FR+ENG, This document is available and can be downloaded on Sétra website: http://www.setra.equipement.gouv.fr

7 Performance evaluation of design concepts

7.1 Life Cycle Evaluation on the Performance of Timber Bridges

7.1.1. General

Life cycle evaluation of bridge projects consists of two aspects: environmental impact and cost. Structural performance affects the lifetime of structural members, hence leads to different maintenance intervals and actions and affects total cost and environmental impact of the structure eventually. In order to optimise timber bridges for low environmental impact and low cost, Life Cycle Assessment (LCA) and Life Cycle Costing (LCC) is applied.

Life cycle in the analyses can be cradle (raw material) to gate (product), gate to gate, or cradle to grave (end of life, e.g. demolition, waste processing). Traditionally, cost of gate to gate (for example product to bridge) is the only stage considered for decision makers; nowadays, entire lifetime (cradle to grave) cost and environmental impact are expected to be considered. In the early design phase of a bridge, LCA and LCC calculations can be used for comparisons, and "best" bridge solution could be sorted out from different design alternatives. Thus, LCA and LCC are generally used as comparative tools for helping decision-making for a specific bridge site at a specific construction time.

7.1.2. Methodology of LCA

LCA addresses the environmental aspects and impacts of a product system. International Organization for Standardization (ISO) published standards ISO 14040 - Principles and framework and ISO 14044 - Requirements and guidelines for LCA (ISO 14040:2006, ISO 14044:2006). The European Commission published ILCD (International Reference Life Cycle Data System) handbook which is in line with the above international standards (ILCD Handbook, 2010). In addition, European standards EN 15804 and EN 16485 could be used as reference when conducting LCA on construction products (EN 15804:2012, EN 16485:2014).

In ISO 14040:2006, life cycle is defined as "*consecutive and interlinked stages of a product system, from raw material acquisition or generation from natural resources to final disposal"*, and LCA is defined as "*compilation and evaluation of the inputs, outputs and the potential environmental impacts of a product system throughout its life cycle"*. Accordingly, stages of LCA are shown in Figure 1:

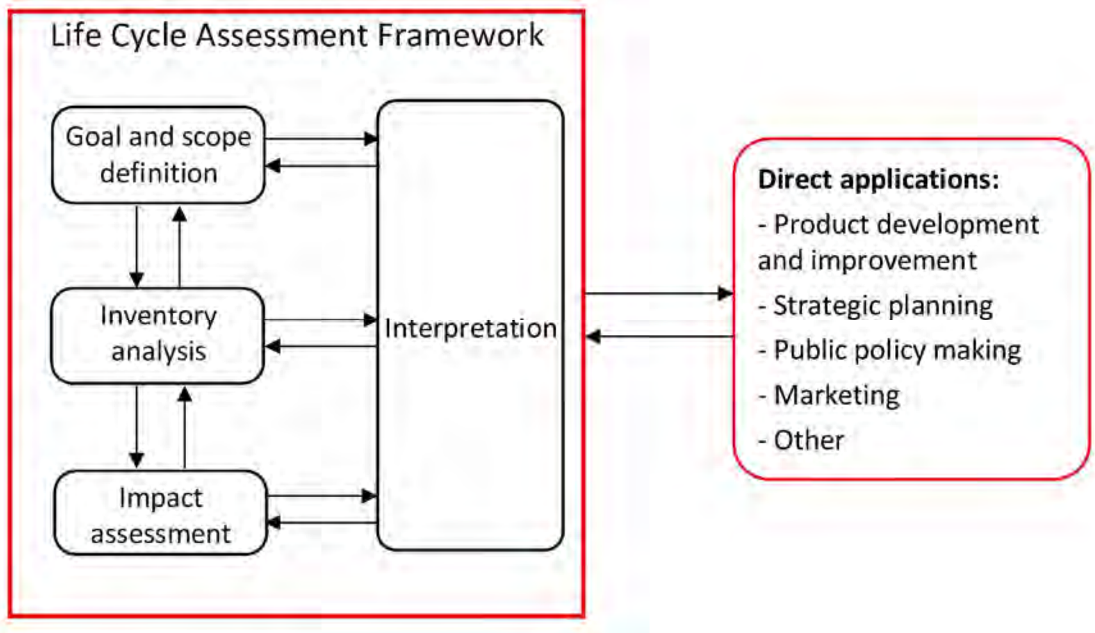

Figure 1. Stages of LCA (ISO 14040:2006).

As shown in Figure 1, LCA is an iterative approach which contributes to the comprehensiveness and consistency of the study and results. The first key point is the "Goal and scope definition", which determines the depth of detail and time frame of an LCA. In this initial stage, what and how to analyse shall be specified; the goal should state the reason and intended application of carrying out the LCA study, and the scope must at least include the following aspects:

- product system
- functional unit
- system boundary
- impact assessment method
- selected impact categories
- data requirement, assumptions, and limitations.

In the above listed aspects, functional unit is the crucial feature for comparing LCA results. A product system may possess multiple functions, the selected one for a given LCA study depends on its goal and scope. ISO 14040:2006 defines the functional unit as "*quantified performance of a product system for use as a reference unit*", and the main reason of defining the functional unit is to ensure that such LCA comparisons are made on a common basis. Provided that the location and traffic capacity of a bridge is known, as well as given length, width, and effective area; then, the functional unit of a bridge can be "the whole bridge structure during its 100-year service life " or "1 m^2 effective area of bridge superstructure in its 100-year service life". The former may be preferred when comparing different alternatives for the same bridge site, the latter may be preferred when comparing different bridge projects. Inventory analysis stage requires Life Cycle Inventory (LCI) data for elementary flows of materials and energy, either from suppliers or from commercial LCI databases. Then the input data (materials and quantities contained in the bridge project) and LCI data will be processed through Life Cycle Impact Assessment (LCIA) method. The LCIA phase evaluates significance of potential environmental impact in terms of various impact categories, e.g. global warming potential (CO_2-equivalents) and ozone depletion potential (CFC-11 equivalents). Finally, the LCA results can be generated as value(s); then the user can interpret the values for “decision making”, strategic planning, and other intentions.

Data quality and transparency of LCI data is very important as this is the primary input for conducting LCA studies and the basis to allow comparisons between different products or designs. When interpreting LCA results, location and source of manufacturing and energy production shall be taken into consideration and specified. However, there is no single or standardised method for conducting LCA, many LCA software are available with embedding LCI databases and LCIA methods. Table 1 lists some LCA software, LCI databases, and LCIA methods.

Table 1. LCA software and LCI database.

	LCA software	**LCI database**	**LCIA method**
Commercial	SimaPro, GaBi, Umberto, etc.	Ecoinvent, Ökobaudat (in Germany), etc.	CML (baseline), ILCD 2011 (by European Commission), ReCiPe 2008, Eclogical scarcity method (applied in Switzerland and Japan), etc.
Free	openLCA, CMLCA, BridgeLCA (by ETSI project), etc.	ELCD (European reference Life Cycle Database), World steel LCI, Wood for good Lifecycle Database, etc.	

Based on the standards, four stages may be included when conducting LCA on a bridge: raw material and product manufacturing, construction, operation and maintenance, and End-of-Life (EoL). Figure 2 shows the life cycle of a bridge:

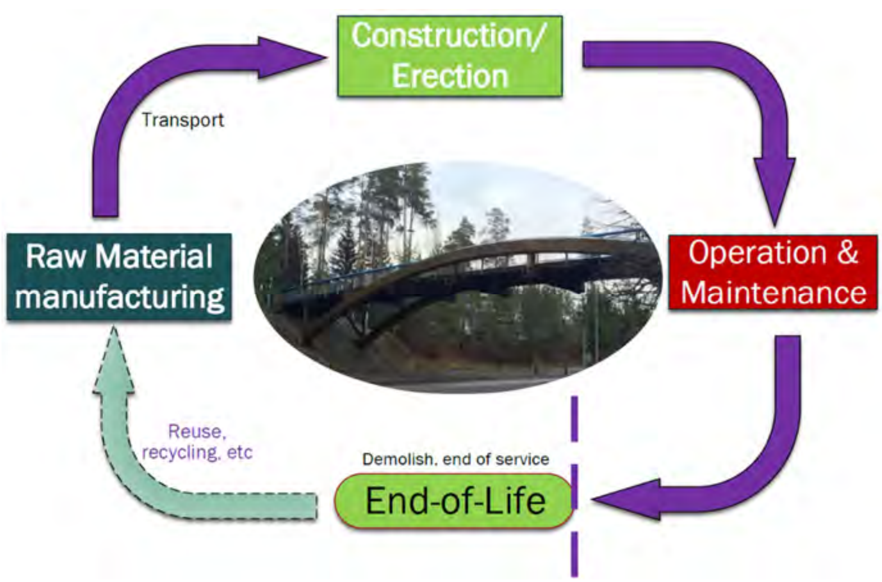

Figure 2. Life cycle of a bridge.

EoL scenarios for different materials can be of great difference, thus processing of the bridge waste in the EoL stage may vary a lot. For instance, should the incineration of timber components in the EoL stage be utilised as secondary source, which of recycling and reusing consumes less processing time and energy? Moreover, whether considering biogenic carbon storage in wood products in the LCA calculation has been argued.

7.1.3. Methodology of LCC

International Organization for Standardization (ISO) published ISO 15686 – Part 5: Life Cycle Costing, which is defined as "*a methodology for the systematic economic evaluation of the life cycle costs over the period of analysis*" (ISO 15686-5:2008). European Commission also published directives regarding LCC: Article 68 in Directive 2014/24/EU of the European Parliament and of the Council (EU.D, 2014), and Article 83 in Directive 2014/25/EU of the European Parliament and of the Council (EU.D, 2014). Elements of LCC defined in ISO 15686-5:2008 are shown in Figure 3:

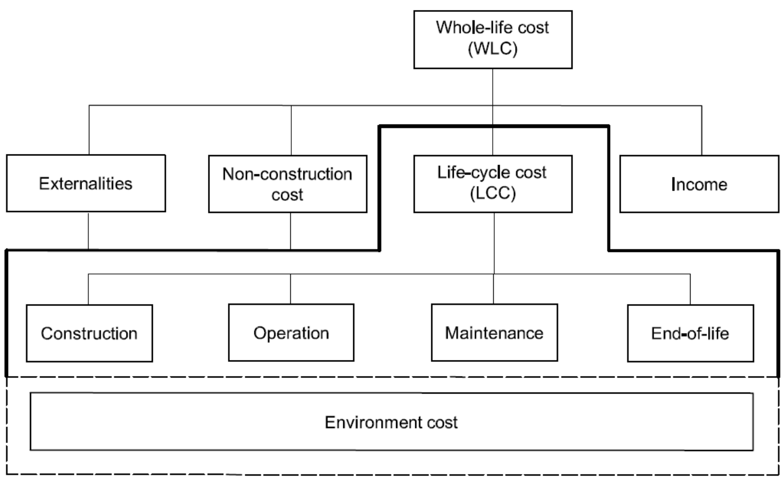

Figure 3. WLC and LCC elements (ISO 15686-5:2008).

In Nordic countries, research and projects regarding LCC has been done or are undergoing since 2000s. The research of LCC on timber bridges for this project is basically based on ETSI project report of Stage 3, which was published in 2013 (Salokangas, 2013). The schematic presentation of LCC analysis is shown in Figure 4:

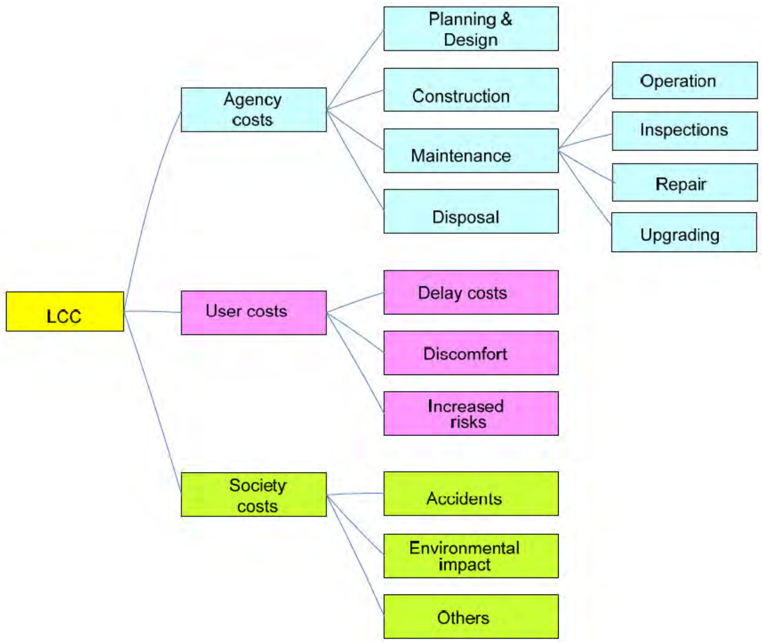

Figure 4. Structure of a complete LCC analysis (Salokangas, 2013).

Figure 4 can be considered as the illustration of LCC part shown in Figure 3. However, the user costs and society costs are out of scope of the research for the DuraTB project, due to lack of time and validated data. For instance, adding environmental impact as cost to "society costs" needs the monetisation of LCA results, and limited research has been done on this aspect (EU.D, 2009), (Finnveden, G., & al., 2013), and (Fourgerit V. & al., 2012). On the other hand, commercial LCA software may provide LCC function, thus monetised LCA results can be added directly to the LCC results inside the software.

Considering the time influence on the cost, decision variables of LCC are listed in (ISO 15686-5:2008, 2008): real costs, nominal costs, discounted costs, and present value. The present value stands for the present monetary sum that should be allocated for future expenditure on an asset, and is used for comparing alternatives over the same period of analysis. The present value should be calculated by applying the expected real discount rate per annum; thus, the expected real discount rate per annum must be paid careful attention in LCC calculation.

Two excel-based tools are available for calculating LCC on bridges, *BridgeLCC* and *Elinkaarikustannusarvio* (Life Cycle Cost) in Finland. The first one is developed in ETSI project (Salokangas, 2013), the other is used internally in Liikennevirasto (Finnish Transport Agency) (Liikennevirasto, 2016). Both of the tools are based on the same structure of LCC, but the Liikennevirasto´s version considers also risks as indirect costs.

7.1.4. Evaluation procedure of LCA and LCC

Drawings and bill of quantities of the bridge should be provided prior to the calculation of LCA and LCC. Besides, maintenance during the service life of the bridge can be based either on the Life Cycle Plan (LCP) provided by the designer and customer, or on the estimation by the LCA and LCC practitioner. The general steps of carrying out LCA and LCC can be as follows:

1) Goal and scope determination, e.g. functional unit, system boundary.

2) Input preparation: collection of design drawings and bill of quantities (material, class, quantity, etc.).

3) Input preparation: available details of material and energy suppliers.

4) Input preparation: Life Cycle Plan or estimated maintenance actions (including relative intervals, required workers, etc.).

5) Input preparation: End-of-Life scenario of materials and corresponding quantities.

6) Assessment preparation: selection of Life Cycle Inventory (LCI) database, e.g. Ecoinvent, GaBi.

7) Assessment preparation: selection of Life Cycle Impact Assessment (LCIA) method, e.g. CML, ELCD.

8) Framework establishment in the LCA and LCC software.

9) Insertion of the collected input information to the corresponding location in the established framework.

10) Running the analysis in the software to obtain the output.

11) Interpretation of the output, e.g. assumption of the calculation, conclusion of the calculation, accuracy, etc.

12) Iteration of the above steps if more input or assessment data is available.

7.1.5. Common maintenance actions and relative maintenance intervals

Timber bridges usually have short construction time and few construction activities, but during the Operation & Maintenance stage of the bridge, service life of structural components influences both LCC and LCA. Based on the records from (Liikennevirasto, 2016), Table 2 lists the results of the three most common maintenance actions and corresponding intervals, details can be found in (Niu & Salokangas, 2016) and (Niu & Salokangas, 2016).

Table 2. Most common actions and intervals of timber bridges in Finland (based on Liikennevirasto, 2016).

Action	**Median value of maintenance intervals (years)**	**Percentage of action on the total amount of studied bridges**
Timber Pedestrian Bridges		
Repair of railing	32	5,2%
Repair of abutment	30	4,5%
Repair of timber handrails	21	4,5%
Timber Road Bridges		
Replacement of timber deck	32	32,3%
Replacement of railings on the deck	32	25,5%
Repair or replacement of embankment railing	34	18,4%

Influencing factors of intervals of maintenance actions on the bridge

Environmental surroundings and traffic conditions may influence the service life of bridge components and the maintenance intervals. If the user wants to consider such effect when applying maintenance intervals, an influencing factor can be introduced. The total influencing factor *f* for estimating the interval of certain maintenance action is expressed as:

$$f = f_1 f_2 f_3 f_i \qquad (7.1)$$

where:

f_1 climate factor,

f_2 salting factor,

f_3 traffic factor (only for timber road bridges),

fi other factors that may affect the maintenance actions and relative intervals.

The function is showing the influencing factors without giving recommended values, because the user should estimate the value of each factor based on the referenced maintenance plan and local conditions.

The final interval of a certain maintenance action should be calculated by multiplying the total influencing factor to corresponding values given in Table 2.

7.2 Case example

Timber pedestrian bridge in Finland: bridge effective area (of the superstructure) 50 m^2, designed service life 50-year according to the suggestion from Liikennevirasto (Finnish Transport Agency). The bridge has a 10 m single span with 12.55 m total length, 4 m effective width. The bridge is supported longitudinally along its full length by five glulam girders, with a plank deck. The sketch of the bridge is shown in Figure 5:

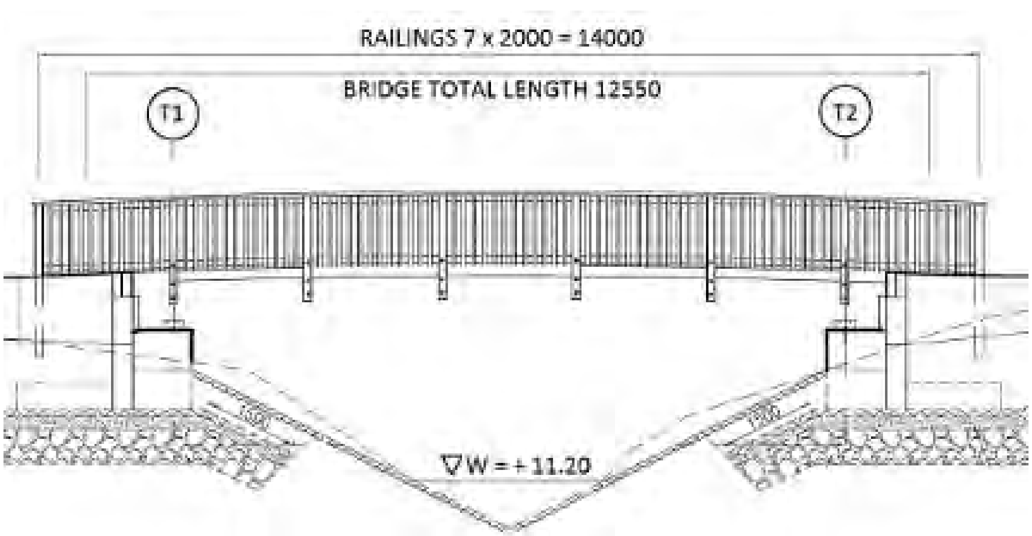

Figure 5. Sketch of the timber pedestrian bridge.

Input:

For the whole structure (both superstructure and substructure), in the whole life cycle, the total bill of quantities for major construction materials and activities (bridge project activities): glulam GL 32c 149 m^3; sawn timber 155 m^3; concrete 40 m^3; reinforcement steel 2 tonnes; diesel 450 litres; electricity 200 kWh.

Unit prices for concrete, steel, timber, etc. For instance: 118€/m^3 for concrete, 110€/ton for reinforcement steel, 450€/m^3 for sawn timber, 900€/m^3 for glulam. Interest rate is assumed to be 2%.

End-of-Life (EoL) for sawn timber is assumed as 100% material recovery, for glulam EoL is assumed as 100% energy recovery.

LCA Tool:

Selected LCA tool: BridgeLCA and openLCA.

Selected Life Cycle Inventory dataset: Ecoinvent v2.

Selected Life Cycle Impact Assessment: ReCiPe v1.06.

Selected Life Cycle impact categories: 3 midpoint indicators: Global Warming Potential (GWP), Ozone Depletion Potential (ODP), Freshwater Eutrophication Potential (EP).

Note: results of LCA can be largely affected by chosen datasets and methods.

LCA Output:

Contribution of different life cycle stages to the total environmental impact:

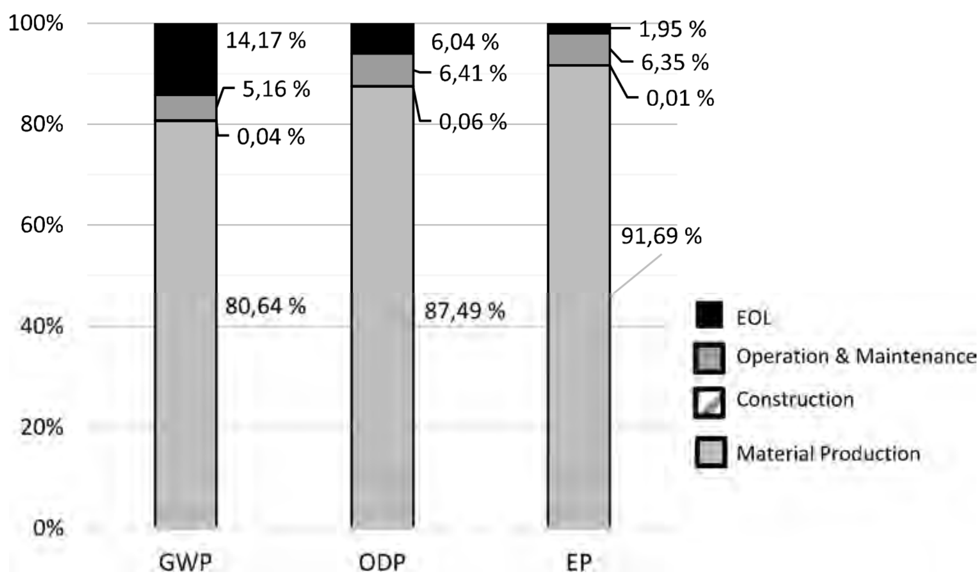

Figure 6. Environmental impact of different life cycle stages.

Energy consumption distribution:

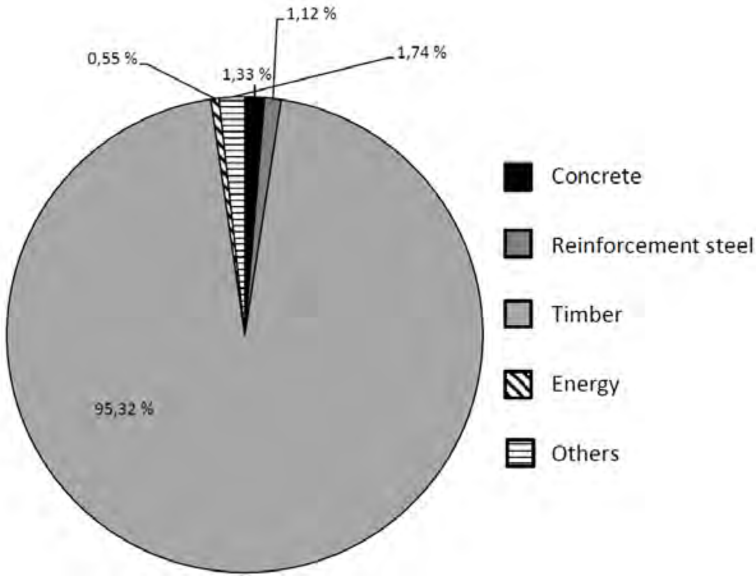

Figure 7. Energy consumption of construction materials and others.

Major energy consumed by timber is renewable, the composition of energy source shown in Figure 8:

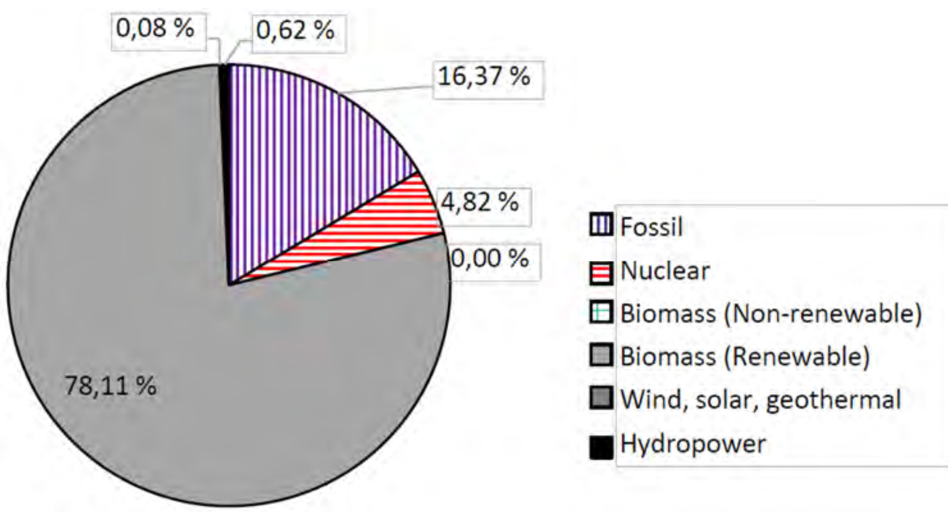

Figure 8. Energy source of timber.

It can be summarised from the above figures that, material production stage contributes the most to the total environmental impact of the bridge. Thus, optimising the bridge design is very important, such as bill of quantities and selection of materials.

LCC Tool:

BridgeLCC created by ETSI project.

Note: repair actions and relative cost vary among bridges, the quality of such data can largely affect the LCC results.

LCC output:

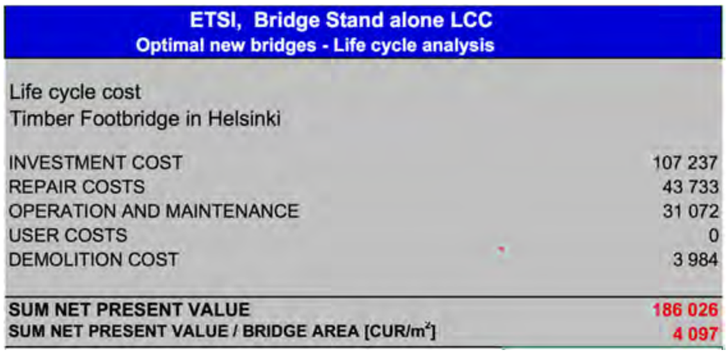

ETSI, Bridge Stand alone LCC
Optimal new bridges - Life cycle analysis

Life cycle cost
Timber Footbridge in Helsinki

INVESTMENT COST	107 237
REPAIR COSTS	43 733
OPERATION AND MAINTENANCE	31 072
USER COSTS	0
DEMOLITION COST	3 984
SUM NET PRESENT VALUE	**186 026**
SUM NET PRESENT VALUE / BRIDGE AREA [CUR/m²]	**4 097**

Figure 9. Total cost of the bridge.

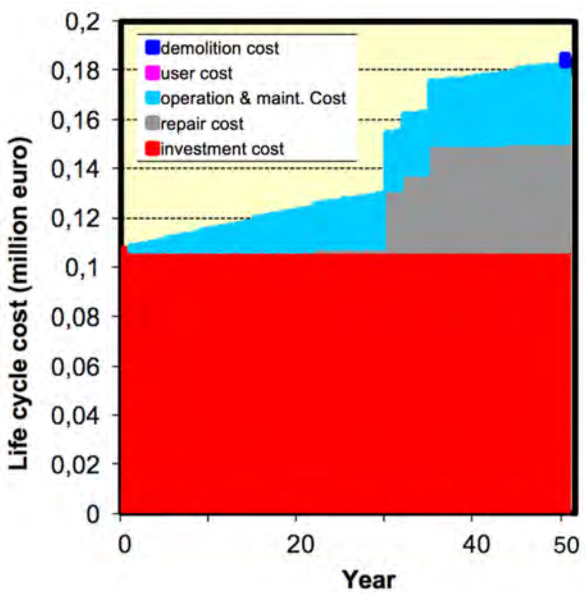

Figure 10. Distribution of operation and maintenance cost.

It can be summarised from Figure 9 and Figure 10 that, the investment cost takes over 50% of the total LCC, other costs during the use and maintenance stage of the bridge take nearly 50%. Thus, both optimising the bridge design and maintenance plan may reduce the total LCC.

7.3 References, chapter 7

EN 15804:2012. (2012). Sustainability of construction works - Environmental product declarations - Core rules for the product category of construction products. CEN.

EN 16485:2014. (2014). Round and sawn timber - Environmental product declarations - Product category rules for wood and wood-based products for use in construction . CEN.

EU, D. (2009). Directive 2009/33/EC of the European Parliament and of the Council of 23 April 2009 on the promotion of clean and energy-efficient road transport vehicles. Official Journal of the European Union, L 120/5-12.

EU, D. (2014). Directive 2014/24/EU of the European Parliament and of the Council of 26 February 2014 on public procurement and repealing Directive 2004/18/EC. Official Journal of the European Union, L94/134-135.

EU, D. (2014). Directive 2014/25/EU of the European Parliament and of the Council of 26 February 2014 on procurement by entities operating in the water, energy, transport and postal services setors and repealing Directive 2004/17/EC. Official Journal of the European Union, L 94/321.

Finnveden, G., & al., (2013). A new set of valuation factors for LCA and LCC based on damage costs - Ecovalue 2012. The 6th International Conference on Life Cycle Management in Gothenburg 2013. Gothenburg.

Fourgerit, V., & al., (2012). Monetary weighting of LCA results to integrate a two-stage management system in the decision process. Proceedings 2nd LCA Conference. Lille.

ISO 14040:2006. (2006). Environmental management - Life cycle assessment - Principles and framework. ISO.

ISO 14044:2006. (2006). Environmental management - Life cycle assessment - Requirements and guidelines. ISO.

ISO 15686-5:2008. (2008). Buildings and constructed assets - Service-life planning - Part 5: Life-cycle costing. CEN.

Liikennevirasto. (2016). Siltarekisteri EXT (Finnish Bridge Register). Helsinki, Finland.

Niu, Y., & Salokangas, L. (2016). Life cycle assessment of timber bridges: a case study. 19th IABSE Congress Stockholm. Stockholm.

Niu, Y., & Salokangas, L. (2016). Life cycle assessment of timiber road bridges: a case study. World Conference on Timber Engineering 2016. Vienna: TU Verlag.

Salokangas, L. (2013). ETSI Project - Bridge Life Cycle Optimisation Stage 3. Aalto University. Helsinki: Aalto University.

ILCD Handbook (2010). International Reference Life Cycle Data System - General guide for Life Cycle Assessment - Detailed guidance. First edition. European Comission, Joint Research Centre, Institute for Environment and Sustainability (JRC-IES), Publications Office of the European Union.

Through our international collaboration programmes with academia, industry, and the public sector, we ensure the competitiveness of the Swedish business community on an international level and contribute to a sustainable society. Our 2,200 employees support and promote all manner of innovative processes, and our roughly 100 testbeds and demonstration facilities are instrumental in developing the future-proofing of products, technologies, and services. RISE Research Institutes of Sweden is fully owned by the Swedish state.

I internationell samverkan med akademi, näringsliv och offentlig sektor bidrar vi till ett konkurrenskraftigt näringsliv och ett hållbart samhälle. RISE 2 200 medarbetare driver och stöder alla typer av innovationsprocesser. Vi erbjuder ett 100-tal test- och demonstrationsmiljöer för framtidssäkra produkter, tekniker och tjänster. RISE Research Institutes of Sweden ägs av svenska staten.

RISE Research Institutes of Sweden
Box 857, 501 15 BORÅS
Telefon: 010-516 50 00
E-post: info@ri.se, Internet: www.sp.se / www.ri.se

Byggteknik
SP Rapport 2017:25
ISSN 0284-5172